TESIS DE LA UNIVERSIDAD DE ZARAGOZA
2021
37

Javier Aragón Fernández

Nanofibrous membranes obtained by electrospinning for bone tissue engineering and wound dressing applications

Departamento
Ingeniería Química y Tecnologías del Medio Ambiente

Director/es
Irusta Alderete, Silvia
Ricardo, Ana Aguiar
De Bartolo, Loredana

EXTRACTO

http://zaguan.unizar.es/collection/Tesis

ISSN 2254-7606

Prensas de la Universidad
Universidad Zaragoza

El presente documento es un extracto de la tesis original depositada en el Archivo Universitario.

En cumplimiento del artículo 14.6 del Real Decreto 99/2011, de 28 de enero, por el que se regulan las enseñanzas oficiales de doctorado, los autores que puedan verse afectados por alguna de las excepciones contempladas en la normativa citada deberán solicitar explícitamente la no publicación del contenido íntegro de su tesis doctoral en el repositorio de la Universidad de Zaragoza.
Las situaciones excepcionales contempladas son:

- Que la tesis se haya desarrollado en los términos de un convenio de confidencialidad con una o más empresas o instituciones.
- Que la tesis recoja resultados susceptibles de ser patentados.
- Alguna otra circunstancia legal que impida su difusión completa en abierto.

© Universidad de Zaragoza
Servicio de Publicaciones

ISSN 2254-7606

Universidad Zaragoza
1542

Tesis Doctoral [Extracto]

NANOFIBROUS MEMBRANES OBTAINED BY ELECTROSPINNING FOR BONE TISSUE ENGINEERING AND WOUND DRESSING APPLICATIONS

Autor

Javier Aragón Fernández

Director/es

Irusta Alderete, Silvia
Ricardo, Ana Aguiar
De Bartolo, Loredana

UNIVERSIDAD DE ZARAGOZA

Ingeniería Química y Tecnologías del Medio Ambiente

2019

Repositorio de la Universidad de Zaragoza – Zaguan http://zaguan.unizar.es

Nanofibrous membranes obtained by electrospinning for bone tissue engineering and wound dressing applications.

A thesis submitted to obtain the degree of doctor, presented by

Javier Aragón Fernández

Zaragoza, 2018

Nanofibrous membranes obtained by electrospinning for bone tissue engineering and wound dressing applications.

A thesis

Prepared in the framework of

Erasmus Mundus Doctorate in Membrane Engineering (EUDIME) to obtain multiple

Doctoral degrees issue by

Universidad de Zaragoza, Departamento de Ingeniería Química y Tecnología del Medio Ambiente

Departamento de Ingeniería Química y Tecnologías del Medio Ambiente
Universidad Zaragoza

Università della Calabria, Istituto per la Tecnologia delle Membrane (ITM)

Universidade Nova de Lisboa, Facultade de Ciência e Tecnologia

Supervisors:
Dr. Silvia Irusta Alderete, Associate Research Professor, Departamento de Ingeniería Química y Tecnología del Medio Ambiente, Universidad de Zaragoza, Spain
Dr. Loredana De Bartolo, Senior Researcher, Istituto per la Tecnologia delle Membrane, Italy
Dr. Ana Isabel Aguiar-Ricardo, Full Professor, Faculdade de Ciências e Tecnologia of Universidade Nova de Lisboa, Portugal

INDEX

SUMMARY AND OBJECTIVES

The current Doctoral Thesis work has been performed under a co-supervision agreement between University of Zaragoza (Home University), University of Calabria (Host University) and Faculty of Sciences and Technology of the NOVA University of Lisbon (FCT NOVA) (Host University). This research has been carried out inside the Erasmus Mundus Doctorate in Membrane Engineering program (EUDIME), (FPA 2011-0014), funded by the European Union.

This thesis focused mainly on the use of the electrospinning technique to produce different kind of membranes for biomedical applications. Synthesis and production of inorganic and organic nanoparticles to be used as fillers or as carriers (drug delivery system) as well as the production of electrospun nanofibrous membranes. This work was carried out *within the Institute of Nanoscience of Aragon* (INA), specifically in the Nanostructured Films and Particles (NFP) group under the supervision of the Professor Silvia Irusta and Dr Gracia Mendoza. Also an important part of the physical-chemical characterization was done at INA.

The study of different biological signals and the use of specific techniques for membrane characterization were acquired at the University of Calabria under the supervision of Dr. Loredana de Bartolo in the Institute on Membrane Technology (ITM). On the other hand, the mobility carried out at the Faculty of Sciences and Technology (FCT NOVA) of Universidade NOVA (FCT NOVA) under the supervision of Professor Ana Isabel Aguiar-Ricardo, allowed a total characterization of two asymmetric membranes following different International Standards to accomplish testing for primary wound dressing.

The development of novel scaffolds loaded with morphogenetic proteins or antibiotic are of great interest in the field of bone tissue engineering. To promote the cellular viability and extracellular matrix production, electrospun scaffolds with enhanced porosity or micro-scale pores could be beneficial since increasing porosity and pore size can provide a three-dimensional (3D) environment that not

only facilitates cell seeding/diffusion but also provides better diffusion of nutrients and waste throughout the scaffolds. The addition of calcium phosphate ceramics has been extensively investigated to fabricate highly porous scaffolds to bone tissue engineering due to their close similar composition of bone, including excellent biocompatibility, osteoinductive and osteoconductive properties. A homogeneous distribution of the bone morphogenetic protein-loaded particles along the entire scaffold could be ensuring a continuous release of the growth factor to provide the necessary biochemical cues for bone repair and regeneration.

Antibiotic-loaded scaffolds may provide drug targeted and sustained release, avoiding the long-term oral and intravenous systematic multidrug administration, which implies toxic side effects, low delivery to the target site and low patient adherence to the treatment, as well as sustaining enhanced osteogenic properties for the successful regeneration of the bone.

Another interesting biomedical application of electrospun membranes is the fabrication of efficient smart dressings for the treatment of wounds. A rapid wound healing requires developing appropriate membranes with interconnected pores to prevent rapid dehydration and bacteria penetration. A high absorption capacity and adequate water vapor transmission will be necessary to keep a moist environment in the wound bed. Besides, if the electrospun membrane has some bactericidal properties will be better for the healing process.

The main goal of this thesis was the development of fibrous membranes by electrospinning with the appropriate characteristics to be used in bone tissue engineering or as wound dressing materials. To achieve this target, several specific objectives were defined, which are described in **Chapters II** to **V.**

This document was divided in the following sections:

- **CHAPTER I**, is an introduction where the concepts of biomaterials, scaffolds and tissue engineering and the main target of drug delivery systems are described. Also, the classification of biomaterials and tissue engineering according to the origin of the materials is also described. As well as all the factors that must be taken into account to develop and properly apply a wound dressing are

expressed. Different kind of techniques used in the literature to produce scaffolds or membrane for bone tissue engineering and wound dressings were mentioned, focusing on the use of electrospinning and electrospray to produce it.

- **CHAPTER II**, focuses on the development of enhanced 3D scaffolds able to promote efficient bone regeneration together with targeted antibiotic release to prevent bacteria colonization. The aim of this work was to synthesize and characterize a drug delivery system consisting of polycaprolactone (PCL) electrospun nanofibers decorated with rifampicin (RFP) loaded in/into poly(lactic-coglicolic acid) (PLGA) particles. This material would promote bone repair avoiding the impairment of the scaffold mediated by infection. The bactericidal ability of the synthesized electrospun material was assessed *in vitro* against Gram positive (*Staphylococcus aureus*) and Gram negative (*Escherichia coli*) bacteria, as well as its cytocompatibility in human osteoblasts 3D cultures. A manuscript with these results was submitted to the International Journal of Pharmaceutics and is under review (Ms. Ref. No.: IJP-D-18-01794).

- **CHAPTER III**, describes the synthesis and characterization of core-shell membranes of PCL and polyvinyl acetate (PVAc) obtained by electrospinning. The fibers were loaded with synthetic hydroxyapatite nanoparticles (HAn) to increase the bioactivity of the materials. The prepared scaffolds were then treated by laser ablation to create desired microscale topographical features in order to favor cell adhesion and growth.

All membranes obtained exhibited a three-dimensionally interconnected pore network structure and the laser treatment caused an increase in cell viability and cell density. Also, an increase in scaffolds biocompatibility suggests that smaller micropore sizes favor cell adhesion and proliferation. These results are published in the article entitled ***"Laser-treated electrospun fibers loaded with nano-hydroxyapatite for bone tissue engineering".*** Javier Aragon, Nuria Navascues, Gracia Mendoza, Silvia Irusta. International Journal of Pharmaceutics 525,112–122, 2017. DOI:10.1016/j.ijpharm.2017.04.022.

- **CHAPTER IV**, refers to the development of a composite electrospun scaffold of PCL or PCL/PVAc core–shell fibers loaded with synthetic HAn. These

fibers were decorated with bone morphogenetic protein 2 (BMP2) loaded in/into PLGA particles via simultaneous electrospraying and coaxial electrospinning. The aim of this work was to evaluate the structural and physico-chemical properties and biodegradation processes of the newly developed scaffolds and their ability to address the architectural, biochemical, and functional features of bone tissue. For this purpose, the scaffold bioactivity was tested by culturing human osteoblasts on the scaffolds and by monitoring cell viability for up to 4 weeks. The *in vitro* osteogenic activity of cells seeded onto the scaffolds was evaluated by assessing alkaline phosphatase (ALP) activity and the expression of osteogenic proteins osteocalcin (OCN) and osteopontin (OPN). These results are published in the article "***Polymeric electrospun scaffolds for bone morphogenetic protein 2 delivery in bone tissue engineering*".** Javier Aragón, Simona Salerno, Loredana De Bartolo, Silvia Irusta and Gracia Mendoza. Journal of Colloid and Interface Science, 531 (2018) 126–137. DOI:10.1016/j.jcis.2018.07.029.

- **CHAPTER V**, describes the synthesis of an antimicrobial wound dressing material, with appropriate mechanical resistance avoiding rapid dehydration and absorbing exudates. PCL/PVAc asymmetric membranes loaded with carvacrol (CRV) were prepared by electrospinning and electrospraying simultaneously. The membranes consist of two layers; the first is an electrospun PCL sheet; the second, a PVAc sheet that would be in contact with the skin releasing the antimicrobial compound. The use of different solvents results in different morphologies for the PVAc-CRV layer. Strain to failure values are in the range of human skin, being adequate to be deposited over a wound surface. Samples present Water Vapor Transmission (WVTR) values in the required range to keep good moisture balance with water loss from the wound at the optimal rate. In the first week, more than 60 % of the loaded CRV was released while after three weeks membranes released between 85 to 100 % of the loaded CRV through a Fickian diffusion and diffusion due to polymer relaxation. Membranes synthetized are potential candidates to be used for wound dressing applications. The manuscript summing up these results was submitted to Materials Science and Engineering C and is under review (MSEC_2018_3013).

- **CHAPTER VI**, summarizes the general conclusions of the thesis work.
- **APPENDIX 1,** describes the main characterization techniques and the methods to evaluate different properties according to the possible applications.
- **APPENDIX 2,** summarizes the articles published and the participation in scientific forums during the thesis period.

RESUMEN Y OBJETIVOS

Esta tesis doctoral se ha realizado dentro del marco de un acuerdo de co-tutela entre la Universidad de Zaragoza (Universidad de origen), la Universidad de Calabria (Universidad anfitriona) y la Facultad de Ciencias y Tecnología de la Universidad NOVA de Lisboa (FCT NOVA) (Universidad anfitriona). El trabajo de investigación se ha llevado a cabo dentro del programa de Doctorado en Ingeniería de Membranas Erasmus Mundus (EUDIME), (FPA 2011-0014), financiado por la Unión Europea.

La tesis se centró principalmente en el uso de la técnica de electrohilado para producir diferentes tipos de membranas que puedan ser utilizadas en distintas aplicaciones biomédicas. Se sintetizaron y produjeron nanopartículas orgánicas e inorgánicas para ser utilizadas como rellenos o como portadores (sistema de administración de fármacos), así como membranas nanofibrosas electrohiladas. Este trabajo se llevó a cabo en el Instituto de Nanociencia de Aragón (INA), específicamente en el grupo de *Nanostructured Films and Particles* (NFP) bajo la supervisión de la profesora Silvia Irusta y la Dra. Gracia Mendoza. Una parte importante de la caracterización físico-química se realizó en el INA.

En la Universidad de Calabria se trabajó bajo la supervisión de la Dra. Loredana de Bartolo en el Instituto de Tecnología de Membranas (ITM). Allí se utilizaron técnicas específicas tanto para la caracterización como para estudiar diferentes señales biológicas producidas por las membranas sintetizadas, bajo la supervisión. Por otro lado, la movilidad llevada a cabo en la Facultad de Ciencias y Tecnología (FCT NOVA) de la Universidade NOVA (FCT NOVA) bajo la supervisión de la profesora Ana Isabel Aguiar-Ricardo, permitió realizar una caracterización completa de dos membranas asimétricas siguiendo diferentes Normas Internacionales que establecen diferentes ensayos a realizar en apósitos primarios utilizados en heridas.

El desarrollo de nuevos *scaffolds* cargados con proteínas morfogenéticas o antibióticos es de gran interés en el campo de la ingeniería de tejidos óseos. *Scaffolds* electrohilados con una microporosidad mejorada puede ser beneficioso

para mejorar la viabilidad celular debido a que una alta porosidad junto a la presencia de microporos puede proporcionar un entorno tridimensional (3D) que no solamente facilita la siembra y difusión celular sino también proporciona una mejor difusión de los nutrientes y residuos a través del *scaffolds*. La adición de cerámica de fosfato de calcio ha sido ampliamente investigada para fabricar *scaffolds* altamente porosos para la ingeniería de tejidos óseos debido a que presentan una composición muy similar al hueso, incluyendo excelentes propiedades de biocompatibilidad, osteoinductivas y osteoconductoras. Partículas cargadas con proteínas morfogenéticas de hueso distribuidas homogéneamente en el *scaffolds* podrían asegurar una liberación continua del factor de crecimiento proporcionando de esta forma las señales bioquímicas necesarias para la reparación y regeneración ósea.

Los *scaffolds* cargados con antibióticos pueden proporcionar una liberación sostenida del fármaco en el sitio de interés, así como el mantenimiento de propiedades osteogénicas mejoradas para la regeneración exitosa del hueso. Evitando de esta forma que se alcancen niveles de toxicidad o niveles ineficaces en la zona de interés, así como la aparición de efectos secundarios indeseados en los pacientes que provocan un rechazo a los tratamientos prolongados de fármacos por vía sistemática (vía oral e intravenosa).

Otra aplicación biomédica interesante de las membranas electrohiladas es la fabricación de apósitos inteligentes eficientes para el tratamiento de heridas. Para lograr una curación rápida de la herida es necesario desarrollar membranas apropiadas con poros interconectados capaces de prevenir la deshidratación rápida y la penetración de bacterias. Para mantener un ambiente húmedo en el lecho de la herida se necesita una alta capacidad de absorción y una adecuada transmisión de vapor de agua. Además, si la membrana electrohilada presenta propiedades bactericidas facilitará el proceso de curación.

El objetivo principal de esta tesis fue el desarrollo mediante electrohilado de membranas fibrosas con las características apropiadas para ser utilizadas en la ingeniería de tejidos óseos o como apósito para heridas. En los **Capítulos II** al **V** se plantean una serie de objetivos específicos con el fin de cumplir el objetivo principal.

Este documento de tesis se dividió en las siguientes secciones:

- **CAPÍTULO I,** corresponde a la introducción general donde se describen los conceptos de biomateriales, *scaffolds*, ingeniería de tejidos y el objetivo principal de los sistemas de liberación de fármacos. Así como, la clasificación de los biomateriales y la ingeniería de tejidos según el origen de los materiales. Además se ponen de manifiesto todos los factores que deben tenerse en cuenta para desarrollar y aplicar adecuadamente los apósitos para heridas. Se mencionaron las diferentes técnicas utilizadas en la literatura haciendo énfasis en el uso de electrohilado y electropulverización para producir *scaffolds* o membranas para su uso en la ingeniería del tejido óseo y como apósitos para heridas.
- **CAPÍTULO II,** se enfoca en el desarrollo y mejora de andamios 3D capaces de promover una eficiente regeneración ósea junto con la liberación de antibióticos dirigidos para prevenir la colonización de bacterias. El objetivo de este trabajo fue sintetizar y caracterizar un sistema de liberación de fármacos que consiste en nanofibras electrohiladas de policaprolactona (PCL) decoradas con partículas de poli (ácido láctico-coglicólico) (PLGA) cargadas con rifampicina (RFP). Este material debe promover la reparación ósea evitando el deterioro del *scaffolds* provocado por una infección. Se realizó la evaluación *in vitro* de la capacidad bactericida del material electrohilado sintetizado contra bacterias Gram positivas (Staphylococcus aureus) y Gram negativas (Escherichia coli), así como su citocompatibilidad en cultivos 3D con osteoblastos humanos. Estos resultados se enviaron a la Revista de farmacia *"International Journal of Pharmaceuitics"* para su publicación en formato de artículo y está bajo revisión.
- **CAPÍTULO III,** se describe la síntesis y caracterización de membranas con estructura de núcleo-envoltura de PCL y acetato de polivinilo (PVAc) obtenidas por electrohilado. Las fibras se cargaron con nanopartículas de hidroxiapatita sintética (HAn) para aumentar la bioactividad de los materiales. Los *scaffolds* desarrollados se trataron con ablación láser para crear características topográficas deseadas a nivel micrométrico con el objetivo de favorecer la adhesión y crecimiento celular.

Todas las membranas obtenidas presentaron una estructura de poros tridimensionalmente interconectados y el tratamiento con láser provocó un aumento en la viabilidad y densidad celular. Además, el aumento en la biocompatibilidad de los *scaffolds* sugiere que los microporos pequeños favorecen la adhesión y proliferación celular. Estos resultados fueron publicados en el artículo titulado ***"Laser-treated electrospun fibers loaded with nano-hydroxyapatite for bone tissue engineering".*** Javier Aragon, Nuria Navascues, Gracia Mendoza, Silvia Irusta. International Journal of Pharmaceutics 525,112–122, 2017. DOI:10.1016/j.ijpharm.2017.04.022.

- **CAPÍTULO IV,** se refiere al desarrollo de un *scaffold* electrohilado compuesto por fibras con estructura de núcleo-cubierta de PCL o PCL/PVAc cargado con HAn sintética. Estas fibras se decoraron con partículas de PLGA cargadas con proteína morfogenética ósea 2 (BMP2) mediante el uso simultaneo de electrohilado coaxial y electropulverización. El objetivo de este trabajo fue evaluar las propiedades estructurales y físico-químicas así como el proceso de biodegradación de los nuevos *scaffolds* desarrollados y su capacidad para abordar las características arquitectónicas, bioquímicas y funcionales del tejido óseo. Para esto, se probó la bioactividad del *scaffold* mediante el cultivo de osteoblastos humanos sobre ellos y se monitoreo de la viabilidad celular durante 4 semanas. Se evaluó la actividad osteogénica *in vitro* de las células sembradas sobre los *scaffolds* determinando la actividad de la fosfatasa alcalina (ALP) y la expresión de osteocalcina (OCN) y osteopontina (OPN) como proteínas osteogénicas. Estos resultados fueron publicados en el artículo titulado "***Polymeric electrospun scaffolds for bone morphogenetic protein 2 delivery in bone tissue engineering*".** Javier Aragón, Simona Salerno, Loredana De Bartolo, Silvia Irusta and Gracia Mendoza. Journal of Colloid and Interface Science, 531 (2018) 126–137. DOI:10.1016/j.jcis.2018.07.029.

- **El CAPÍTULO V,** describe la síntesis de un apósito antimicrobiano para heridas, con una resistencia mecánica adecuada que es capaz de absorber exudados y evitar la deshidratación rápida de una herida. Se prepararon membranas asimétricas de PCL/PVAc cargadas con carvacrol (CRV) mediante el

uso simultáneo de electrohilado y electropulverización. Las membranas constan de dos capas; la primera es una capa de PCL electrohilado; la segunda, una lámina de PVAc que estaría en contacto con la piel liberando a su vez el compuesto antimicrobiano. Se demostró que el uso de diferentes disolventes pueden dar lugar a la obtención de diferentes morfologías de la capa PVAc-CRV. Los valores obtenidos de elongación máxima de las membranas antes de romperse son adecuados para ser utilizados como apósitos para heridas ya que están en el mismo rango reportado de elongaciones en la piel humana. Las membranas presentan una tasa óptima de Transmisión de vapor de agua (WVTR) con valores que se encuentran en el rango requerido para mantener un buen balance entre humedad y pérdida de agua en la herida. En la primera semana, se liberó más del 60 % del CRV cargado, mientras que después de tres semanas, las membranas liberaron entre el 85 y el 100 % del CRV cargado mediante la contribución de un proceso de difusión de tipo Fickiano y la relajación delas cadenas poliméricas. Las membranas sintetizadas son candidatas potenciales para ser utilizadas como apósitos para heridas. El manuscrito que resume estos resultados se envió a la revista *"Materials Science and Engineering C"* y está bajo revisión (MSEC_2018_3013).

- **CAPÍTULO VI,** resume las conclusiones generales del trabajo de tesis.
- **APÉNDICE 1,** describe las principales técnicas de caracterización y los métodos para evaluar diferentes propiedades en función de las posibles aplicaciones.
- **APÉNDICE 2,** resume los artículos publicados y la participación en foros científicos durante el período de tesis.

SOMMARIO E OBIETTIVI

La presente tesi di dottorato è stata svolta in base ad un accordo di co-supervisione tra l'Università di Saragozza (Università di appartenenza), l'Università della Calabria (Università ospitante) e la Facoltà di Scienze e Tecnologia dell'Università NOVA di Lisbona (FCT NOVA) (Università ospitante) . Questa ricerca è stata condotta all'interno del programma *Erasmus Mundus Doctorate in Membrane Engineering (EUDIME)*, (FPA 2011-0014), finanziato dall'Unione Europea.

Questa tesi si è concentrata principalmente sull'uso della tecnica di elettrofilatura per produrre diversi tipi di membrane per applicazioni biomediche. Sintesi e produzione di nanoparticelle inorganiche e organiche da utilizzare come fillers o vettori (sistema di somministrazione di farmaci) e produzione di membrane nanofibrose elettrofilate. Questo lavoro è stato condotto all'interno *dell'Institute of Nanoscience of Aragon* (INA), in particolare nel gruppo *Nanostructured Films and Particles* (NFP) sotto la supervisione della Professoressa Silvia Irusta e della dott.ssa Gracia Mendoza. All'interno dello stesso istituto INA si è svolta una parte importante della caratterizzazione fisico-chimica.

Lo studio di diversi segnali biologici e l'uso di tecniche specifiche per la caratterizzazione delle membrane è stato effettuato presso l'Università della Calabria sotto la supervisione della dott.ssa Loredana de Bartolo presso l'Istituto per la Tecnologia delle Membrane (ITM). Infine, la mobilità svolta presso la Facoltà di Scienze e Tecnologia (FCT NOVA) dell'Universidade NOVA (FCT NOVA) sotto la supervisione della prof.ssa Ana Isabel Aguiar-Ricardo, ha permesso una caratterizzazione completa di due membrane asimmetriche in accordo a diversi standard internazionali sull'esecuzione dei test per il trattamento primario di una ferita.

Lo sviluppo di nuovi scaffold caricati con proteine morfogenetiche o antibiotici sono di grande interesse nel campo dell'ingegneria del tessuto osseo. Gli

scaffold elettrofilati con una maggiore porosità o pori microscopici potrebbero essere utili per promuovere la vitalità cellulare e la produzione di matrice extracellulare. Infatti un incremento della porosità e della dimensione dei pori potrebbe fornire un ambiente tridimensionale agevolando la semina/diffusione cellulare e migliorando la diffusione di nutrienti e rifiuti attraverso gli scaffold. L'addizione di ceramiche di fosfato di calcio è stata ampiamente studiata per la fabbricazione di scaffolds altamente porosi utili per l'ingegneria del tessuto osseo alla composizione chimica simile al tessuto osseo, l'eccellente biocompatibilità, le proprietà osteoinduttive e osteoconduttive. Una distribuzione omogenea delle particelle caricate con la proteina morfogenetica ossea lungo l'intero scaffold potrebbe garantire un rilascio continuo del fattore di crescita, stimolo biochimico necessario per la riparazione e la rigenerazione ossea.

Gli scaffold caricati con antibiotici possono fornire un rilascio mirato e prolungato di farmaci, evitando la somministrazione multifarmaco orale e endovenosa a lungo termine, che implica effetti collaterali tossici, bassa erogazione al sito target e bassa aderenza al trattamento da parte del paziente, oltre a sostenere un incremento dell'osteogenicità utile per la rigenerazione dell'osso.

Un'altra interessante applicazione biomedica delle membrane elettrofilate è la realizzazione di medicazioni intelligenti per il trattamento delle ferite. Una guarigione rapida delle ferite richiede lo sviluppo di membrane appropriate con pori interconnessi per prevenire la rapida disidratazione e la penetrazione dei batteri. Un'elevata capacità di assorbimento e una trasmissione adeguata del vapore acqueo saranno necessari per mantenere un ambiente umido nel letto della ferita. Inoltre, proprietà battericide miglioreranno il processo di guarigione.

L'obiettivo principale di questa tesi è lo sviluppo di membrane fibrose mediante elettrofilatura per applicazioni nell'ingegneria del tessuto osseo o per la medicazione delle ferite. Per raggiungere questi obiettivi, sono stati definiti diversi obiettivi specifici, descritti nei **Capitoli** da **II** a **V**.

Questo documento è stato diviso nelle seguenti sezioni:

- **CAPITOLO I,** è un'introduzione in cui vengono descritti i concetti di biomateriali, scaffold e ingegneria tissutale e l'obiettivo principale dei sistemi di somministrazione di farmaci. Inoltre, viene descritta anche la classificazione dei biomateriali e dell'ingegneria tissutale in base all'origine dei materiali. Vengono inoltre elencati tutti i fattori per lo sviluppo e l'applicazione di una medicazione. Sono stati menzionati diversi tipi di tecniche utilizzate in letteratura per produrre scaffold o membrane per l'ingegneria del tessuto osseo e le medicazioni delle ferite, concentrandosi sull'uso di electrospinning ed electrospray.
- **CAPITOLO II,** si concentra sullo sviluppo di impalcature 3D avanzate in grado di promuovere una rigenerazione ossea efficiente insieme a rilascio di antibiotici mirati per prevenire la colonizzazione dei batteri. Lo scopo di questo lavoro è sintetizzare e caratterizzare un sistema di somministrazione di farmaci costituito da nanofibre elettrofilate di policaprolattone (PCL) decorate con rifampicina (RFP) caricate in particelle di acido poli(lattico-co-glicolico) (PLGA). Questo materiale promuoverebbe la riparazione ossea evitando il danneggiamento dello scaffold a causa dell'infezione. La capacità battericida del materiale elettrofilato sintetizzato è stata valutata in vitro contro i batteri Gram positivi (Staphylococcus aureus) e Gram negativi (Escherichia coli), nonché la citocompatibilità nelle colture umane di osteoblasti 3D. Un manoscritto con questi risultati è stato presentato all'*International Journal of Pharmaceutics* ed è in fase di revisione (Ms. Ref. No.: IJP-D-18-01794).
- **CAPITOLO III,** descrive la sintesi e la caratterizzazione delle membrane core-shell di PCL e polivinilacetato (PVAc) ottenute per elettrospinning. Le fibre sono state caricate con nanoparticelle di idrossiapatite sintetica (HAn) per aumentare la bioattività dei materiali. Gli scaffold preparati sono stati quindi trattati mediante ablazione laser per creare le caratteristiche topografiche su microscala desiderata al fine di favorire l'adesione e la crescita delle cellule.

Tutte le membrane ottenute hanno mostrato una struttura reticolare dei pori interconnessa tridimensionalmente e il trattamento laser ha causato un aumento della vitalità e della densità cellulare. Inoltre, un aumento della biocompatibilità

degli scaffold suggerisce che dimensioni di micropori più piccole favoriscono l'adesione e la proliferazione cellulare. Questi risultati sono pubblicati nell'articolo "***Laser-treated electrospun fibers loaded with nano-hydroxyapatite for bone tissue engineering***". Javier Aragon, Nuria Navascues, Gracia Mendoza, Silvia Irusta. *International Journal of Pharmaceutics* 525, 12-122, 2017. DOI: 10.1016 / j.ijpharm.2017.04.022.

- **CAPITOLO IV,** si riferisce allo sviluppo di un'impalcatura elettrofilata composita di fibre core-shell PCL o PCL / PVAc caricate con HAn sintetico. Queste fibre sono state decorate con la proteina morfogenetica ossea 2 (BMP2) caricata in particelle di PLGA mediante elettrofiltrazione simultanea ed elettrofilatura coassiale. Lo scopo di questo lavoro è di valutare le proprietà strutturali e fisico-chimiche e i processi di biodegradazione degli scaffold recentemente sviluppati e la loro capacità di affrontare le caratteristiche architettoniche, biochimiche e funzionali del tessuto osseo. A tale scopo, la bioattività dello scaffold è stata testata coltivando gli osteoblasti umani sugli scaffold e monitorando la vitalità cellulare fino a 4 settimane. L'attività osteogenica in vitro delle cellule seminate sugli scaffold è stata esaminata valutando l'attività della fosfatasi alcalina (ALP) e l'espressione delle proteine osteogeniche osteocalcina (OCN) e osteopontina (OPN). Questi risultati sono pubblicati nell'articolo ***"Polymeric electrospun scaffolds for bone morphogenetic protein 2 delivery in bone tissue engineering***". Javier Aragón, Simona Salerno, Loredana De Bartolo, Silvia Irusta e Gracia Mendoza. *Journal of Colloid and Interface Science*, 531 (2018) 126-137. DOI: 10.1016 / j.jcis.2018.07.029.

- **CAPITOLO V,** descrive la sintesi di un materiale per la medicazione delle ferite antimicrobiche, con un'adeguata resistenza meccanica che evita la rapida disidratazione e l'assorbimento degli essudati. Le membrane asimmetriche PCL / PVAc caricate con carvacrolo (CRV) sono state preparate mediante elettrospinning e elettrospray simultaneamente. Le membrane sono costituite da due strati; il primo è un foglio elettrofilato di PCL; il secondo, un foglio di PVAc che durante il contatto con il tessuto epidermico dovrebbe rilasciare il composto antimicrobico. L'uso di diversi solventi determina morfologie differenti per lo strato PVAc-CRV. I valori di deformazione fino a rottura sono nella gamma della

pelle umana, essendo adeguati per essere depositati su una superficie della ferita. I campioni presentano valori di trasmissione del vapore acqueo (WVTR) nell'intervallo richiesto per mantenere un buon equilibrio idrico con la perdita di acqua dalla ferita alla frequenza ottimale. Nella prima settimana, oltre il 60 % del CRV caricato è stato rilasciato mentre dopo tre settimane le membrane sono state rilasciate tra l'85 e il 100 % del CRV caricato attraverso una diffusione di Fick e una diffusione dovuta al rilassamento del polimero. Le membrane sintetizzate sono potenzialmente candidabili per le applicazioni di medicazione. Il manoscritto che riassume questi risultati è stato presentato alla Materials Science and Engineering C ed è in fase di revisione (MSEC_2018_3013).

- CAPITOLO VI, riassume le conclusioni generali del lavoro di tesi.
- APPENDICE 1, descrive le principali tecniche di caratterizzazione e i metodi per valutare le diverse proprietà in base alle possibili applicazioni.
- APPENDICE 2, riassume gli articoli pubblicati e la partecipazione a forum scientifici durante il periodo della tesi.

RESUMO E OBJETIVOS

O presente trabalho de Tese de Doutoramento foi realizado sob um acordo de co-supervisão entre a Universidade de Saragoça (Universidade de Origem), a Universidade de Calábria (Universidade Anfitriã) e a Faculdade de Ciências e Tecnologia da Universidade NOVA de Lisboa (FCT NOVA) (Universidade Anfitriã). Esta investigação foi realizada no âmbito do programa de Doutoramento Erasmus Mundus em Engenharia de Membranas (EUDIME), (FPA 2011-0014), financiado pela União Europeia.

Esta tese enfocou principalmente o uso da técnica de eletrofiação para produzir diferentes tipos de membranas para aplicações biomédicas. Síntese e produção de nanopartículas inorgânicas e orgânicas para serem utilizadas como cargas ou como transportadores (sistema de liberação de fármacos), bem como a produção de membranas nanofibrosas eletrofuncionais. Este trabalho foi realizado no Instituto de Nanociência de Aragão (INA), especificamente no grupo de *Nanostructured Films and Particles* (NFP) sob a supervisão da Professora Silvia Irusta e Dr Gracia Mendoza. Também uma parte importante da caracterização físico-química foi feita no INA.

O estudo de diferentes sinais biológicos e o uso de técnicas específicas para caracterização de membranas foram adquiridos na Universidade da Calábria sob a supervisão do Dr. Loredana de Bartolo no Institute on Membrane Technology (ITM). Por outro lado, a mobilidade realizada na Faculdade de Ciências e Tecnologia (FCT NOVA) da Universidade NOVA (FCT NOVA), sob a supervisão da professora Ana Isabel Aguiar-Ricardo, permitiu uma caracterização total de duas membranas assimétricas seguindo diferentes Normas Internacionais para realizar testes de curativos primários.

O desenvolvimento de novos scaffolds carregados com proteínas morfogenéticas ou antibióticos é de grande interesse no campo da engenharia de tecidos ósseos. Para promover a viabilidade celular e a produção de matriz extracelular, os suportes elétricos com poros de micro-incrustação ou porosidade aumentada podem ser benéficos, pois o aumento da porosidade e do tamanho dos

poros pode proporcionar um ambiente tridimensional (3D) que não apenas facilita a disseminação e difusão celular melhor difusão de nutrientes e resíduos em todos os andaimes. A adição de cerâmica de fosfato de cálcio tem sido extensivamente investigada para fabricar estruturas de suporte altamente porosas para engenharia de tecido ósseo devido à sua composição semelhante próxima do osso, incluindo excelentes propriedades de biocompatibilidade, osteoindutoras e osteocondutoras. Uma distribuição homogênea das partículas carregadas de proteína óssea morfogenética ao longo de todo o arcabouço poderia assegurar uma liberação contínua do fator de crescimento para fornecer as pistas bioquímicas necessárias para o reparo e a regeneração óssea.

Suportes carregados com antibióticos podem fornecer liberação direcionada e sustentada, evitando a administração sistêmica por via oral e intravenosa de múltiplos fármacos a longo prazo, o que implica efeitos colaterais tóxicos, baixa entrega ao local alvo e baixa adesão do paciente ao tratamento, bem como propriedades para a regeneração bem sucedida do osso.

Outra aplicação biomédica interessante de membranas electrospun é a fabricação de pensos inteligentes eficazes para o tratamento de feridas. Uma rápida cicatrização de feridas requer o desenvolvimento de membranas apropriadas com poros interconectados para evitar desidratação rápida e penetração de bactérias. Uma alta capacidade de absorção e uma transmissão adequada de vapor de água serão necessárias para manter um ambiente úmido no leito da ferida. Além disso, se a membrana electrospun tiver algumas propriedades bactericidas, será melhor para o processo de cicatrização.

O objetivo principal desta tese foi o desenvolvimento de membranas fibrosas por eletrofiação com as características adequadas para uso em engenharia de tecido ósseo ou como material de curativo. Para atingir esses objetivos, vários objetivos específicos foram definidos, descritos nos **Capítulos II** a **V**.

Este documento foi dividido nas seguintes seções:

- **CAPÍTULO I,** é uma introdução onde são descritos os conceitos de biomateriais, scaffolds e engenharia de tecidos e o principal alvo dos sistemas de liberação de drogas. Além disso, a classificação de biomateriais e engenharia de tecidos de acordo com a origem dos materiais também é descrita. Bem como todos

os fatores que devem ser levados em conta para desenvolver e aplicar corretamente um curativo são expressos. Diferentes tipos de técnicas usadas na literatura para produzir scaffolds ou membranas para engenharia de tecidos ósseos e curativos foram mencionados, com foco no uso de eletrofiação e eletropulverização para produzi-lo.

- **CAPÍTULO II,** enfoca o desenvolvimento de andaimes 3D aprimorados capazes de promover a regeneração óssea eficiente, juntamente com a liberação de antibióticos direcionados para evitar a colonização de bactérias. O objetivo deste trabalho foi sintetizar e caracterizar um sistema de liberação de fármaco constituído por nanofibras de eletrofun policaprolactona (PCL) decoradas com partículas de poli (ácido láctico-coglicólico) (PLGA) carregadas com rifampicina (RFP). Este material promoveria a reparação óssea evitando o comprometimento da estrutura mediada pela infecção. A capacidade bactericida do material sintetizado foi avaliada in vitro contra bactérias Gram positivas (Staphylococcus aureus) e Gram negativas (Escherichia coli), bem como sua citocompatibilidade em culturas 3D de osteoblastos humanos. Um manuscrito com estes resultados foi submetido ao International Journal of Pharmaceutics e está sob-revisão (Ms. Ref. No .: IJP-D-18-01794).
- **CAPÍTULO III,** descreve a síntese e caracterização de membranas de núcleo-casca de PCL e acetato de polivinila (PVAc) obtidas por eletrofiação. As fibras foram carregadas com nanopartículas de hidroxiapatita sintética (HAn) para aumentar a bioatividade dos materiais. Os andaimes preparados foram então tratados por ablação a laser para criar características topográficas em microescala desejadas de modo a favorecer a adesão e crescimento celular.

Todas as membranas obtidas exibiram uma estrutura de rede de poros interconectados tridimensionalmente e o tratamento com laser causou um aumento na viabilidade celular e na densidade celular. Além disso, um aumento na biocompatibilidade dos scaffolds sugere que tamanhos menores de microporos favorecem a adesão e a proliferação celular. Estes resultados estão publicados no artigo intitulado ***"Laser-treated electrospun fibers loaded with nano-hydroxyapatite for bone tissue engineering".*** Javier Aragon, Nuria Navascues,

Gracia Mendoza, Silvia Irusta. *International Journal of Pharmaceutics* 525,112–122, 2017. DOI:10.1016/j.ijpharm.2017.04.022.

- **CAPÍTULO IV,** refere-se ao desenvolvimento de um andaime de eletropneio compósito de fibras de núcleo-casca PCL ou PCL PVAc carregadas com HAn sintético. Estas fibras foram decoradas com partículas de PLGA carregada com proteína morfogenética óssea 2 (BMP2) por eletropulverização e eletrofiação coaxial simultaneamente. O objetivo deste trabalho foi avaliar as propriedades estruturais e físico-químicas e os processos de biodegradação dos novos scaffolds desenvolvidos e sua capacidade de abordar as características arquitetônicas, bioquímicas e funcionais do tecido ósseo. Para este propósito, a bioatividade do andaime foi testada cultivando osteoblastos humanos nos andaimes e monitorando a viabilidade celular por até 4 semanas. A atividade osteogênica in vitro de células semeadas nos arcabouços foi avaliada pela avaliação da atividade da fosfatase alcalina (ALP) e da expressão das proteínas osteogênicas osteocalcina (OCN) e osteopontina (OPN). Estes resultados estão publicados no artigo "***Polymeric electrospun scaffolds for bone morphogenetic protein 2 delivery in bone tissue engineering*".** Javier Aragón, Simona Salerno, Loredana De Bartolo, Silvia Irusta and Gracia Mendoza. *Journal of Colloid and Interface Science,* 531 (2018) 126–137. DOI:10.1016/j.jcis.2018.07.029.

- **CAPÍTULO V,** descreve a síntese de um material antimicrobiano para curativos, com resistência mecânica adequada, evitando a rápida desidratação e absorvendo exsudatos. As membranas assimétricas de PCL/PVAc carregadas com carvacrol (CRV) foram preparadas por electrospinning e electropulverização simultaneamente. As membranas consistem em duas camadas; o primeiro é uma folha de PCL electrospun; o segundo, uma folha de PVAc que estaria em contato com a pele liberando o composto antimicrobiano. O uso de diferentes solventes resulta em diferentes morfologias para a camada PVAc-CRV. Os valores de tensão para falha estão na faixa da pele humana, sendo adequados para serem depositados sobre uma superfície da ferida. As amostras apresentam valores de Transmissão de Vapor de Água (WVTR) na faixa necessária para manter um bom equilíbrio de umidade com a perda de água da ferida na taxa ideal. Na primeira

semana, mais de 60 % do CRV carregado foi liberado, enquanto após três semanas as membranas foram liberadas entre 85 a 100 % do CRV carregado através de difusão e difusão de Fick, devido ao relaxamento do polímero. Membranas sintetizadas são potenciais candidatos a serem usadas em aplicações de curativos. O manuscrito resumindo estes resultados foi submetido à *Materials Science and Engineering C* e está em revisão (MSEC_2018_3013).

- **CAPÍTULO VI,** resume as conclusões gerais do trabalho de tese.
- **APÊNDICE 1,** descreve as principais técnicas de caracterização e os métodos para avaliar diferentes propriedades de acordo com as possíveis aplicações.
- **APÊNDICE 2,** resume os artigos publicados e a participação em fóruns científicos durante o período da tese.

CHAPTER I

Introduction

I.1 Biomaterials

The loss of a body part or an organ generates, besides the loss of function, social and psychological disorders. This has determined not only the interest of finding new materials, but constantly new technologies are developed to improve them and provide materials that meet the most modern requirements in this field. For more than a century, efforts have been devoted to finding materials with the appropriate characteristics to solve the problems related to the reconstruction of tissues and organs injured due to aging diseases or due to trauma from accidents or falls.

The widespread definition of biomaterials was suggested by the American National Institute of Health, "biomaterial is any substance or combination of substances, other than drugs, synthetic or natural in origin, which can be used for any period of time, which augments or replaces partially or totally any tissue, organ or function, in order to maintain or improve the quality of life of the individual" (1).

Gold and ivory were the first materials used by Egyptians and Romans as biomaterials for replacements of cranial defects (1). Amniotic membrane (innermost layer of the placenta) was the first biological material documented for its use as a surgical material in skin transplantation with better results when compared to xenograft or cadaveric coverings (2). Polymethyl methacrylate (PMMA) is a non-degradable polyacrylate and was one of the first polymers accepted to be used in orthopedics applications in the mid-1950s (3). The tissue biocompatibility of this polymer became further apparent when Plexiglas fragments were accidentally implanted in eyes and other body tissues of World War II fighter pilots during aircraft crashes (3).

The advance in modern medicine has implied the increase in human life and, thus, a greater use of biomaterials. Nowadays, biomaterials play an essential role in medicine facilitating healing and reestablishing the main functions of tissues after injury or disease. The modern field of biomaterials combines not only chemistry, physics, biology and medicine but also recent influences from materials science, regenerative medicine and tissue engineering (Figure I.1) (4).

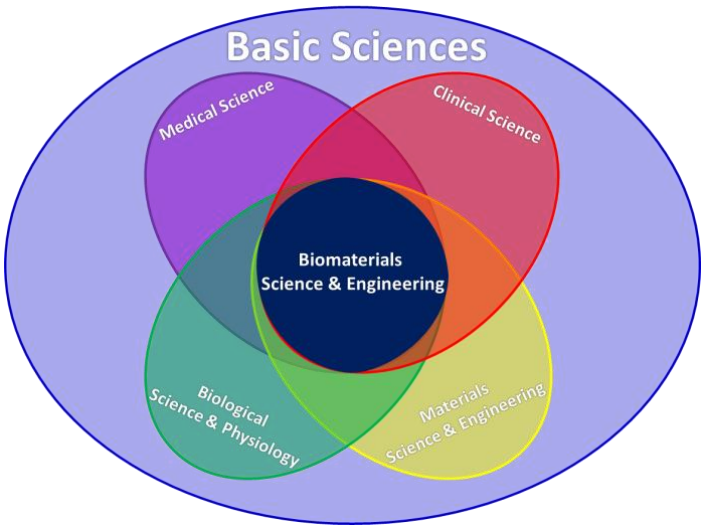

Figure I.1. Main disciplines that integrate the biomaterials sciences and engineering. Modified from von Recum and LaBerge (4).

Biomaterials science and engineering is an interdisciplinary research field that requires knowledge from different areas, which are mentioned in Table I.1.

Table I.1. Disciplines required for the development of biomaterials.

Discipline	***Essential Knowledge***
Basic Science	Physics, chemistry and Biology.
Materials Science and Engineering	Structure, property, relationship of synthetic and biological materials including metals, ceramics, polymers, composites, body tissues, design and prototype development, applied mechanics, thermodynamics, etc.
Medical Science	Composition of human body (cells, tissues, organs and systems), anatomy, physiology, pharmacology, immunology and pathology with some biochemistry, microbiology, molecular biology, genetics, etc.
Clinical Science	Clinical specialties, among which are includes: surgery, orthopedics, maxillofacial, plastic and reconstructive surgery, dentistry, ophthalmology, neurosurgery, obstetrics and gynecology, , cardiovascular surgery, veterinary medicine, etc

The global market of biomaterials was around 70 billion of USD in 2016 and is expected to reach about 150 Billion of USD by 2021 with a compound annual growth rate (CAGR) of 16.0% (5). According to their applications, the biomaterials market is sectioned into cardiovascular, orthopedic, ophthalmology, dental, plastic surgery, wound healing, tissue engineering, neurological/central nervous system, and other applications (5). The plastic surgery and wound healing segments and the polymeric biomaterials are expected to grow at the highest CAGRs during the forecast period. As well as, polymethylmethacrylate (PMMA) is expected to lead the polymer biomaterials market. Among the main companies that commercialize biomaterials we can find: Royal DSM (Netherlands), BASF SE (Germany), Corbion N.V. (Netherlands), Covestro (Germany), Invibio Ltd. (U.K.), Carpenter Technology Corporation (U.S.), Evonik Industries AG (Germany), Berkeley Advanced Biomaterials, Inc. (U.S.), CAM Bioceramics BV (Netherlands), and Celanese Corporation (U.S.) (5).

I.1.1 Biomaterial classification

Biomaterials can be classified according to the nature of the material, being the most important groups: ceramics, metals, polymers and composites. They can be defined either as passive biomaterials (generally remain neutral in their biological environment and have no inherent power of action) or active biomaterials (able of interact with their environment and may even become an integral part of the body) with different bioactivity (6).

I.1.1.1 Metallic biomaterials

Metallurgic industry is able to produce a large number of metals and alloys, but only a few are biocompatible and long-term successful as an implant material. The combination of high mechanical strength and fracture toughness makes metals more suitable for load-bearing applications compared with ceramics or polymeric materials. At the beginning, metallic implants were developed to be used mainly in bone repair (internal fracture fixation of long bones), playing a major role in most orthopedic devices, including temporal and permanent devices (e.g. bone plates, pins,

screws and total joint replacements) (7). The main methods to obtain them are by casting, forging, pressing, rolling and machining. Afterwards, the metallic implants developed were used not only in orthopedic surgery, but also in dental and orthodontic practice, including tooth fillings and roots. Currently, several researches point to the use of metallic biomaterials in application of nonconventional reconstructive surgery of hard tissues/organs (NiTi shape memory alloys as vascular stents) and to develop new magnesium-based alloys for bone tissue engineering and regeneration (7).

Chen and Thouas summarized the current status and clinical applications of the four classes of metallic biomaterial (7): ***Stainless steels, Co-based and Ti-based alloys*** are routinely applied in: temporary devices (fracture plates, screws, hip nails, etc.); stem and cup of total hip replacements with cobalt–chromium-molybdenum or ceramic femoral heads; total joint replacements (wrought alloys); dentistry castings and other permanent devices (nails, pacemakers). The last category corresponds to "***Miscellaneous***" and within there are different alloys such as ***tantalum alloys,*** used as a radiographic marker and wire sutures for plastic surgery and neurosurgery, both approved by US Food and Drug Administration (FDA); ***magnesium alloys,*** that have been reported in different papers as a biodegradable orthopedic implants and ***nickel-titanium alloys*** (known as Nitinol), which have been FDA approved for different applications: orthodontic dental archwires, vascular stents, vena cava filter, intracranial aneurysm clips, catheter guide wires, orthopedic staples and contractile artificial muscles for an artificial heart.

Despite all its advantages for bone repair current metallic biomaterials present limitations or disadvantages, among which can be highlighted (8):

- ✓ possible release of toxic metallic ions and/or particles through corrosion or wear processes, reducing biocompatibility, leading to the beginning of the inflammatory cascades and triggering tissue loss

- ✓ the elastic moduli are not well matched with that of natural bone tissue, producing stress shielding effects reducing the remodeling and stimulations of new bone growth, compromising the implant stability
- ✓ are essentially neutral *in vivo*, remaining as permanent fixtures, causing a second surgical procedure after the tissue has healed sufficiently to remove them safely, such are the cases of plates, screws and pins used to secure serious fractures.

I.1.1.2 Ceramic biomaterials

Ceramic materials are composed of inorganic, non-metallic substances crystalline, semi-crystalline or non-crystalline (amorphous compounds), glasses and glass-ceramics (partially crystallized glasses).

Ceramic biomaterials (Table I.2) can be categorized according with the interactions or attachment between material and host tissue (bioinert or bioactive). Furthermore, the bioactive ceramics may be divided as resorbable or non-resorbable and they may be manufactured either in granulates, as coatings, porous or dense in bulk form (9).

Ceramic biomaterials have been widely used to repair the skeletal system, comprising bone, joints and teeth and to augment both hard and soft tissue (10). Additionally, these materials have been used as carriers for enzymes, antibodies, antigens and as microinjectable delivery system for radioactive isotopes for in situ treatment of tumors. They are also used for eyeglasses, diagnostic instruments, chemical ware, thermometers, tissue culture flasks and fiber optics for endoscopy (9). In dentistry, ceramics are used as restorative materials (including inlays and onlays), in gold-porcelain crowns, glass-filled ionomer cements, multi-unit bridges and dentures (1,9).

Table I.2. Types of Ceramic biomaterials (9).

Interaction with host tissue	*Properties*	*Implant–Tissue Response*	*Ceramic*
Bioinert	Non-toxic material dense or non-porous and biologically inactive (nearly inert)	A fibrous tissue of variable thickness is formed and adhered by growth into surface irregularities by cementing the device into the tissues or by press-fitting into a defect	Aluminum oxide (single crystal and polycrystalline) Zirconia (10)
	Non-toxic material porous (pore diameter between 50-150μm) and biologically inactive (nearly inert)	An ingrown occurs that mechanically attaches the tissue to the material	Aluminum oxide (polycrystalline) Hydroxyapatite-coated porous metals
Bioactive	Non-toxic material biologically active, dense or non-porous, glasses and glass-ceramics with a reactive surface	They connect directly by chemical bonding with the tissue forming an interfacial bond	Bioactive glasses Bioactive glass-ceramics Hydroxyapatite (HA)
	Non-toxic resorbable material biologically active, dense, non-porous or porous able to dissolve in biological environment	The surrounding tissue replaces it slowly	Calcium sulfate Tricalcium phosphate Calcium–phosphate salts

The main methods of manufacturing ceramic biomaterials are plasma spraying, liquid phase sintering (vitrified), hydrothermal synthesis and solid state sintering (9).

In addition, the main advantages of the use of ceramic biomaterials are their high biocompatibility, high resistance to compression, lower wear rates, resistance to corrosion, chemical inertness, release of very low concentrations of 'inert' wear particles, low thermal and electrical conductivity, easy obtaining and low production costs (10,11). Its main disadvantages are associated with the low impact resistance and the difficulties in processing specific geometric forms (11).

I1.1.3 Polymeric biomaterials

Polymers are the biomaterials most used in medicine because they show several unique properties which make them useful in a wide range of applications, such as hard and soft tissue replacements, orthopedics, dental or cardiovascular devices (12). The polarity, stiffness and organization of the polymeric chains into very interesting architectures are the main characteristics of polymeric biomaterials (12). These materials are often mechanically weaker than other classes of biomaterials (metals and ceramics), because they are linked by secondary interactions, such as hydrogen bonding, dipole-dipole interactions and London forces. Nonetheless, they can exhibit physical behavior more similar to native tissue (12).

Polymers biomaterials can be classified regarding its origin in natural or synthetic. Biodegradability is considered the main characteristic of natural polymers, but synthetic polymers are more available and usually have a more cost-effective fabrication compared with the obtaining of natural polymers (13). Many researchers consider that natural polymers are finding increasing applications in the area of bone replacement and hard tissue augmentation but its availability and cost of obtaining is its main disadvantage (13). Among the most used natural polymers can be found: collagen, chitosan, alginate, starch, cellulose, hyaluronic acid, elastin, keratin, silk, etc. (14,15) . Some of them have a highly desirable to induce rapid bone colonization since they can provide a template for biomimetic apatite formation (15).

The main methods to process synthetic polymers are thermally induced phase separation, porogen leaching/solvent casting, electrospinning, gas foaming, rapid prototyping or 3D printing are some of the methods used to process synthetic polymers (16). Synthetic polymers such as, poly(ε -caprolactone) (PCL), poly lactic acid (PLA), poly glycolic acid (PGA) and their copolymers, e.g. poly(lactide-co-glycolic acid) (PLGA) have been widely used to create 3D constructs for bone regeneration due to its biocompatibility and their tailorable biodegradation (16,17).

In 2016, Teo and collaborators reported a list of synthetic polymers approved by the FDA (Table I.3), commonly used as medical implants (13).

Table I.3. Synthetic polymers approved by FDA for biomedical applications.

Synthetic Polymer	***Biomedical Applications***
Polyethylene	Anesthesiology, Cardiovascular, Otolaryngology, Gastroenterology, Urology, Hematology, Pathology, Neurology, Ophthalmic and Orthopedic
Polytetrafluorethylene	Anesthesiology, Cardiovascular, Gastroenterology, Urology, General Surgery, Plastic Surgery, Hematology, Pathology, Neurology and Ophthalmic
Polyamide	Anesthesiology, Cardiovascular, Gastroenterology, Urology, Hematology, Pathology, Neurology General Surgery, Plastic Surgery and Ophthalmic
Polypropylene	Cardiovascular, Gastroenterology, Urology, General Surgery, Plastic Surgery, Obstetric and Gynecologic
Polyethylene terephthalate	Cardiovascular, General Surgery and Plastic Surgery
Polydimethylsiloxane	Cardiovascular, Otolaryngology, Gastroenterology, Urology, General Surgery, Plastic Surgery and Neurology
Polyhydroxyalkanoates	Cardiovascular, Gastroenterology, Urology, Neurology and Orthopedic
Polymethylmethacrylate	Dental and Ophthalmic
Liquid crystal polymer	Otolaryngology and Neurology
Silicone	Otolaryngology, Gastroenterology, Urology, General Surgery, Plastic Surgery, Obstetric and Gynecologic
Parylene	Otolaryngology, Neurology
Polyimides	Neurology
SU-8	Neurology
Polyether Ether Ketone	Orthopedic
Polyurethane	Obstetric and Gynecologic

Despite all its advantages and applications, polymeric biomaterials present a low mechanical resistance and several of them are easily biodegradable. These two properties must be taken into account when developing a new biomaterial (11).

I.1.1.4 Composite biomaterials

Composite materials were defined by William in the Dictionary of Biomaterials, as a "structural material made of two or more distinctly different materials, where each component contributes positively to the final properties" (18). In our body, many tissues are considered "composite" with an additional complexity due to their hierarchical structure, such as extracellular matrix (ECM), tendons, ligaments, skin, and bone, among others (19). Generally, composite biomaterials are associated to combinations of two or more components from the basic biomaterials classes, metals, ceramic and polymers, rather than a combination of materials within the same class (18). Components present in a composite should be distinguishable at a microscopic level. Distribution, content and interaction of the constituent materials together with their physical, chemical and mechanical properties, have a strong repercussion over the final properties of the composite biomaterials (19).

Composite biomaterials usually consist of one or more discontinuous phases (commonly known as filler or reinforcing material) embedded within a continuous phase (known as matrix). The principal functions of the filler are to increase the mechanical properties and bioactivity and change the physical and chemical properties. Ceramic and glass particles as well as carbon, polymer and glass fibers have been the main reinforcing materials used in composite biomaterials (Table I.4).

Most composite biomaterials used in biomedical applications have a polymeric matrix (Table I.5), that can be bio absorbable or not. Ceramic and metallic matrices composites are used mainly in non-biomedical applications, only a few composite biomaterials have a ceramic matrix, such as calcium phosphate bone cements (19).

Table I.4. Advantages/Disadvantage of reinforcing materials.

Reinforcing materials	*Main properties*	*Disadvantage*
Carbon fiber	Lightweight, flexible; high strength; and high tensile modulus	Poor shear strength and may be fragile
Polymer fibers	Biocompatibility, biodegradation; high strength and fatigue resistance; controlled release	Poor mechanical properties
Ceramic	Biocompatibility; bioactivity; reinforce polymers	Poor shear strength and may be fragile
Glasses	High strength-to-weight ratio; good dimensional stability; good resistance to heat, cold, moisture; and corrosion; good electrical insulation properties; ease of fabrication and relatively low cost.	Poor shear strength

Table I.5. Some biomedical composite systems used and its applications.

Matrix/Reinforcement	*Applications*
Epoxy resin/CF	External fixator
Epoxy resins/CF; PMMA/CF; PSU/CF; PP/CF, PE/CF; PBT/CF; PEEK/CF; PEEK/GF; PLLA/HA; PLLA/PLLA fibers and PGA/PGA fiber.	Bone fracture fixation plates, pins, screws
PMMA/HA particles; PMMA/Glass beads; Calcium phosphate/aramid fibers, CF, GF, PLGA fibers and PMMA/UHMWPE fiber	Bone cement
PU/Bioglass; PSU/Bioglass; PEEK/CF; Hydrogels/PET fibers and PLA/PLA fibers/CP	Spine surgery, bone substitute
Bis-GMA/inorganic particles	Dental cements and other dental applications
PEEK/CF	Acetabular cups
PEI/CF-GF; PEEK/CF and CF/PA12	Hip prostheses stem
PE/HA particles	Bone replacement, substitute
Poly(propylene fumarate)/TCP; PEG-PBT/HA PLGA/HA fibers; P(DLLA-CL)/HA particles and Starch/HA particles	Bone filling, regeneration
Hydrogels/PET and Polyolefins/UHMWPE fiber	Tendons and ligaments
PELA/Polyurethane fiber	Vascular grafts
Epoxy resins/CF, GF, KF	Prosthetic limbs

Bis-GMA: Bis-glycidyl dimethacrylate; CF: carbon fibers ; CP: calcium phosphate; GF: glass fibers; KF: Kevlar fiber; HA: hydroxyapatite; PA12: polyamide 12; PBT: poly(butylene terephthalate); P(DLLA-CL): poly(D,L-lactide/-caprolactone); PE: polyethylene; PEEK: poly(ether-ether-ketone); PEG: poly(ethyleneglycol); PEI: poly(ether-imide); PELA: poly(ethylene oxide)-b-poly(lactic acid) block copolymer; PET: poly(ethylene terephthalate); PGA: poly(glycolic acid); PLA: poly(lactic acid); PLGA: poly(lactic-co-glycolic acid); PLLA: poly(L-lactic acid); PMMA: poly(methylmethacrylate); PP: polypropylene; PSU: polysulfone; PU: polyurethane; TCP: tricalciumphosphate; UHMWPE: ultra-high molecular weight polyethylene

I.2 Drug delivery system

Drug delivery systems are focused on enhancing the therapeutic effect of an active molecule at a specific target site, controlling drug release and protecting it under physiological conditions. Toxic and ineffective dose levels are unwanted effects from systemic delivery that can be avoided with the use of these systems (Figure I.2) (20–23). The goal of controlled release systems is to prevent the variability of dose levels and maintain an appropriate therapeutic dose for the desired time.

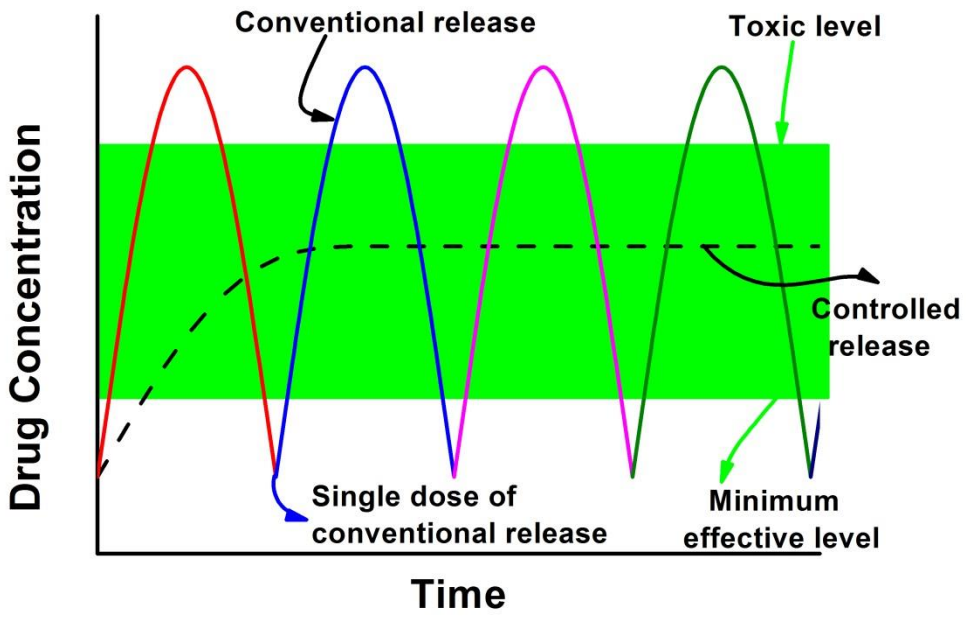

Figure I.2. Drug levels from conventional and controlled drug delivery.

Drug controlled release is associated with different phenomena such as diffusion, swelling, degradation, erosion and dissolution, it depends mainly on composition, structure of the vehicles used and drug distribution. The most used materials to develop controlled release systems are polymers (natural or synthetic), ceramics (calcium phosphate including hydroxyapatite), glass (bioglass), metals, and metal alloys (21).

Hydrophilic drugs release from polymer materials are controlled by Fickian or non-Fickian diffusion and erosion process. When the polymers reach the rubbery state (above glass transition temperature) the surrounding medium can penetrate allowing dissolution and subsequent diffusion of the drug.

On the other hand, hydrophobic drugs are released by erosion process. *In vivo* erosion or degradation (biological environment) can be passive (by hydrolysis) or active (by enzymes) producing surface or bulk erosion. Surface erosion is considered ideal for

several drug delivery applications, because the drug release is usually correlated with the expected erosion rate. In bulk erosion the drug is released in three stages (21):

1. Burst release (drug located on the surface)
2. Drug release during the initial biodegradation process
3. Release of residual drug during complete biodegradation

In addition, the controlled release systems can be sensitive to certain stimuli (responsive drug delivery systems), such as pH and temperature.

The main applications of drug delivery systems are transdermal, topical, gastrointestinal, nasal, mucoadhesive, parenteral, and implantable carrier systems. Kohrs *et al.* (21) summarizes the major advantages and disadvantages for the different applications (TABLE I.6).

The active compounds used in wound management have evolved in parallel to the pharmaceutical agents and wound dressings used as drug delivery systems. New generation of wound dressings that incorporate new active compounds is in continue development. Hydrocolloids, hydrogels, alginates, polyurethane foam/films, and silicone gels are widely used as wound dressing to deliver active molecules (24).

Active compounds loaded in wound dressings play an active role in the wound healing process, as debriding or cleansing agents to eliminate necrotic tissue. Wound dressing loaded with antimicrobial agents prevents or treats infection to aid tissue regeneration(24). When growth factors are loaded into wound dressings, several processes (migration, cell division, differentiation, protein expression, and enzyme production) could be activated at different phases of wound healing (inflammatory, proliferation and migratory phases) (24–26).

Vitamins (A, C, E) and mineral supplements (copper and zinc) are other active compounds involved in the wound healing process that can be released from the dressings. The dressings most employed with this kind of active molecules are oil-based liquid emulsions, creams, ointments, gauze, and silicone gel sheets (24).

Table I.6 Advantages and disadvantages of common drug delivery approaches (21).

Approach	Advantages	Disadvantages
Transdermal/topical	1. Sustained delivery 2. Avoids first-pass metabolism 3. Reduced dosing frequency 4. Steady absorption 5. Noninvasive	1. Possible skin reaction 2. Delayed drug action 3. Variability in drug absorbance rates due to application location 4. Adhesion failure
Gastrointestinal	1. Convenient 2. Simple design 3. Safest administration route 4. Low cost	1. Gastric retention time 2. Requires high levels of gastric liquid and food 3. Drugs with solubility and stability issues in highly acidic environment cannot be used 4. First-pass metabolism
Nasal	1. Rapid absorption 2. Quick drug action 3. Avoids first-pass metabolism	1. Possible nasal irritation 2. Potential toxicity of absorption enhancers 3. Difficult to halt after administration
Mucoadhesive	1. Prolonged residence times 2. Localization of treatment 3. High drug flux at absorbing tissues 4. Avoids first-pass metabolism	1. Potential for damage to mucosa 2. Patient discomfort
Parenteral	1. Highest bioavailability 2. Immediate physiological response 3. Avoids first-pass metabolism 4. Dosing control	1. Pain 2. Potential injection site infection 3. Patient aversion to needles 4. Difficult to halt after administered
Implantable	1. Eliminates need for patient compliance 2. Avoids first-pass metabolism 3. Potential for zero-order release	1. Invasive 2. Limited loading capacity 3. Biocompatibility considerations 4. Surgical removal at therapy termination 5. Possible device failure and drug dumping

Drug delivery systems with long-term therapeutic properties and high clinical efficacy have a growing interest in tissue engineering to release bioactive molecules (mainly growth factors). Biological signals are an important characteristic tissue engineering and both surface-bound and soluble factors can be incorporated within the scaffold as drug delivery systems (20,27).

I.3 Wound dressing materials

Human skin is the most susceptible tissue to suffer an injury because is the largest and most external organ of the human body. Skin is about 15% of the total body weight and it has an average surface area of 1.6-2 m^2 (27). A "wound" is commonly known when the normal skin structure is broken or destroyed, but not only includes lacerations or tears in the skin layer with exposure of the subcutaneous tissue (an open wound), also contusions from blunt objects (a closed wound). In pathology, wounds are restricted to cases in which the trauma sustained by skin structures has penetrated through the epidermis and inflicted damage on the dermis (28).

Wounds can be classified in base on several criteria (29):

a) Severity. In accordance with the amount of tissue damage, the involvement of muscle, bone, nerve and whether the infection is present. These wounds are usually caused by trauma (burn and ulcer wounds), pressure sores, abrasions and iatrogenic wounds, such as skin graft donor sites and dermabrasions

b) Morphology and thickness. Depending on the layers involved, wounds can be superficial wounds (only the epidermis is involved); partial-thickness wounds (epidermis and dermis and involved); and full-thickness wounds (involve the subcutaneous fat or deeper tissue).

c) Surgical. According to the degree of contamination, i.e., clean, clean-contaminated, contaminated and infected, as per the USA National Research Council

d) Aetiology. Based on the cause of wound formation, wounds are classified as pressure ulcers, neuropathic ulcers, vascular ulcers (arterial and venous) and burns.

e) Wounds with and without tissue loss (skin, muscle, bone, tendon).

Normal wound healing physiological process requires skin restoration via re-epithelialization and collagen formation (30,31). Several type of dressing are widely used to protect the wound, to increase the speed and quality of wound healing.

The main characteristic of a wound dressing is to provide the optimum conditions for wound healing and, at the same time, offer protection to the wound from invasion by pathogenic microorganisms and further trauma (31). It is also essential that the dressing does not integrate into the tissue and can be detached without causing any trauma to the wound surface during dressing changes (32).

The obtaining of an ideal dressing is very complicated because not only must take into account the characteristics of each type of wound, but also should mimic the properties and functions of human skin (33):

- ✓ Protecting the organism from its environment even while maintaining it in uninterrupted communication with the environment;
- ✓ Preventing body fluid from escaping and external fluids from penetrating;
- ✓ Thermoregulation;
- ✓ Synthesis (vitamin D and melanin)
- ✓ Storage (lipids, melanin and water);
- ✓ Resistance to mechanical stress;
- ✓ Absorption;
- ✓ Excretion; etc.)

To select an appropriate wound dressing, it is necessary to take into account multiple factors, based on their functional and performance characteristics (24).

✓ Debridement (wound cleansing): Enhances the migration of leukocytes into the wound bed and supports the accumulation of enzymes. Necrotic tissue, foreign bodies and particles prolong the inflammatory phase and serve as a medium for bacterial growth.

✓ Provide or maintain a moist wound environment: Prevents desiccation and cell death, enhances epidermal migration, promotes angiogenesis and connective tissue synthesis, and supports autolysis *via* the rehydration of desiccated tissue.

- ✓ Absorption. Removal of blood and excess exudate: In chronic wounds, there is an excess of exudate, containing tissue-degrading enzymes, which block the proliferation and activity of cells, and break down extracellular matrix materials and growth factors, thus delaying wound healing. The excess of exudate can also macerate the surrounding skin.
- ✓ Gaseous exchange (water vapor and air): Permeability to water vapor controls the management of exudate. Low tissue oxygen levels stimulate angiogenesis. Raised tissue oxygen stimulates epithelialization and fibroblasts.
- ✓ Prevent infection: protect the wound from bacterial invasion: Infection prolongs the inflammatory phase and delays collagen synthesis, inhibits epidermal migration and induces additional tissue damage.
- ✓ Provision of thermal insulation: Normal tissue temperature improves the blood flow to the wound bed and enhances epidermal migration.
- ✓ Low adherence. Protects the wound from trauma: Adherent dressings may be painful and difficult to remove, and cause further tissue damage.
- ✓ Cost-effective low frequency of dressing change: Dressing comparisons based on treatment costs rather than unit or pack costs should be made (cost-benefit-ratio). Although many dressings are more expensive than traditional materials, the more rapid response to treatment may save considerably on the total cost.

Global wound dressings market was estimated to be valued at 6.3 billion of USD in 2016, and is expected to grow at a CAGR of 6.0% from 2016 to 2021, to reach around 8.5 Billion of USD by 2021 (34). Advanced wound dressings segment registered the largest market share in 2015 and it is expected to grow at a CAGR of 6.9%. Increasing knowledge regarding wound care management, the high growth potential of emerging economies, and the increasing number of acquisitions by key companies have opened up a wide range of opportunities for the growth of this market in upcoming years. Among the main companies that market wound dressings are Smith & Nephew plc (U.K.), Acelity L.P., Inc. (U.S.), Integra Lifesciences Corporation (U.S.), Coloplast Corporation (Denmark), 3M Company (U.S.),

Organogenesis Inc. (U.S.), ConvaTec Inc. (U.S.), Hollister Wound Care (U.S.), Mölnlycke Health Care AB (Sweden), and BSN Medical (Germany) (34).

In the estimated global prevalence by wound type according to the report from MedMarket Diligence, LLC (Figure I.3), it is expected that the most frequent injuries in the world in 2020 will be surgical wounds (about 450 million of people), followed by diabetic ulcers (more than 60 million of people), venous ulcers (about 40 million of people), pressure ulcers and lacerations (more than 20 million of people) and burn wounds (about 10 million of people) (35). This indicates the importance of developing new wound dressings for the efficient treatment of these types of wounds.

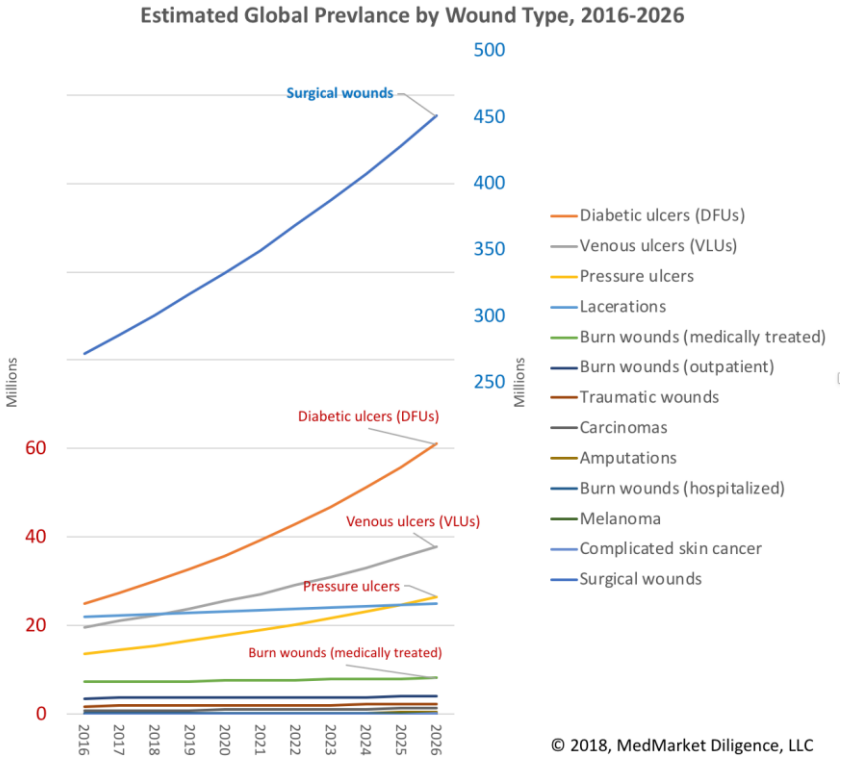

Figure I.3. Estimate global prevalence by wound type reported by MarketsandMarkets™ in 2016 (34).

I.3.1 Wound dressing classification

Traditionally, wound dressings are classified based on its nature or action as: passive products (gauze and tulle dressings, which is the largest market segment); interactive products (polymeric films and foams recommended for low exuding

wounds, which are mostly transparent, permeable to water vapor and oxygen but impermeable to bacteria); and bioactive products (dressings constructed from material which has endogenous activity or dressings able to act as a drug delivery system of bioactive compounds in wound healing) (36).

In 1999, wound dressing categories were reclassified by the FDA as follow (36):

- ✓ ***Nonresorbable Gauze/Sponge Dressing for External Use*** (sterile or nonsterile device, to be placed directly on a patient's wound to absorb exudates).
- ✓ ***Hydrophilic Wound Dressing*** (non-resorbable materials with hydrophilic properties available in sterile or nonsterile form, to cover a wound and absorb exudates).
- ✓ ***Occlusive Wound Dressing*** (non-resorbable material sterile or nonsterile with or without an adhesive backing, intended to cover a wound, to provide or support a moist wound environment and to allow the exchange of gases such as oxygen and water vapor through the device).
- ✓ ***Hydrogel Wound and Burn Dressing*** (non-resorbable matrix sterile or nonsterile made of hydrophilic polymers or other material in combination with at least a 50 % of water, designed to cover a wound, to absorb wound exudates, to control bleeding or fluid loss, and to protect against abrasion, friction, desiccation and contamination).
- ✓ ***Interactive Wound and Burn Dressings*** (reduces the colonization count, exudates level, improves the wound bed moisture retention, improves the wound collagen matrix, removes cellular products and provides protection for the epithelializing bed).

At present, wound dressing market offers more than 3,000 of dressing products registered to suit the needs according to the condition of the wound (37) and according to the base of dressings they can be divided into 8 main categories (Table I.7).

Table I.7. Wound dressing categories and its applications.

Dressing categories	*Main features*	*Applications*	*Disadvantages*
Gauze and Impregnated Gauze Dressings	Highly permeable and relatively non-occlusive, inexpensive, and used as a non-time or short-term use.	Secondary dressings commonly used for both infected and non-infected wounds of any size, shape, depth, or etiology.	Require more force to remove and may leave residue or lint in the wound bed.
Films	Flexible, permeable to water vapor and gas, but impermeable to bacteria and water.	Superficial wounds such as lacerations, abrasions, partial thickness wounds, sutured wounds, and graft donor sites with minimal drainage. They may also be used on granular wounds and areas of friction.	Not to be used on infected wounds, wounds with moderate to heavy drainage (little absorptive capabilities), or patients with fragile skin.
Hydrogels	Permeable to gas and water, provide moisture to dry wounds and absorbs a minimal amount of fluid, effective for softening eschars.	Available in sheets, gels, or impregnated gauzes are indicated for any thickness wounds with minimal or moderate drainage. They can decrease pain and provide padding to decrease shear forces.	Most hydrogels are almost non-adhesive, thus requiring a secondary dressing. Should not be used on infected wounds and on heavily draining wounds.
Foams	Porous 3 layered polyurethane foams able to quickly and effectively draw the exudates deeply into the absorbent material and reliably hold it there. Hydrophobic outer layer prevents bacteria from penetrating. Middle absorption layer is devised to retain absorbed wound exudates. The inner contact layer is hydrophilic with specifically pores size.	Universally used on wounds with minimal to heavy exudates, because they are easy to place and provide thermal insulation. Foams dressing should be able to quickly and effectively draw the exudates deeply into the absorbent material and reliably hold it there. It should also provide soft cover to the wound site, in order to manage the wound environment.	Semipermeable foams are not indicated for dry or eschar covered wounds because it can adhere to the wound

Table I.7. Continued			
Hydrocolloids	Hydrophilic colloidal particles with a strong film or a foam adhesive backing sheet provide thermal insulation. Impermeable to water, gas, and bacteria and therefore can be effective barriers against urine, stool, and pathogenic microorganisms.	Indicated for any thickness wounds, may be safely used on both granular and necrotic wounds. They should only be used with skin sealants on patients with good skin integrity.	Often leave residues after removal. Not appropriate for bleeding or heavily draining wounds. They are contraindicated for infected wounds and must be used with caution on immuno-compromised patients.
Alginates and Hydrofibers	React with serum and wound exudates to form a hydrophilic gel to provide a moist wound environment. They are highly permeable and non-occlusive.	Ideal dressings for moderate to highly draining wounds (they can absorb up to 20 times their weight of exudates). Indicated for partial and full thickness draining wounds and can also be used for infected wounds.	They require a secondary dressing and are not indicated for dry or minimally draining wounds and on wounds with exposed tendon, capsule, or bone
Biological Dressings	Derived from natural tissues, such as skin or amnion. Generally, they provide and maintain moist wound environment that is conducive to regeneration and migration of fibroblasts and epithelial cells and act as a bacterial barrier to protect the wound from infection and fluid loss. Decrease the pain associated with open wounds. Some types may adhere firmly to the wound by vascular connections.	Temporary coverage of open and large wounds. Ideal skin substitute for use in acute and chronic wounds (38).	Low availability and high produce cost. (38) The most serious potential liability of biologic wound dressings is transmission of infection; however, the actual incidence of such transmission is extremely low.

Table I.7. Continued			
Composite Dressings and Adjunctives	Multiple layers and each layer is physiologically distinct. They usually have 3 layers: inner contact layer (is non adherent, preventing trauma to the wound bed), middle layer (absorbs moisture and wicks it away to prevent maceration yet maintaining a moist wound bed) and outer layer (commonly a semipermeable film, serves as a bacterial barrier).	Convenient for both partial and full thickness wounds. It can be used as primary or secondary dressings.	Less flexibility and more expensive (30).

As described above, each dressing variety has unique properties, which makes it suitable for different wound conditions. The disadvantage of a dressing for a specific type of wound may be beneficial for the treatment of another wound. Some of the commercial products are described in Table I.8 (36). However, there is still no superior product that heals chronic wounds like venous leg ulcers, diabetic wound and pressure ulcers which often fail to achieve complete healing. Hence, developing a dressing material that addresses the major interfering factors of normal healing process will help patients and wound care practitioners (30).

Table I.8. Some commercial dressing materials (36)**.**

Dressing	*Type*	*Company*	*Material*
Bioclusive®	Film	Johnson & Johnson	PU
Cica-Care	Film	Smith & Nephew	Silicone
Mepiform®	Film	Mölnlycke Health Care	Silicone
Mepilex®	Film/form	Mölnlycke Health Care	Silicone/PU
Mefilm®	Film	Mölnlycke Health Care	PU
Mitraflex®	Film	Mölnlycke Health Care	PU
Omiderm®	Film	Iatro Medical	PU
Opsite®	Film	Smith & Nephew	PU
Spyrosorb®	Film	BritCair	PU
Tegaderm®	Film/pad/foam	3M Health Care	Hydrocolloid/acrylic
Biatain®	Foam/film	Coloplast	PU
PolyMem®	Foam/film	Ferris Mfg. Corp.	PU
Contreet®	Foam/film	Coloplast	PU containing silver
Cavi-careTM	Foam	Smith & Nephew	Silicone
Lyofoam®	Foam	Seton Healthcare	PU
Allevyn®	Foam	Smith & Nephew	PU
Tielle®	Foam	Johnson & Johnson	PU
Actisorb plus®	Deodorizing	Johnson & Johnson	Activated charcoal cloth with silver
Carbonet®	Deodorizing	Smith & Nephew	Activated charcoal cloth
Alione	Bioactive	Coloplast	Hydrocolloid
Biofilm	Bioactive	Biotrol	Hydrocolloid
CombiDERM®	Bioactive	ConvaTec	Hydrocolloid
Comfeel Contour®	Bioactive	Coloplast AS	Hydrocolloid
Cutinova Hydro	Bioactive	Smith & Nephew	Hydrocolloid

Table I.8. Continued			
Kaltocarb®	Deodorizing	ConvaTec	Activated charcoal cloth with alginate
GranuGel® Paste	Bioactive	ConvaTec	Hydrocolloid paste
Granuflex®	Bioactive	ConvaTec	Hydrocolloid
Tegasorb®	Bioactive	3M Health Care	Hydrocolloid
Duoderm®	Bioactive	ConvaTec	Hydrocolloid
Mesitran®	Bioactive	Theo Manufacturing BV	Hydrocolloid with honey
Aquacel®	Bioactive	ConvaTec	Hydrofiber
Versiva®	Bioactive	ConvaTec	Carboxymethyl cellulose
Aquaform®	Bioactive	Aspen Medical	Hydrogel
Geliperm®	Bioactive	Geistlich Sons Ltd.	Hydrogel
Granugel®	Bioactive	ConvaTec	Hydrogel
Intrasite Gel®	Bioactive	Smith & Nephew	Hydrogel
Nu-Gel®	Bioactive	Johnson & Johnson	Hydrogel
Purilon Gel®	Bioactive	Coloplast Ltd.	Hydrogel
Sterigel®	Bioactive	Seton	Hydrogel
Vigilon	Bioactive	Bard	Hydrogel
Algisite®	Bioactive	Smith & Nephew	Alginates
Algosteril®	Bioactive	Brothier	Alginates
Kaltostat®	Bioactive	ConvaTec	Alginates
Melgisorb	Bioactive	Mölnlycke Health Care	Alginates
SeaSorb®	Bioactive	Coloplast AS	Alginates
Sorbsan®	Bioactive	Pharma-Plast Ltd.	Alginates
Tegagel®	Bioactive	3M Health Care	Alginates
Tegagen	Bioactive	3M Health Care	Alginates
Mepore®	Traditional	Mölnlycke Health Care	Nonwoven polyester fabric
Debrisan®	Beads	Pharmacia and Upjohn Ltd.	Polysaccharide
Iodosorb	Beads	Smith & Nephew	Polysaccharide
Iodoflex	Beads	Smith & Nephew	Polysaccharide
Acticoat	Silver	Smith & Nephew	High-density polyethylene mesh and nonwoven fabric of rayon and polyester

Table I.8. Continued			
Promogran	Form	Johnson & Johnson	Collagen/regenerated cellulose
KytoCel®	Form	Aspen Medical	Chitosan fibers
CeloxTM	Form/pad/granules	Medtrade Products Ltd.	Chitosan
HemCon®	Form	HemCon Medical Tech., Inc.	Chitosan
AquanovaTM	Pad	MedTrade Products Ltd.	Chitosan
Beschitin®	Sponge/film	Unitika Medical Products	Chitin

I.4 Tissue engineering

One of the most devastating, costly and frequent problem in human health care is the loss or failure of an organ or tissue (39). Every year, millions of people suffer tissue loss or end stage organ failure. Tissue engineering is considered a new field dating from late 80's, that benefits/takes advantage of the principles of engineering and biology to the development of functional substitutes for damaged tissue.

In 1988, tissue engineering was defined by Y.C. Fung as "an interdisciplinary field that applies the principles of engineering and the life sciences toward the development of biological substitutes that restore, maintain, or improve tissue function" (17).

In 1993, three general strategies were proposed for the creation of new tissue (39):

✓ Isolated cells or cell substitutes. It allows the replacement of only the affected cells and permits manipulation of cells before using them. Its limitations include failure of the cells used to maintain their function in the recipient and immunological rejection.

✓ Tissue-inducing substances. This approach not only depends on the large-scale production and purification of appropriate signal molecules, but also on the development of methods to deliver these molecules (growth factors, drugs or any bioactive ingredient) to their targets.

✓ Cells placed on or within matrices. The matrices are produced from natural or synthetic materials (commonly known as scaffolds). Immunological

rejection may be prevented by using autologous cells or by immunosuppressive drugs. In this approach, it is possible to find open and closed system. In open systems, cells attached to matrices are implanted and become incorporated into the body. In closed systems, the cells are isolated from the body by a membrane that allows permeation of nutrients and wastes but prevents large entities such as antibodies or immune cells from destroying the transplant. These systems can be implanted or used as extracorporeal devices.

Twenty years later, some general strategies have been adopted to obtain new tissues, such as: use of autogenous (or autologous) cells sources; production of a scaffold for damaged target tissue; tissue culture systems; and use of substances that can induce the regeneration of damaged tissue (Figure I.4) (39–41). Among the main current research areas in tissue engineering, the engineering of bone, bone marrow, skin, nerves, cartilage, blood vessels, corneal epithelia, arteries, heart valves, and heart myocardium are the most relevant (42).

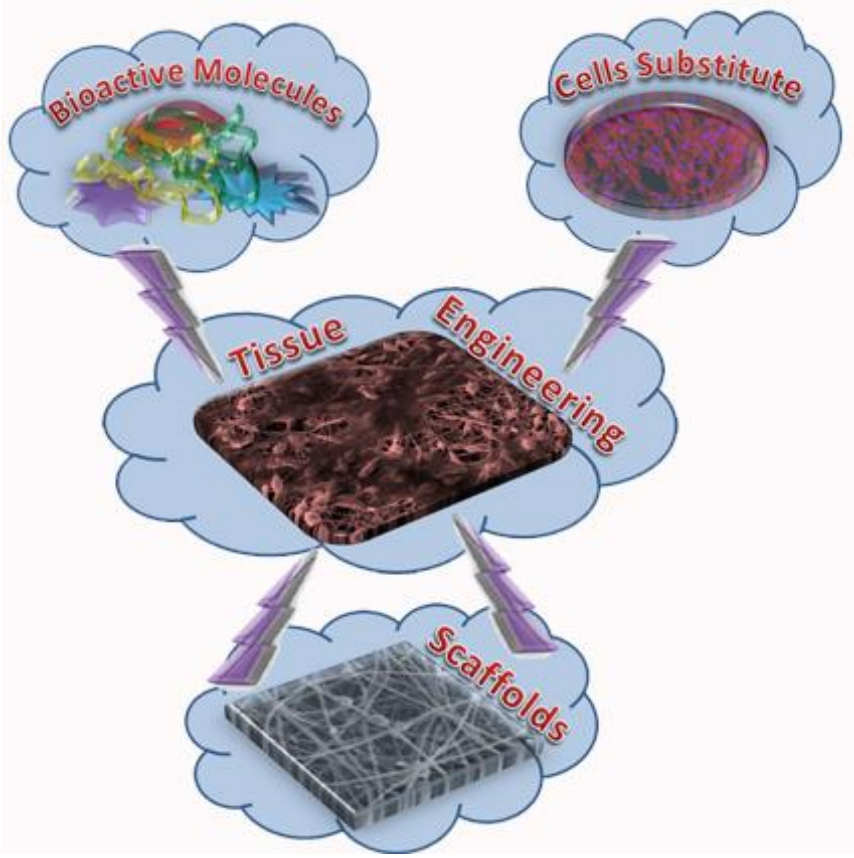

Figure I.4. Tissue engineering strategy currently used.

In the mid 80's, Dr. Joseph Vacanti proposed the idea "to design appropriate scaffoldings for cell delivery as opposed to seeding cells onto available naturally occurring scaffolds having physical and chemical properties that could not be manipulated". Dr. Vacanti worked intensely to generate functional tissue equivalents utilizing a branching network of synthetic biocompatible/biodegradable polymers configured as scaffolds seeded with viable cells (43). In 1999, the concept of scaffolds based tissue engineering was defined in Williams Dictionary of Biomaterials as "a porous structure, usually polymeric, which serves as a substrate and guide for tissue regeneration (18).

Nowadays, a combination of biological and engineering requisites should be taken into account to design a scaffold for a specific application. The biocompatibility of the material used involves that the scaffold should not demonstrate immunogenicity or bring out an adverse inflammatory response (44,45). A suitable degradation/tissue regeneration rate will be necessary to be sure that mechanical properties and functionality of the scaffolds are not compromised. Bioresorbable scaffolds developed must also be sterilizable and degraded without significant cytotoxic, inflammatory or immunogenic degradation components. Scaffold design should take into account also bulk properties, porosity, pore diameter, surface area, chemical properties, micro and macro-environments to regulate cell adhesion, spreading, motility, survival, and differentiation (46).

In 2016, the global tissue engineering market size was valued at around USD 5 billion and according to a new report by Grand View Research, Inc., it is expected to reach USD 11.5 billion by 2022 with a CAGR about 13%.(47) This market growth is supported by a growing potential of tissue engineering procedures in the treatment of tissue damages (48).

Every year, around 1.3 million case of breast cancer are reported, over 1.5 million people are diagnosed with Parkinson's disease (47). Moreover, factors such as rising geriatric population and lifestyle-oriented diseases are positively affecting the market growth of tissue engineering. More than 900 million surgeries are performed

for bone reconstruction or replacement. Increasing cases of chronic diseases, road accidents, and trauma injuries are contributing to the growth of the development of tissue engineering (47). Among the various applications covered in the global tissue engineering market, orthopedics, musculoskeletal, and spine currently holds the highest 55 % revenue share in 2016 (48). Stryker Corporation, Medtronic Inc., Organogenesis Inc., Zimmer Biomet, Acelity, Acell Inc., Athersys Inc., Tissue Regenix, Group Plc, RTI surgical Inc., and ReproCell Inc., are some of the key players operating in this market (47–49).

I.4.1 Bone tissue engineering

For more than a century, efforts have been devoted to find materials with the appropriate characteristics for the restoration of bone tissue in humans. Constantly, new technologies are developed to improve these materials and provide surgeons with biomaterials that meet the most modern requirements in this field. It is necessary to understand the properties and functions of bone tissue in order to develop successful materials for bone tissue engineering.

Bone tissue is a heterogeneous natural material composed of an inorganic part, an organic matrix and water. Inorganic content of bone ranges from 30 to 98 % dry weight, but most of the bones have approximately 60–70 % of the total bone/dry weight, depending upon site, species and stage of development (50). In 1926, de Jong (51) found that X-ray diffraction patterns obtained from ground bone are similar to geologic hydroxyapatite [$Ca_5(PO_4)_3(OH)_2$]. The inorganic phase of bone tissue is commonly known as biological apatite. The main difference between them is the variety of substitutions and vacancies in the bone apatite nanocrystals, different Ca/P molar ratio and crystallinity (52) that result in different reabsorptions properties. Bone organic phase is formed mainly by a matrix of collagen type I (around 90 %), non-collagenous proteins (around 5 %), lipids (around 2 %) and water. Several families of non-collagenous proteins have been identified in the bone matrix: albumin, alpha 2-HS Glycoprotein, osteocalcin, fibronectin, proteoglycans, osteopontin, osteonectin, thrombospondins, alkaline phosphatase, among others (53). All these proteins are closely linked to collagen and fulfil important functions in matrix

organization, cell signaling, metabolism and mineralization. If noncollagenous proteins are extracted from the bone tissue, it cannot be re-mineralized (54). Lipids are fat soluble and plays an important function for cell, they surround the cell body and regulate the flux of signaling molecules and ions into and out of the cell (50). Water in our body has many functions and in the bone tissue is responsible for filling the pores, interacting with collagen fibrils and binding to mineral crystals.

Bone tissue is a complex organ and supports the living structures that give the body form and shape. Bones protect our vital organs and act as a reservoir for critical vitamins and nutrients, such as calcium, and also act as the levers and pivots that permit control for direction and range of movement (55). Bone tissue has an innate ability to remodel and regenerate itself and it is completely renewed every 10 years (56–58). The bone remodeling process is a homeostatic balance between bone deposition and bone resorption by osteoblasts and osteoclasts, respectively. The health and wellbeing of patients can be affected if serious complications occur during bone healing. When normal repair process becomes dysregulated or interrupted, or bone defects are too large, bone tissue unable to completely heal without external intervention (55). Large bone defects were originally defined as critical size defects (CSDs) and experimentally a 12-week healing period is acceptable (59,60). Several investigating models suggests that during the CSD healing processes only around 10 % of the defect is normally repaired in the studied period (no more than 12 weeks) (61).

In 2007, the "diamond concept" of bone tissue engineering was proposed and described by Giannoudis and collaborators, as a “standard tissue engineering approach to provide solutions for impaired fracture healing, bone restoration and regeneration”. This concept has become widely accepted and acknowledged in the field of bone tissue engineering (55,62,63).

Following the "diamond concept" (Figure I.5), to develop a functional bone graft substitute able to promote vascularization by bone tissue engineering, it is necessary to use a osteoconductive three-dimensional structure (scaffolds or matrix), usually composed by a natural or synthetic polymer loaded with bioactive molecules (such as

growth factors, among others) and osteoinductive materials (such as calcium phosphate biomaterials). Furthermore, they can also act as mechanical reinforcement to increase the mechanical properties. Mesenchymal stem cells (MSCs) and/or differentiated osteoblasts can also be used to enhance fracture healing in a number of in vitro and in vivo studies (55,62,63).

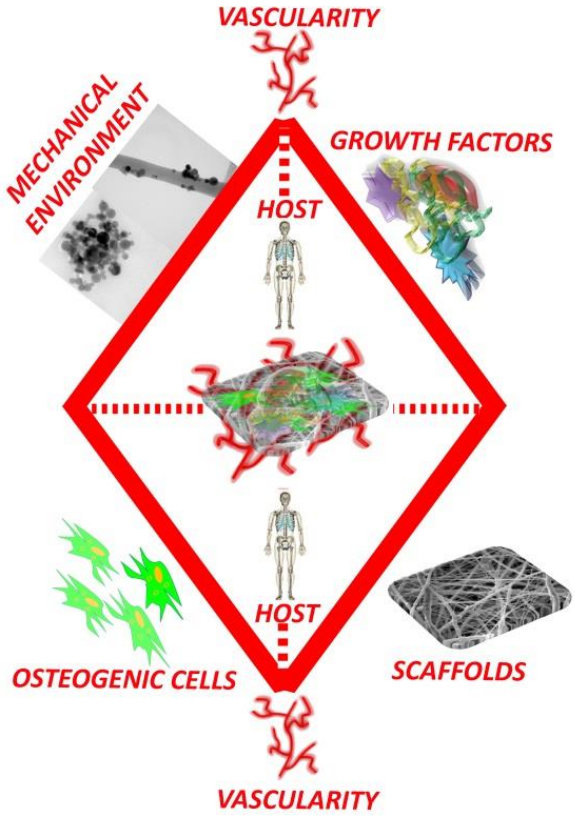

Figure I.5. Diamond model of bone fracture healing interactions. Modified from Giannoudis et al.(63)

The Department of Economic and Social Affairs (United Nations, Population Division) expects that people aged over 60 reach 2 billion worldwide in 2050 (64). This fact will bring an increase in the number of orthopedic surgeries, because this population is more prone to orthopedic ailments and the market is anticipated to witness a significant demand during the next 30 years. The global bone grafts and substitutes market is expected to reach around $4 billion by the period 2022-2025, registering a CAGR between 4 and 5% since 2015 (65–68).

Table I.9 shows some of the most successful commercially available bone tissue engineered scaffolds.

Table I.9. Some of the most successful commercially available bone tissue engineered products and its description.

Product	*Product description*	*Company*
Vertigraft® Allograft	Variety of structural allografts and an array of osteobiological properties, including, but not limited to, VG1 ALIF, VG2 PLIF, VG2 RAMP and VG2 TLIF.	DePuy Orthopaedics, Inc., Warsaw, IN, USA
Symphony® I/C Graft Chambers	Osteoinductive and osteoconductive product comprised of a mixture of allograft cancellous chips and DBM. Also contains naturally occurring cascade of BMP's and growth factors.	
Restore® Orthobiologic Soft Tissue Implant	Resorbable scaffold to reinforce weakened or damaged soft tissue repair including rotator cuff, patellar, Achilles, biceps, quadriceps and other tendons.	
Optium DBM® System	Includes both Optium DBM® Gel and Putty. Both contain osteoinductive and osteoconductive properties.	
Healos® Fx Injectable Bone Graft Replacement	An osteoconductive and easy to use bone graft replacement which provides a scaffold. It has potentially osteogenic properties when autologous bone marrow is added.	
Healos Bone Graft Replacement	Osteoconductive matrix comprised of cross-linked collagen fibers that are fully coated with hydroxyapatite. When combined with BMA, product provides an environment for osteoprogenitor cell attachment, proliferation, and differentiation.	
Conduit® TCP Granules	Osteoconductive synthetic porous ceramic graft material made of tricalcium phosphate which provides a scaffold for bone cell attachment.	
Infuse® bone graft	Solution containing rhBMP-2 and an ACS used to fill the LT-CAGE® lumbar tapered fusion device.	Medtronic Inc., Minneapolis, MN, USA

Table I.9. Continuation		
Actifuse	Silicate substituted calcium phosphate.	Baxter International Inc., Deerfield, IL, USA
Vitoss	Bioactive glass and calcium phosphate.	Orthovita Inc. Malvern, PA, USA
OP-1® Putty	rhBMP-7, Type I bovine collagen matrix and putty additive carboxymethylcellulose sodium.	Olympus Biotech, Hopkinton, MA, USA
OP-1 Implant	Osteoinductive and osteoconductive bone graft material consisting of collagen matrix, 1 g of Type I bovine collagen, 3.3 mg of rhBMP-7 and 2–3 cc of saline.	

I.4.1.1 Classifications of scaffolds in bone tissue engineering

Scaffolds used in bone tissue engineering must provide a stable mechanical environment and adequate degradation rate over a certain period of time in order to achieve optimal bone tissue ingrowth and regeneration. In 2013, Henkel and Hutmacher proposed a novel approach to design scaffolds-based bone tissue engineering (Figure I.6) (69).

Scaffolds designed for bone tissue engineering should provide a suitable microenvironment for the tissue regeneration capacity, promote the crucial steps in the organ maturation process and tissue remodeling (69). Scaffolds can be classified according to the nature of the material (metals, ceramic and polymer scaffolds with or without modifications). Polymeric scaffolds with modifications (addition of ceramics) are the most used in this field.

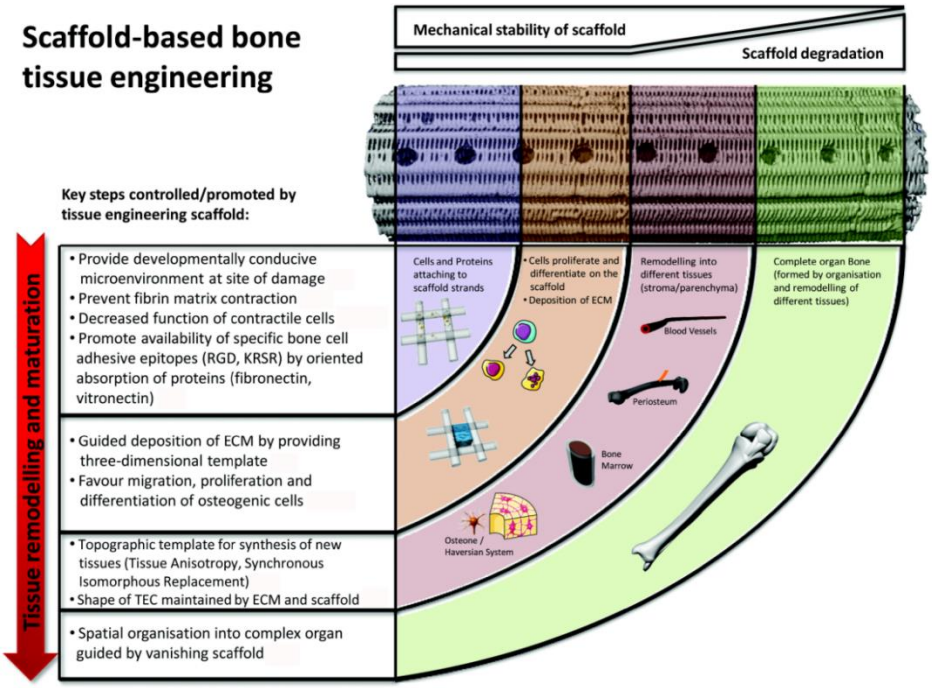

Figure I.6. Targeted design and application of scaffolds for bone tissue engineering. Images from Servier Medical Art, © 2013 SERVIER. All Rights Reserved (55,69).

I.4.1.1.1 Metallic scaffolds in bone tissue engineering.

Metallic scaffolds act more like permanent implants than scaffolding. Pure metals like iron, magnesium, titanium, tantalum, zirconium and niobium, and different alloys such as, chrome-cobalt, magnesium-calcium, iron-magnesium, titanium-aluminum-vanadium, nickel-titanium and stainless steel, have been used. Clinical applications as well as their advantages and disadvantages are discussed in I.***1.1.1 section***

I.4.1.1.2 Ceramic scaffolds in bone tissue engineering.

Bio-ceramics practically mimic the bone tissue and provide a higher osteoblasts adherence and proliferation because solubility and surface topography have a significant influence in cell behavior compared to other materials. Calcium phosphate ceramics such as hydroxyapatite, tricalcium phosphate, biphasic and amorphous calcium phosphates have been greatly studied for bone tissue repair in the form of scaffolding or in combination with polymers or metals.

I.4.1.1.3 Polymeric scaffolds in bone tissue engineering.

Several physiochemical characteristics (solubility, porosity, pore size, enzymatic reactions, biocompatibility and allergic response) are usually more controllable in polymeric materials used to design scaffolds. Natural polymer scaffolds could be tissue or cell derived that show osteoinductive properties. They are composed mainly by proteins (collagen, elastin, gelatin, keratin, fibrinogen and silk), polysaccharides (cellulose, glycosaminoglycans, amylose, chitin and dextran), polynucleotides (DNA, RNA) and extracellular matrix .

Table I.10. Most used polymeric scaffolds in bone repair. Modified from *Ghassemi et al* (70).

Name	***Mechanical Properties***	***Modifications***	***Advantages***
Synthetic polymers			
PLLA*	+++	HA incorporation to enhance cell growth.	- biocompatible - biodegradable - support cell adhesion
PGA*	+++	Alkaline hydrolysis for increasing cell replacement and cells biomaterials interaction improvement.	- biocompatible - biodegradable - support cell adhesion
PCL*	++	- High RGD concentration for increasing osteoblast attachment. - CNT addition for mechanical properties, BMSCs proliferation and differentiation enhancement.	- biodegradable
PLGA*	+	- HA incorporation for enhancing compressive strength. - Diamond nanoparticles incorporation for higher mechanical resistance. Incorporation of CNTs for higher rate of cell attachment, proliferation, and differentiation.	- biodegradable - support cell adhesion
PET*	+++	-	- highly biocompatible - biodegradable - impact resistance
PAG	+	-	- biocompatible
PAA*	+	-	- non-biodegradable

Table I.10. Continued			
PBT*	++	-	- highly biocompatible - biodegradable - impact resistance
PEG*	+	RGD peptides for facilitating cell adhesion and spreading.	- biocompatible - steering cells into scaffolds - osmotic effects in body
PVA	+++	CNT and CNF incorporation for higher concentration of ALP and mineralised matrix.	- Non-biodegradable - great resistance against organic solvents
PPF*	++	linked RGD peptides for osteoblast migration regulation.	- biocompatible - suitable physical properties and decomposition rate
PU	+	-	- variable degradability - injectable
Natural polymers			
Collagen (type I, II and III)	+	- mixing with calcium for mechanical integrity increase. - blending with PCL for mechanical improvement.	- biocompatible - degradable
Chitosan	-	Nanocrystalline hydroxyapatite and SWCNT incorporation for mechanically and cytocompatibility enhancement.	-
Chitin	+	-	- biocompatible - biodegradable
Alginate	+	Addition of HA, calcium phosphate cements, bioglass and other natural and synthetic polymers for upgrading cell adhesion and mechanical properties.	- biocompatible - degradable - minimally invasive manner (gel-forming) - ease of chemical modification with adhesion ligands and controlled release of tissue induction factors (e.g., BMP, TGF-β)

Mechanical properties: +++ good, ++ average, + poor

FDA approved: *

On the other hand, biocompatible and biodegradable synthetic polymers such as PCL, PLA and PGA have been the most utilized in bone tissue engineering for their excellent mechanical properties and its low cost of obtaining. But some polymers lose their compressive strength due to rapid degradation *in vivo* (poly(propylene fumarate), generating a local acidic environment which can cause adverse tissue responses. Table I.10 shows some of the most used polymeric scaffolds modified and their advantages.

I.5 Techniques to produce materials for biomedical applications

Biomaterials may be designed and fabricated using all kind of materials: polymers, ceramics and metals, as well as their combinations (71). In the literature, there are diverse methods to produce biomaterials for medical applications, specifically for wound dressing applications and bone tissue engineering (71–73). Salerno and Netti summarized some of them (Freeze drying, Particles sintering, Phase inversion, Solid freeform fabrication, Reverse templating, Spraying, Textiles, Emulsion, Gas foaming, Bioprinting, Microfluidic, Self-assembly) (71).

The design of an appropriate biomaterial depends not only on its specific medical application but also on the characteristics of the particular patient. It is very difficult to describe specific characteristics to take into account in such developments, but any device used should be able to maintain its functionality during all the accurate time without rejection and safely.

On the other hand, to prepare 3D porous scaffolds, the most used methods are fiber bonding, compression molding, extrusion, high internal phase emulsion templating, emulsion freeze drying, solvent casting/particulate leaching, high pressure processing, superstructure engineering, supercritical fluid processing, gas foaming/particulate leaching, thermally induced phase separation, electrospinning and rapid prototyping (46,74).

Electrospinning is a versatile, simple, scalable and cost-effective spinning technique to produce scaffolds or membranes in form of fibers with a random orientation or with a certain degree of alignment (Figure I.7). Currently, several natural (hyaluronic acid, collagen, alginate, cellulose, chitosan, gelatin, pullulan, zein,

silk fibroin) or synthetic (polyamide, polycaprolactone, polylactic acid, poly (lactic-co-glycolic acid), polyvinyl alcohol, polyurethane, poly (ethylene-co-vinil alcohol), polystyreneetc, etc.) (75,76) polymers are electrospun and the fibers obtained by these technique have been used in various applications such as tissue engineering scaffolds, wound dressing and in numerous biomedical applications (75–77).

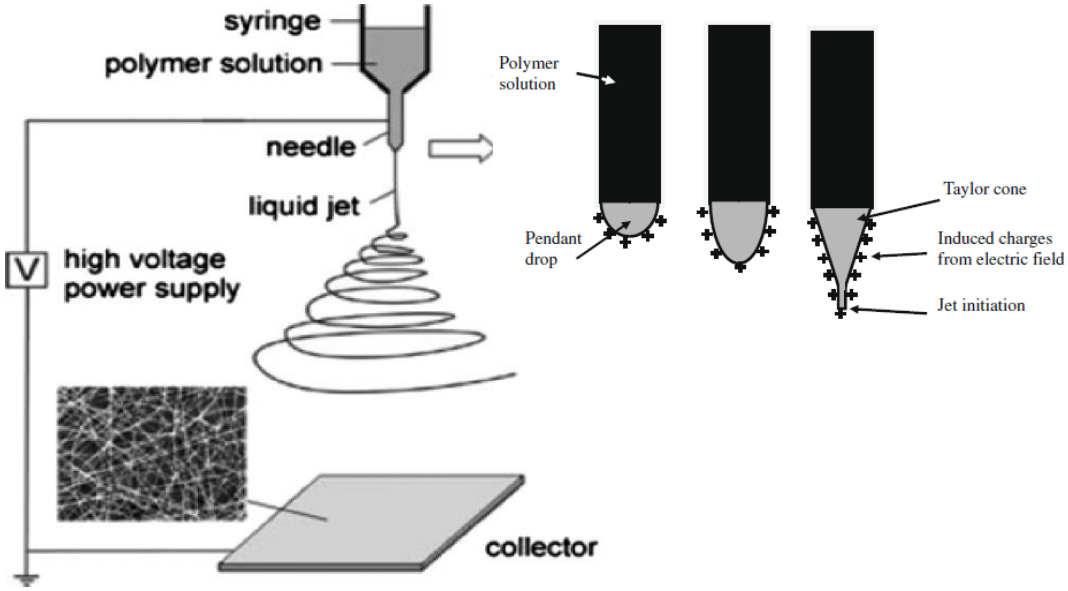

Figure. I.7. Schematic diagram of a typical vertical set up of electrospinning apparatus.

Electrospinning technique is governed by electrostatic forces to produce fibers with different diameters from nanometer to micrometer (76,77). To produce an electrospun material polymer solutions are pumped through a needle under an electric field generated by a voltage source. When the electric field applied to the needle reaches a critical value and the repulsive electrical forces overcome the surface tension forces, a Taylor cone is formed on the needle tip (Figure I.7) (76,78–81). Solvent evaporation of the polymers solution occurs between the needle tip and the collector, leaving a solid polymer in fiber form on the collector(76,77,82–86).

Several parameters must be taken into account to produce electrospun material, such as solution properties, process parameters, and environmental conditions

(76,86,87). All of them affect the process in a different way, Table I.11 summarizes these effects.

Table I.11. Effects and results of different parameters on electrospun morphology (76,83).

Parameters	Effect on fiber morphology	Results
Solution parameters		
Polymer concentration	Directly proportional.	Increase in polymer concentration produce an increase in fiber diameter.
Molecular weight (Mw) of polymer	Directly proportional.	Number of beads and droplets are reduced with high Mw.
Viscosity	Directly proportional. Viscosity, polymer concentration and Mw are strongly related.	Optimal viscosity range is needed to produce fibers.
Surface tension	It is not clear.	Instability of jets is obtained when surface tension is high.
Conductivity/surface charge density	Inversely proportional.	Decrease in conductivity induces an increase in fiber diameter.
Processing parameters		
Applied voltage	Inversely proportional.	Increase in voltage cause an decrease in fiber diameter.
Feed rate/Flow rate	Directly proportional.	A decrease in flow rate generates a decrease in fiber diameter. Particles can be obtained if the flow decreases considerably.
Tip to collector distance	A minimum distance is necessary to facilitate the solvent evaporation and produce homogeneous fibers.	Too large and too small distance can generate beads formation.
Ambient parameters		
Humidity	It must controlled	A high humidity can result in beads formations and small circular pores can appear on the surface of the fiber.
Temperature	Inversely proportional.	Increase in temperature cause a decrease in fiber diameter.

Scaffolds obtained by electrospinning for bone tissue engineering have received a special attention, due to its high porosity (> 90 % porosity) and its similarities with the structure and morphology of the native ECM (85). A successful delivery of differentiation and proliferation factors (growth factors, such as, BMP-2 and BMP7) (88) with the electrospun structures composed by biodegradable polymer filled or impregnated with calcium phosphate could solve the exigency of bone tissue engineering (89).

On the other hand, electrospun membranes have shown a great capability for wound dressing due to the extremely high surface area, allowing adjustment of the wound moisture. The electrospun materials preserve the wound from bacterial infections due to their small pore size. The high porosity allows a good exchange of oxygen and water vapor (75–77,82–88,90–94).In the electrospinning process, it is also possible to load antibiotics and antimicrobial agents to obtain controlled delivery systems of one or multiple bioactive factors (20,76,88,94–99). Furthermore, these systems have the potential to be used as wound dressing materials, bone tissue engineering scaffolds, augmentation devices, and antimicrobial filters (29,30,34,37,75,100,101).

Micro and/or nanoparticles can be obtained by electrospraying technique, using the same equipment and governed by the same principle of electrospinning (87,88). Loaded and unloaded particles can be obtained in a single step process by electrospraying without the use of any surfactant (87,93,102,103). For this purpose, the polymer solution should fulfill certain characteristics related to flow rate, polymer concentration, viscosity, and polymer molecular weight Mw. On the other hand, the use of highly volatile solvents together with the appropriate needle-collector distance could help the particles synthesis(93,103–105). Particles obtained by electrospray have a higher encapsulate ion efficiency compared with other particles production technique (88,103).

Electrospinning/Electrosprayed techniques allow obtaining The polymer solution can incorporate more than just one polymer and also other materials such as

drugs, biomolecules, essential oils or inorganic particles (dissolved or dispersed) with the objective to obtain an adequate material for a specific application (88). With only one needle it is possible to obtain an appropriate scaffold or membrane for bone tissue engineering or wound dressing. The use of coaxial or triaxial needles also the simultaneous use of both techniques allows design very specific materials with core/shell structures for biomedical applications (17,20,46,75–77,83–85,87,88,90,93,94,96–98,105–129,129–136).

References

1. Bergmann CP, Stumpf A. Biomaterials. In: Bergmann CP, editor. Dental Ceramics Microstructure, Properties and Degradation. Springer-Verlag Berlin Heidelberg; 2013. p. 84.

2. Davis JS. Skin transplantation with a review of 550 cases at the Johns Hopkins hospital. Johns Hopkins Med J. 1910;15:307–96.

3. Hacker MC, Krieghoff J, Mikos AG. Synthetic Polymers. In: Atala A, Lanza R, Nerem R, Mikos AG, editors. Principles of Regenerative Medicine. Third. Academic Press; 2019. p. 559–90.

4. Von Recum AF, Laberge M. Educational goals for biomaterials science and engeneering: perspective view. J Appl Biomater. 1995;6:137–44.

5. Biomaterials Market by Type of Materials (Metallic, Ceramic, Polymers, Natural) & Application (Cardiovascular, Orthopedic, Dental, Plastic Surgery, Wound Healing, Neurology, Tissue Engineering, Ophthalmology) - Global Forecast to 2021 [Internet]. MarketsandMarkets. 2016 [cited 2018 Jul 24]. Available from: https://www.marketsandmarkets.com/Market-Reports/biomaterials-393.html?gclid=CjwKCAjwspHaBRBFEiwA0eM3kXnsj7wpCUj3UMF-4SfNYz4shf_LOBeDjvto5uJAFl11Y5V0po5FNBoC_RUQAvD_BwE

6. Ducheyne P. Comprehensive Biomaterials II. 2nd ed. Ducheyne P, editor. Elsevier; 2017. 4858 p.

7. Chen Q, Thouas GA. Metallic implant biomaterials. Mater Sci Eng R Reports. Elsevier B.V.; 2015;87:1–57.

8. Staiger MP, Pietak AM, Huadmai J, Dias G. Magnesium and its alloys as orthopedic biomaterials: A review. Biomaterials. 2006;27(9):1728–34.

9. Hench LL, Best SM. Ceramics, Glasses, and Glass-Ceramics: Basic Principles. In:

Ratner B, Hoffman AS, Schoen FJ, Lemons JE, editors. Biomaterials Science : An introduction to materials in medicine. Third. Academic Press; 2013. p. 128–51.

10. Huang J, Best S. Ceramic biomaterials for tissue engineering. In: Baccaccini AR, Ma PX, editors. Tissue Engineering Using Ceramics and Polymers. Second. Woodhead Publishing; 2014. p. 3–34.

11. Sáenz A, Rivera-Muñoz E, Brostow W, Castaño VM. Ceramic biomaterials: An introductory overview. J Mater Educ. 1999;21(5–6):297–306.

12. Heath DE, Cooper SL. POLYMERS: BASIC PRINCIPLES. In: Ratner B, Hoffman AS, Schoen FJ, Lemons JE, editors. Biomaterials science : an introduction to materials in medicine. Third. Academic Press; 2013. p. 64–111.

13. Teo AJT, Mishra A, Park I, Kim YJ, Park WT, Yoon YJ. Polymeric Biomaterials for Medical Implants and Devices. ACS Biomater Sci Eng. 2016;2(4):454–72.

14. Love B. Polymeric Biomaterials. In: Love B, editor. Biomaterials. Academic Press; 2017. p. 205–38.

15. He W, Benson R. Polymeric Biomaterials. In: Ebnesajjad S, editor. Plastics Design Library Handbook of Biopolymers and Biodegradable Plastics: Properties, Processing and Applications. William Andrew; 2013. p. 87–107.

16. Dubruel P, Van Vlierberghe S. Biomaterials for Bone Regeneration. Novel Techniques and Applications. Dubruel P, Van Vlierberghe S, editors. Woodhead Publishing; 2014. 502 p.

17. Boccaccini AR, Ma PX. Tissue Engineering Using Ceramics and Polymers. Second. Boccaccini AR, Ma PX, editors. Woodhead Publishing; 2014. 728 p.

18. Williams DF. The Williams Dictionary of Biomaterials. Williams DF, editor. Liverpool University Press; 1999. 343 p.

19. Migliaresi C. COMPOSITES. In: Ratner BD, Hoffman AS, Schoen FJ, Lemons JE,

editors. Biomaterials Science An Introduction to Materials in Medicine. Third. Academic Press; 2013. p. 223–41.

20. Lühmann TC, Meinel L, Groll J, Dalton PD. 4.29 Electrospun Fibers for Drug Delivery ☆. In: Ducheyne P, editor. Comprehensive Biomaterials II. 2nd ed. Elsevier Ltd.; 2017. p. 527–48.

21. Kohrs NJ, Liyanage T, Venkatesan N, Najarzadeh A, Puleo DA. Drug Delivery Systems and Controlled Release. In: Narayan R, editor. Encyclopedia of Biomedical Engineering. Elsevier Inc.; 2019. p. 316–29.

22. Brannon-Peppas L. Biomaterials: Polymers in controlled drug delivery. Medical Plastics and Biomaterials Magazine [Internet]. 1997; Available from: https://www.mddionline.com/polymers-controlled-drug-delivery

23. Robinson JR, Lee VHL. Controlled drug delivery: Fundamentals and applications. Second. Robinson JR, Lee VHL, editors. New York: CRC Press; 1987. 744 p.

24. Boateng JS, Matthews KH, Stevens HNE, Eccleston GM. Wound healing dressings and drug delivery systems: A review. J Pharm Sci. 2008;97(8):2892–923.

25. Abdal-Hay A, Hamdy AS, Khalil KA, Lim JH. A novel simple one-step air jet spinning approach for deposition of poly(vinyl acetate)/hydroxyapatite composite nanofibers on Ti implants. Mater Sci Eng C. 2015;49:681–90.

26. Abdal-Hay A, Hamdy AS, Khalil KA, Lim JH. A novel simple one-step air jet spinning approach for deposition of poly(vinyl acetate)/hydroxyapatite composite nanofibers on Ti implants. Mater Sci Eng C. 2015;49:681–90.

27. Paul W, Sharma CP. The Anatomy and Functions of Skin. In: Paul W, Sharma CP, editors. Advances in Wound Healing Materials : Science and Skin Engineering. Smithers Rapra Technology Ltd; 2015. p. 25–34.

28. Han S-K. Basics of Wound Healing. In: Han S-K, editor. Innovations and

Advances in Wound Healing. Second Edi. Berlin, Heidelberg: Springer Berlin Heidelberg; 2016. p. 1–38.

29. Paul W, Sharma CP. Classification of Wound Dressing Products. In: Paul W, Sharma CP, editors. Advances in Wound Healing Materials : Science and Skin Engineering. Smithers Rapra Technology Ltd; 2015. p. 49–60.

30. Dhivya S, Padma VV, Santhini E. Wound dressings – a review. BioMedicine. 2015;5(4):24–8.

31. Longaker MT, Gurtner GC, Werner S, Barrandon Y. Wound repair and regeneration. Nature. 2008;453(7193):314–21.

32. FDA. FDA Executive Summary: Classification of Wound Dressings Combined with Drugs. 2016;83. Available from: https://www.fda.gov/downloads/AdvisoryCommittees/CommitteesMeetingMaterials/MedicalDevices/MedicalDevicesAdvisoryCommittee/GeneralandPlasticSurgeryDevicesPanel/UCM518494.pdf

33. Montagn W, Parakkal PF. An Introduction to Skin. In: Montagn W, Parakkal PF, editors. THE STRUCTURE AND FUNCTION OF SKIN. Third Edit. New York and London: Academic Press; 1974. p. 1–17.

34. Wound Dressings Market by Type (Advanced Wound Dressings, Traditional Wound Dressings), Application (Surgical Wounds, Ulcers, Burns), End User (Inpatient Facilities, Outpatient Facilities) - Global Forecast to 2021 [Internet]. MarketsandMarkets. 2016 [cited 2018 Jul 24]. Available from: https://www.marketsandmarkets.com/Market-Reports/wound-dressings-market-123903496.html

35. Wound Management, Forecast 2016 to 2026. Report #S254 [Internet]. MedMarket Diligence, LLC. 2018 [cited 2018 Jul 27]. Available from: http://mediligence.com/s254/

36. Paul W, Sharma CP. Wound Management – An Introduction to Wound Healing. In: Advances in Wound Healing Materials : Science and Skin Engineering. Smithers Rapra Technology Ltd; 2015. p. 1–14.

37. Han S-K. Interactive Wound Dressings. In: Han S-K, editor. Innovations and Advances in Wound Healing. Second Edi. Berlin, Heidelberg: Springer Berlin Heidelberg; 2016. p. 39–62.

38. Chern PL, Baum CL, Arpey CJ. Biologic dressings: Current applications and limitations in dermatologic surgery. Dermatologic Surg. 2009;35(6):891–906.

39. Langer R, Vacanti JP. Tissue Engineering. Sience. 1993;260(May):920–6.

40. Santos Jr. AR, de Carvalho Zavaglia CA. Tissue Engineering Concepts. Ref Modul Mater Sci Mater Eng Elsevier,. 2016;1–5.

41. Santos ARJ, Lombello CB, Genari SC. Technologies Applied to Stimulate Bone Regeneration. In: Davies J, editor. Tissue Regeneration From Basic Biology to Clinical Application. IntechOpen; 2012. p. 339–66.

42. Chiu LLY, Chu Z, Radisic M, Mozafari M. Tissue Engineering. Ref Modul Mater Sci Mater Eng. 2017;2:1–31.

43. Vacanti CA. The history of tissue engineering. J Cell Mol Med. 2006;10(3):569–76.

44. Anderson JM. Biocompatibility and the Relationship to Standards: Meaning and Scope of Biomaterials Testing. In: Comprehensive Biomaterials. Elsevier; 2011. p. 7–26.

45. Spector M. 4.1 The Concept of Biocompatibility. In: Comprehensive Biomaterials II. 2017. p. 1–6.

46. Singh M, Kasper FK, Mikos AG. Tissue Engineering Scaffolds. In: Ratner B, Hoffman A, Schoen F, Lemons J, editors. Biomaterials Science: An Introduction

to Materials: Third Edition. Third Edit. Academic Press; 2013. p. 1138–59.

47. Tissue Engineering Market Size, Share & Trends Analysis Report By Application (Cord Blood & Cell Banking, Cancer, GI & Gynecology, Dental, Skin/Integumentary, Orthopedics), And Segment Forecasts, 2018 - 2025 [Internet]. Grand View Research. 2018 [cited 2018 Aug 7]. Available from: https://www.grandviewresearch.com/industry-analysis/tissue-engineering-and-regeneration-industry/methodology

48. Global Tissue Engineering Market Forecasts, 2017-2025 [Internet]. Bizwit Research. 2018 [cited 2018 Aug 7]. Available from: http://www.orbisresearch.com/reports/index/global-tissue-engineering-market-forecasts-2017-2025

49. Global Tissue Engineering Market by Manufacturers, Regions, Type and Application, Forecast to 2023 [Internet]. Global Info Research. 2018 [cited 2018 Aug 7]. p. 149. Available from: http://www.orbisresearch.com/reports/index/global-tissue-engineering-market-by-manufacturers-regions-type-and-application-forecast-to-2023

50. Boskey AL. Bone composition: relationship to bone fragility and antiosteoporotic drug effects. Bonekey Rep. Nature Publishing Group; 2013;2(September):1–11.

51. de Jong WF. La substance minérale dans les os. Recl des Trav Chim des Pays-Bas. 1926;45(6):445–8.

52. Young RA. Biological Apatite vs Hydroxyapatite at the Atomic Level. Clin Orthop Relat Res. 1975;113:249–62.

53. Young MF. Bone matrix proteins: their function, regulation, and relationship to osteoporosis. Osteoporos Int. 2003;14(S3):35–42.

54. Boskey AL. Mineralization of Bones and Teeth. Elements. 2007;3(6):385–91.

55. Baldwin J, Henkel J, Hutmacher DW. 6.3 Engineering the Organ Bone. In: Ducheyne P, editor. Comprehensive Biomaterials II. 2nd ed. Elsevier Ltd.; 2017. p. 54–74.

56. Spruyt D, Gillet C, Rasschaert J. Bone and Bone Marrow; Interactions. In: Huhtaniemi I, Martini L, editors. Reference Module in Biomedical Sciences. second. Academic Press; 2019. p. 31–9.

57. Clarke B. Normal bone anatomy and physiology. Clin J Am Soc Nephrol. 2008;3 Suppl 3:131–9.

58. Bartl R, Frisch B. Biology of Bone. In: Osteoporosis. second. Springer, Berlin, Heidelberg; 2009. p. 7–28.

59. Schmitz JP, Hollinger JO. The Critical Size Defect as an Experimental Model for Craniomandibulofacial Nonunions. Clin Orthop Relat Res. 1986;205:299–308.

60. Boyan BD, Cohen DJ, Schwartz Z. 7.17 Bone Tissue Grafting and Tissue Engineering Concepts ☆. In: Ducheyne P, editor. Comprehensive Biomaterials II. 2nd ed. Elsevier Ltd.; 2017. p. 298–313.

61. Cowan CM, Soo C, Ting K, Wu B. Evolving Concepts in Bone Tissue Engineering. Curr Top Dev Biol. 2005;66:239–85.

62. Giannoudis P V., Einhorn TA, Marsh D. Fracture healing: The diamond concept. Injury. 2007;38(Supplement 4):3–6.

63. Giannoudis P V., Einhorn TA, Schmidmaier G, Marsh D. The diamond concept - open questions. Injury. 2008;39(Supplement 2):5–8.

64. Bone Grafts and Substitutes Market Size, Share & Trends Analysis Report By Material Type (Natural, Synthetic), By Application Type (Spinal Fusion, Craniomaxillofacial, Long Bone), By Region, And Segment Forecasts, 2018 - 2025 [Internet]. Grand View Research, Inc. 2018 [cited 2018 Aug 10]. p. 87.

Available from: https://www.grandviewresearch.com/industry-analysis/bone-grafts-substitutes-market

65. Global Bone Grafts and Substitutes Market Analysis & Trends - Industry Forecast to 2025 [Internet]. Research and Markets. 2017 [cited 2018 Aug 10]. p. 173. Available from: https://www.researchandmarkets.com/reports/4039804/global-bone-grafts-and-substitutes-market#rela3-992759

66. Bone Graft and Substitutes - Global Market Outlook (2016-2022) [Internet]. Research and Markets. 2017 [cited 2018 Aug 10]. Available from: https://www.researchandmarkets.com/reports/4335734/bone-graft-and-substitutes-global-market#rela3-4039804

67. Global Bone Graft and Substitute Market Insights, Opportunity, Analysis, Market Shares And Forecast 2017 – 2023 [Internet]. Research and Markets. 2017 [cited 2018 Aug 10]. p. 140. Available from: https://www.researchandmarkets.com/reports/4263768/global-bone-graft-and-substitute-market-insights#relb1-4039804

68. Bone Grafts and Substitutes Market by Product (Allografts, Bone Grafts Substitutes, and Cell-based Matrices), by Application (Spinal Fusion, Long Bone, Foot & Ankle, Craniomaxillofacial, Joint Reconstruction, and Dental Bone Grafting) - Global Opportunity [Internet]. Allied Market Research. 2016 [cited 2018 Aug 10]. p. 130. Available from: https://www.alliedmarketresearch.com/bone-graft-substitutes-market

69. Henkel J, Hutmacher DW. Design and fabrication of scaffold-based tissue engineering. BioNanoMaterials. 2013;14(3–4):171–93.

70. Ghassemi T, Shahroodi A, Ebrahimzadeh MH, Mousavian A, Movaffagh J, Moradi A. Current Concepts in Scaffolding for Bone Tissue Engineering. Arch bone Jt Surg. 2018;6(2):90–9.

71. Salerno A, Netti PA. 1 – Introduction to biomedical foams. In: Netti PA, editor. Biomedical Foams for Tissue Engineering Applications. Woodhead Publishing; 2014. p. 3–39.

72. Picheth GF, Pirich CL, Sierakowski MR, Woehl MA, Sakakibara CN, de Souza CF, et al. Bacterial cellulose in biomedical applications: A review. Int J Biol Macromol. Elsevier B.V.; 2017;104:97–106.

73. Aragon J, Navascues N, Mendoza G, Irusta S. Laser-treated electrospun fibers loaded with nano-hydroxyapatite for bone tissue engineering. Int J Pharm. 2017;525(1):112–22.

74. Aramwit P. 1 – Introduction to biomaterials for wound healing. Wound Healing Biomaterials. Elsevier Ltd; 2016. 3-38 p.

75. Miguel SP, Figueira DR, Simões D, Ribeiro MP, Coutinho P, Ferreira P, et al. Electrospun polymeric nanofibres as wound dressings: A review. Colloids and Surfaces B: Biointerfaces. Elsevier; 2018. p. 60–71.

76. Bhardwaj N, Kundu SC. Electrospinning: A fascinating fiber fabrication technique. Biotechnol Adv. 2010;28(3):325–47.

77. Uyar T, Kny E. Electrospun Materials for Tissue Engineering and Biomedical Applications: Research, Design and Commercialization. Electrospun Materials for Tissue Engineering and Biomedical Applications: Research, Design and Commercialization. 2017.

78. Doshi J, Reneker DH. Electrospinning Process and Applications of Electrospun Fibers Jayesh. J Electrostat. 1995;35:151–60.

79. Formhals A. Process and apparatus for preparing artificial threads. US1975504, 1934.

80. Zeleny J. The Electrical Discharge from Liquid Points, and a Hydrostatic Method of Measuring the Electric Intensity at Their Surfaces. Phys Rev. American

Physical Society; 1914 Feb;3(2):69–91.

81. Taylor GI. Electrically driven jets. Proc R Soc London A Math Phys Eng Sci. 1969 Dec 2;313(1515):453–75.

82. Stocco TD, Bassous NJ, Zhao S, Granato AEC, Webster TJ, Lobo AO. Nanofibrous scaffolds for biomedical applications. Nanoscale [Internet]. 2018;10(26):12228–55. Available from: http://xlink.rsc.org/?DOI=C8NR02002G

83. Ramakrishna S, Fujihara K, Teo W-E, Lim T-C, Ma Z. An introduction to Electrospinning and Nanofibers. Ramakrishna S, Fujihara K, Teo W-E, Lim T-C, Ma Z, editors. World Scientific Publishing Co. Pte. Ltd.; 2005. 382 p.

84. Bosworth LA, Downes S. Electrospinning for Tissue Regeneration [Internet]. 1 Edition. Bosworth LA, Downes S, editors. Electrospinning for Tissue Regeneration. Woodhead Pub; 2011. 409 p. Available from: http://www.sciencedirect.com/science/article/pii/B9781845697419500094

85. Min Ju Y, Lee J, Jin Lee S, Xu W. Tissue Engineering Scaffolding Using Electrospinning. In: Neves NM, editor. Electrospinning for Advanced Biomedical Applications and Therapies. Smithers Rapra Technology; 2012. p. 89–134.

86. Doshi J, Reneker DH. Electrospinning process and applications of electrospun fibers. J Electrostat. Elsevier; 1995 Aug 1;35(2–3):151–60.

87. Soares RMD, Siqueira NM, Prabhakaram MP, Ramakrishna S. Electrospinning and electrospray of bio-based and natural polymers for biomaterials development. Mater Sci Eng C. Elsevier; 2018 Nov 1;92:969–82.

88. Wang M, Zhao Q. Electrospinning and Electrospray for Biomedical Applications. Encycl Biomed Eng. Elsevier; 2019 Jan 1;330–44.

89. Aragón J, Salerno S, Bartolo L De, Irusta S, Mendoza G. Polymeric electrospun scaffolds for bone morphogenetic protein 2 delivery in bone tissue engineering.

J Colloid Interface Sci. 2018;

90. Stanger J, Tucker N, Staiger M. Report 190. Electrospinning. Smithers Rapra Technology; 2005.

91. Ramakrishna S, Fujihara K, Teo W, Yong T, Ramaseshan R. Electrospun nanofibers: solving global issues. Mater Today. 2006;9(3):40–50.

92. Ramakrishna S, Fujihara K, Teo W-E, Yong T, Ma Z, Ramaseshan R. Electrospun nanofibers: solving global issues. Mater Today. Elsevier; 2006 Mar 1;9(3):40–50.

93. Zamani M, Prabhakaran MP, Ramakrishna S. Advances in drug delivery via electrospun and electrosprayed nanomaterials. Int J Nanomedicine. Dove Press; 2013 Aug 9;8(1):2997–3017.

94. Wang L, Ryan AJ. Introduction to electrospinning. In: Bosworth LA, Downes S, editors. Electrospinning for tissue regeneration. Woodhead Pub; 2011. p. 1–33.

95. El-Naggar ME, Abdelgawad AM, Salas C, Rojas OJ. Curdlan in fibers as carriers of tetracycline hydrochloride: Controlled release and antibacterial activity. Carbohydr Polym. Elsevier Ltd.; 2016;154:194–203.

96. Huang ZM, He CL, Yang A, Zhang Y, Han XJ, Yin J, et al. Encapsulating drugs in biodegradable ultrafine fibers through co-axial electrospinning. J Biomed Mater Res - Part A. 2006;77(1):169–79.

97. Ulubayram K, Calamak S, Shahbazi R, Eroglu I. Nanofibers Based Antibacterial Drug Design, Delivery and Applications. Curr Pharm Des. 2015;21(15):1930–43.

98. Ali M, Yang F, Jansen J. Smart Drug Delivery Systems for Tissue Engineering. In: Wang Q, editor. Smart Materials for Tissue Engineering: Applications. The Royal Society of Chemistry; 2017. p. 505–28.

99. Gaikwad V V., Patil AB, Gaikwad M V. Scaffolds for drug delivery in tissue

engineering. Int J Pharm Sci Nanotechnol. 2008;1(2):113–22.

100. Han SK. Innovations and Advances in Wound Healing. 2 Edition. Innovations and Advances in Wound Healing. Springer-Verlag Berlin Heidelberg; 2015. 1-38 p.

101. Paul W, Sharma CP. Wound-healing Dressings and Drug Delivery. In: Advances in Wound Healing Materials : Science and Skin Engineering. Smithers Rapra Technology Ltd; 2015. p. 81–102.

102. Gao Y, Zhao D, Chang MW, Ahmad Z, Li X, Suo H, et al. Morphology control of electrosprayed core-shell particles via collection media variation. Mater Lett. North-Holland; 2015 May 1;146:59–64.

103. Bock N, Dargaville TR, Woodruff MA. Electrospraying of polymers with therapeutic molecules : state of the art. Prog Polym Sci. Elsevier; 2012;37(11):1510–51.

104. Hao S, Wang Y, Wang B, Deng J, Zhu L, Cao Y. Formulation of porous poly(lactic-co-glycolic acid) microparticles by electrospray deposition method for controlled drug release. Mater Sci Eng C. 2014;39(1):113–9.

105. Luo CJ, Edirisinghe M. Core-liquid-induced transition from coaxial electrospray to electrospinning of low-viscosity poly(lactide- co -glycolide) sheath solution. Macromolecules. 2014;47(22):7930–8.

106. Song W, Yu X, Markel DC, Shi T, Ren W. Coaxial PCL/PVA electrospun nanofibers: Osseointegration enhancer and controlled drug release device. Biofabrication. 2013;5(3).

107. Li J, Feng H, He J, Li C, Mao X, Xie D, et al. Coaxial electrospun zein nanofibrous membrane for sustained release. J Biomater Sci Polym Ed. 2013;24(17):1923–34.

108. Raheja A, Chandra TS, Natarajan TS. Design of a low cost spinneret assembly for

coaxial electrospinning. Appl Phys Lett. 2015;106(August 2016):254101.

109. Wei QL, Xu FY, Xu XJ, Geng X, Ye L, Zhang AY, et al. The multifunctional wound dressing with core-shell structured fibers prepared by coaxial electrospinning. Front Mater Sci. 2016;10(2):113–21.

110. Zhang L, Si T, Fischer AJ, Letson A, Yuan S, Roberts CJ, et al. Coaxial Electrospray of Ranibizumab-Loaded Microparticles for Sustained Release of Anti-VEGF Therapies. Jablonski MM, editor. PLoS One. Public Library of Science; 2015 Aug;10(8):e0135608.

111. Song W, Yu X, Markel DC, Shi T, Ren W. Coaxial PCL/PVA electrospun nanofibers: Osseointegration enhancer and controlled drug release device. Biofabrication. 2013 Sep;5(3):35006.

112. Song W, Yu X, Markel DC, Shi T, Ren W. Coaxial PCL/PVA electrospun nanofibers: osseointegration enhancer and controlled drug release device. Biofabrication. 2013 Sep;5(3):35006.

113. Wang Y, Wei Y, Zhang X, Xu M, Liu F, Ma Q, et al. PLGA/PDLLA core shell submicron spheres sequential release system: Preparation, characterization and promotion of bone regeneration in vitro and in vivo. Chem Eng J. 2015;273:490–501.

114. Aragon J, Navascues N, Mendoza G, Irusta S. Laser-treated electrospun fibers loaded with nano-hydroxyapatite for bone tissue engineering. Int J Pharm. 2017 Jun;525(1):112–22.

115. Yang JC, Lee SY, Tseng WC, Shu YC, Lu JC, Shie HS, et al. Formation of highly aligned, single-layered, hollow fibrous assemblies and the fabrication of large pieces of PLLA membranes. Macromol Mater Eng. 2012;297(2):115–22.

116. Ribeiro N, Sousa SR, Van Blitterswijk CA, Moroni L, Monteiro FJ. A biocomposite of collagen nanofibers and nanohydroxyapatite for bone regeneration.

Biofabrication. IOP Publishing; 2014;6(3).

117. Paletta JRJ, Mack F, Schenderlein H, Theisen C, Schmitt J, Wendorff JH, et al. Incorporation of osteoblasts (MG63) into 3D nanofibre matrices by simultaneous electrospinning and spraying in bone tissue engineering. Eur Cells Mater. 2011;21:384–95.

118. Pilehvar-Soltanahmadi Y, Akbarzadeh A, Moazzez-Lalaklo N, Zarghami N. An update on clinical applications of electrospun nanofibers for skin bioengineering. Artif cells, nanomedicine, Biotechnol. 2015;(January):1–15.

119. Murray E, Thompson BC, Sayyar S, Wallace GG. Enzymatic degradation of graphene/polycaprolactone materials for tissue engineering. Polym Degrad Stab. Elsevier Ltd; 2015;111:71–7.

120. Sridhar R, Lakshminarayanan R, Madhaiyan K, Amutha Barathi V, Lim KHC, Ramakrishna S. Electrosprayed nanoparticles and electrospun nanofibers based on natural materials: applications in tissue regeneration, drug delivery and pharmaceuticals. Chem Soc Rev. Royal Society of Chemistry; 2015;44(3):790–814.

121. Puhl S, Ilko D, Li L, Holzgrabe U, Meinel L, Germershaus O. Protein release from electrospun nonwovens: Improving the release characteristics through rational combination of polyester blend matrices with polidocanol. Int J Pharm. Elsevier B.V.; 2014;477(1–2):273–81.

122. Ambrosio L. Biomedical composites. Ambrosio L, editor. Woodhead Publishing; 2010. 648 p.

123. Wendorff JH, Agarwal S, Greiner A. Electrospinning Materials, Processing, and Applications. Wendorff JH, Agarwal S, Greiner A, editors. Wiley-VCH Verlag GmbH & Co. KGaA; 2012. 254 p.

124. Andreu V, Mendoza G, Arruebo M, Irusta S. Smart dressings based on

nanostructured fibers containing natural origin antimicrobial, anti-inflammatory, and regenerative compounds. Materials (Basel). 2015;8(8):5154–93.

125. Unnithan AR, Gnanasekaran G, Sathishkumar Y, Lee YS, Kim CS. Electrospun antibacterial polyurethane-cellulose acetate-zein composite mats for wound dressing. Carbohydr Polym. Elsevier Ltd.; 2014;102(1):884–92.

126. Hung WC, Lin LH, Tsen WC, Shie HS, Chiu HL, Yang TCK, et al. Permeation of biological compounds through porous poly(l-lactic acid) (PLLA) microtube array membranes (MTAMs). Eur Polym J. Elsevier Ltd; 2015;67:166–73.

127. Ou KL, Chen CS, Lin LH, Lu JC, Shu YC, Tseng WC, et al. Membranes of epitaxial-like packed, super aligned electrospun micron hollow poly(l-lactic acid) (PLLA) fibers. Eur Polym J. Elsevier Ltd; 2011;47(5):882–92.

128. Sarhan WA, Azzazy HME, El-Sherbiny IM. The effect of increasing honey concentration on the properties of the honey/polyvinyl alcohol/chitosan nanofibers. Mater Sci Eng C. Elsevier B.V.; 2016;67:276–84.

129. Alhusein N, Blagbrough IS, de Bank PA. Zein/polycaprolactone electrospun matrices for localised controlled delivery of tetracycline. Drug Deliv Transl Res. 2013;3(6):542–50.

130. Guarino V, Altobelli R, Cirillo V, Cummaro A, Ambrosio L. Additive electrospraying: A route to process electrospun scaffolds for controlled molecular release. Polym Adv Technol. 2015;26(12):1359–69.

131. Prabhakaran MP, Ghasemi-Mobarakeh L, Ramakrishna S. Electrospun Composite Nanofibers for Tissue Regeneration. J Nanosci Nanotechnol. 2011;11(4):3039–57.

132. Bosworth LA, Downes S. Electrospinning for tissue regeneration. Bosworth LA, Downes S, editors. Woodhead Pub; 2011. 409 p.

133. Kim TG, Lee DS, Park TG. Controlled protein release from electrospun biodegradable fiber mesh composed of poly(??-caprolactone) and poly(ethylene oxide). Int J Pharm. 2007;338(1–2):276–83.

134. Biomedical Textiles for Orthopaedic and Surgical Applications.

135. Lin J, Li C, Zhao Y, Hu J, Zhang LM. Co-electrospun nanofibrous membranes of collagen and zein for wound healing. ACS Appl Mater Interfaces. 2012;4(2):1050–7.

136. Allen-Hoffmann BL, Rooney PJ. Skin Tissue Engineering and Regenerative Medicine. In: Albanna MZ, Holmes IV JH, editors. Skin Tissue Engineering and Regenerative Medicine. Academic Press; 2016. p. 265–87.

CHAPTER II

Composite scaffold obtained by electro-hydrodynamic technique for infection prevention and treatment in bone repair

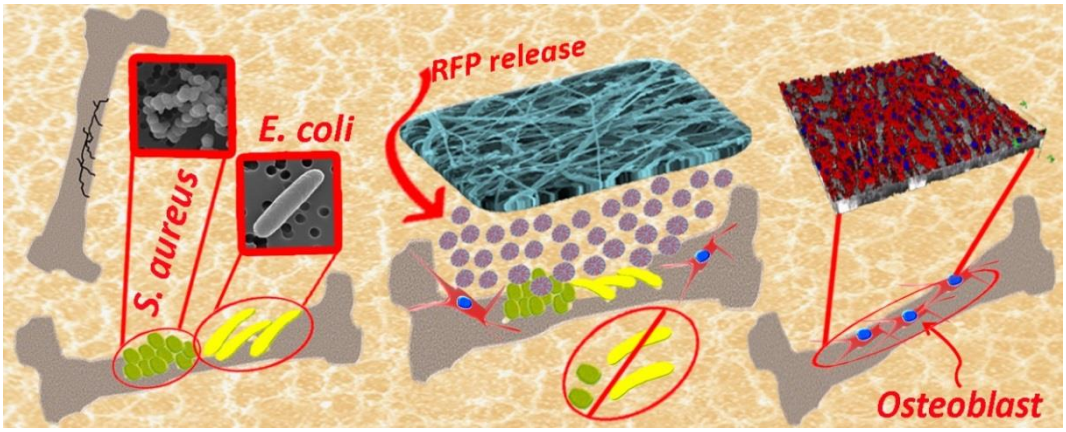

The contents of this chapter have been adapted from the following submitted work (under review):

Composite scaffold obtained by electro-hydrodynamic technique for infection prevention and treatment in bone repair. Javier Aragón, Sergio Feoli, Silvia Irusta, Gracia Mendoza. **International Journal of Pharmaceutics** (Ms. Ref. No.: IJP-D-18-01794)

"Bone infection is a devastating condition after implant or orthopedic surgery. Its therapeutic approach is extremely complicated and may imply serious side-effects or even disabilities. The development of enhanced 3D scaffolds, able to promote efficient bone regeneration together with targeted antibiotic release to prevent bacteria colonization, appears as a promising tool for the successful repair of bone defects. Herein, polymeric electrospun scaffolds composed of polycaprolactone (PCL) nanofibers decorated with poly(lactic-coglicolic acid) (PLGA) particles loading rifampicin were fabricated to obtain a local and sustained drug release for a more efficient prevention of infection. The release profile showed an initial burst of rifampicin at the first six hours, enabling the complete elimination of bacteria. Then, a sustained and long-term release was observed until the end of the experiments (28 days), facilitating a prolonged effect on the inhibition of bacteria growth, consistent with the acidic degradation of the microparticles. In addition, bactericidal effects against Gram negative (Escherichia coli) and Gram positive (Staphylococcus aureus) bacteria were demonstrated at concentrations of released rifampicin after 24 h up to 58 ppm, being more effective against S. aureus (13 ppm vs 58 ppm for E. coli). Cell morphology and cytocompatibility studies highlighted the suitability of the fabricated scaffolds to support cell growth, as well as their promising clinical application for bone regeneration combined with the prevention or treatment of bacterial infection."

CHAPTER III

Laser-treated electrospun fibers loaded with nano-hydroxyapatite for bone tissue engineering.

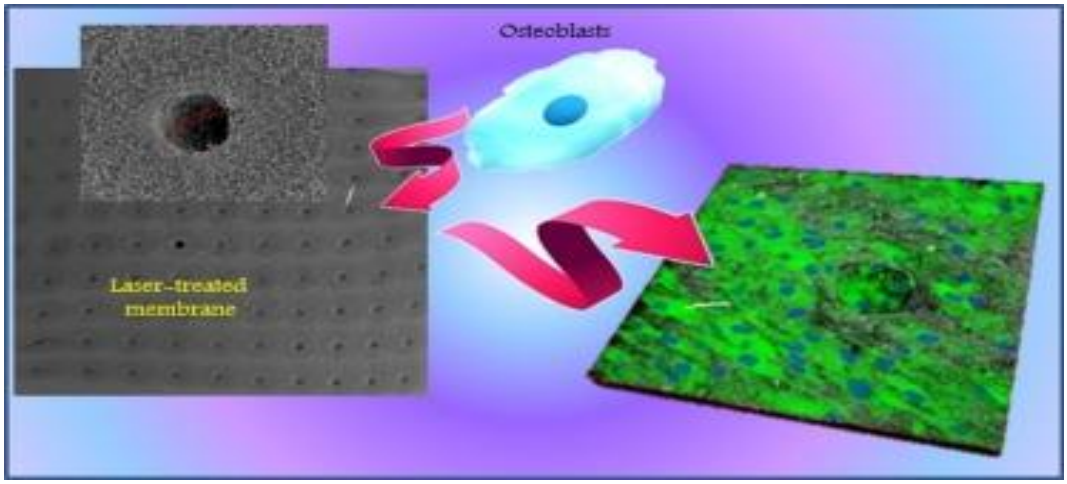

The contents of this chapter have been adapted from the following published work:

Laser-treated electrospun fibers loaded with nano-hydroxyapatite for bone tissue engineering. Javier Aragon, Nuria Navascues, Gracia Mendoza, Silvia Irusta. International Journal of Pharmaceutics 525,112–122, 2017.
DOI:10.1016/j.ijpharm.2017.04.022

"Core-shell polycaprolactone/polycaprolactone (PCL/PCL) and polycaprolactone/polyvinyl acetate (PCL/PVAc) electrospun fibers loaded with synthesized nanohydroxyapatite (HAn) were lased treated to create microporosity. The prepared materials were characterized by XRD, FTIR, TEM and SEM. Uniform and randomly oriented beadless fibrous structures were obtained in all cases. Fibers diameters were in the 150–300 nm range. Needle-like HAn nanoparticles with mean diameters of 20 nm and length of approximately 150 nm were mostly encase inside the fibers. Laser treated materials present micropores with diameters in the range 70–120 μm for PCL-HAn/PCL fibers and in the 50–90 μm range for PCL-HAn/PVAC material. Only samples containing HAn presented bioactivity after incubation during 30 days in simulated body fluid. All scaffolds presented high viability, very low mortality, and human osteoblast proliferation. Biocompatibility was increased by laser treatment due to the surface and porosity modification."

III.1 Introduction

Scaffolds are specially designed biomaterials that provide a support for cell growth, migration and finally proliferation to allow tissue regeneration (1). In order to satisfy the required adhesion and proliferation of cells geometric factors are of great importance (2). The matrix architecture is vital for the success of bone tissue engineering which includes microstructure of scaffold, its porosity percentage and surface topography (3). Polymer nanofibers obtained by electrospinning mimic the bone extracellular matrix structure and the potential to enhance the osseointegration is very promising (4). They also exhibit high surface area to volume ratios favorable for cells and bioactive molecules attachment to the fibers surface. However, the small pore size of electrospun scaffolds hinders cell infiltration and ultimately reduces their use in replacing large tissues that require ample vascularization and nutrient diffusion (5). To promote cellular viability and extracellular matrix production, electrospun scaffolds with enhanced porosity or micro-scale pores could be beneficial since increasing porosity and pore size can provide a three-dimensional (3D) environment that not only facilitates cell seeding/diffusion but also provides better diffusion of nutrients and waste throughout the scaffolds (6).

Different techniques were studied to obtain electrospun materials with larger pores or higher porosity. Among them the addition of porogens during electrospinning and the posterior elimination by leaching was used (7). Collection in liquid increases the pore size but the fabrication is highly dependent on the surface tension, flow rate and weight fraction of the polymer solution (8). Another promising technique to improve electrospun materials porosity is the surface modification by laser technologies for scaffold microstructuring. Laser has become an invaluable tool in processing and treating biological tissues due to its possibility of precise material processing with clean surfaces and reduced thermal damage. Pulsed laser ablation is a well-established universal tool for direct surface modification of almost all type of materials. Ultra-short laser pulses (picosecond and femtosecond) enable to obtain 3D microstructures with high precision, taking advantage of the “cold” ablation process (9). It was demonstrated that laser

machining is an efficient technique to prepare patterning structures in electrospun polycaprolactone (PCL) membranes (10,11). It was found that electrospun poly(l-lactide) scaffolds with laser ablated holes exhibit significant better endothelial cell ingrowth (5). McCullen et al. (12) used laser ablation on electrospun PCL scaffolds to favour the adhesion and growth of human adipose-derived stem cells. Electrospun PCL/β-TCP fibers were also treated by laser irradiation to obtain microsized pores (13). Beside the meaningful cellular activity the material showed enhanced compressive strength.

Naturally occurring polymers are well suited for various *in vivo* applications, promoting cell adhesion and growth. However, scaffolds fabricated from these polymers could exhibit poor mechanical properties or fast degradation rates. Native proteins, such as collagen and fibrinogen, are also more expensive and more difficult to source than synthetic polymers (14). Among the synthetic available polymer used to fabricate three-dimensional (3D) scaffolds aliphatic polyesters undoubtedly represent so far the most extensive studied class, since they combine good physico-chemical and mechanical properties with assessed biocompatibility (15). Particularly PCL is a low cost, biocompatible polymer that has a slow degradation rate and distinct rheological and viscoelastic properties that make it suitable for specific long term implantation (14). Its compatibility with a wide range of drugs enables uniform drug distribution in the matrix and its long term degradation facilitates drug release up to several months (16). Polyvinyl acetate (PVAc) polymer has also been applied in many medical fields because of its strong biocompatibility. The hydrogels containing functional groups such as COOH usually show good biocompatibility with blood, body fluids, and tissues (17). This inert polymer has the advantage that it does not induce a deleterious reaction in living tissue (18). Because of all these characteristics PVAc has been used in many medical fields, including drug and cell carries and in tissue engineering (19).

One important limitation in the use of synthetic biodegradable polymers as scaffold materials is the lack of bioactivity, in particular for bone tissue applications (20). The main approach to develop bioresorbable and bioactive scaffolds is the addition of bioactive materials to the polymer matrix. Calcium

phosphate ceramics have been extensively investigated to fabricate highly porous scaffolds to engineer bone due to their near similar composition of bone, including excellent biocompatibility, osteoinductive and osteoconductive properties (3). It has been found that the addition of hydroxyapatite (HA) not only enhances the tensile strength of PCL scaffolds but also acts as a chelating agent to accelerate the mineralization of human fetal osteoblast cells to form bone-like apatite for bone tissue engineering (21).

Objective

The main objective of this work was to obtain a material with appropriate matrix architecture to favor cells adhesion and proliferation composed of biodegradable polymers, with mechanical resistance, good biocompatibility and high bioactivity. PCL/PVAc and PCL/PCL membranes with core-shell structure loaded with synthetic hydroxyapatite nanoparticles (HAn) to increase the bioactivity of the materials were obtained by electrospinning. In addition, the membranes obtained were treated by laser ablation to create desired microscale topographical features in order to favor cell adhesion and growth.

III.2 Synthesis of inorganic nanoparticles and electrospun scaffolds

III.2.1 Synthesis of hydroxyapatite nanoparticles

Synthesis of HA ($Ca_{10}(PO_4)_6(OH)_2$) nanoparticles was conducted as previously described (22). $CaCO_3$ was used as calcium sources, maintaining a Ca/P ratio of 1.67 during reaction in solution with 0.3 M H3PO4.

III.2.2 Preparation of electrospun scaffolds

Electrospun scaffolds were prepared using an Yflow 2.2.D-500 electrospinner (Coaxial Electrospinning Machines/R&D Microencapsulation, Malaga, Spain). PCL pellets were dissolved in DCM/DMF (1:1) and PVAc was dissolved in DMF, these solutions were stirred overnight at room temperature. To prepare PCL-HAn scaffolds, HAn powder was dispersed in DCM/DMF with the help of TWEEN® 80 by stirring overnight at room temperature, then this solution was added to the PCL solution and stirred overnight at room temperature. The polymers solutions were

loaded into 20 mL plastic syringes. The PCL-HAn suspension was fed through the inner needle of the coaxial system and PCL or PVAc solutions were fed through the outer one. This last needle was connected to the positive voltage power supply, at a voltage ranging from 7 to 13 kV. The shell and core flow rates and the spinning distance were fixed to 0.5 mL/h (in both needles) and 19 cm respectively. The spun fibers were collected on a static plate (covered with aluminum foil) connected to negative voltage power supply, at a voltage ranging from −2 to 4 kV for 18 h. To create macropores in the fibrous membrane structures, a pulse Nd:YAG laser (TECHNOLOGY Q-Switch) was used. Different conditions were used for each material: output power: 16 W, wavelength: 1064 nm for the PCL-HAn/PCL fibers and output power: 1 W, wavelength: 532 nm for PCL-HAn/PVAc fibers.

The characterization techniques and different evaluation methods are described in **Appendix 1**.

III.3 Results and discussion

III.3.1 Hydroxyapatite characterization

The XRD pattern for the synthesized HA nanoparticles is shown in Figure III.1a, it could be seen that all the peaks could be indexed to the hexagonal phase hydroxyapatite (JCPDS N° 09-0432). The diffractogram do not show any other peaks corresponding to secondary phases or intermediate compounds suggesting the formation of pure HAn phase. Intense diffraction peaks with broad width are indicative of the crystalline nature of the prepared material and the small crystallite size respectively (23). Inset of Figure III.1a shows the peaks corresponding to the (002) and (211) diffraction planes of hydroxyapatite. According to the JCPDS card 09-0432, the reference intensity ratio for (211), (002) is RI(211)/RI(002) = 2.61. The calculated degree of texture index (24) for the synthesized hydroxyapatite is 0.51 indicating a preferred growth orientation along the c-axis (25). These results are consistent with electronic microscope images (Figure III.1b and III.1c), which show fibrous needle-like particles with mean diameters of 20 nm and length of approximately 150 nm. The rod-like shape of the nanoparticles is more clearly seen in TEM images (Figure III.1c). The FTIR spectrum (Figure III.1.d) of the material presents the characteristic bands for PO_4^{3-}

appearing at 472, 572 and 603 cm^{-1} related to the asymmetric bending, and signals assigned to symmetric and asymmetric stretching positioned in the 900-1200 cm^{-1} range (26). The broad peak around 3455 cm^{-1} is due to the adsorbed water on HAn structure and the absorption peak at 1635 cm^{-1} is attributed to the bending mode of OH^- groups (27). The absorption peak assigned to apatite hydroxyl bond is observed at 3569 cm^{-1} (28). The shoulder at 878 cm^{-1} together with the doublet at 1415 and 1458 cm^{-1} indicate the existence of CO_3^{2-} (29) probably coming from the atmosphere carbon dioxide during sample preparation and would have been incorporated into the HAn crystal structure (30). All these results imply that the synthesis of rod-like shaped hydroxyapatite nanoparticles was successful.

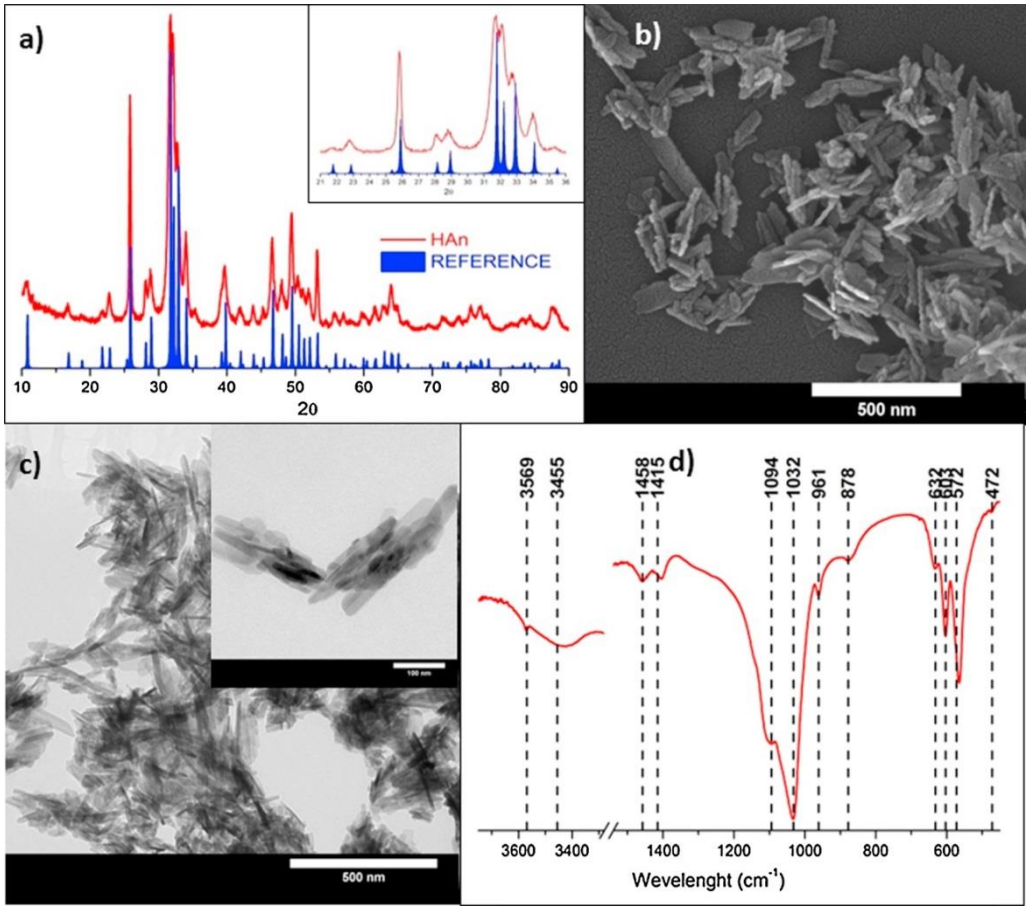

Figure III.1. Characterization of the synthesized HAn: a) XRD, b) SEM images, c) TEM micrographs, d) FTIR spectrum.

III.3.2 Scaffolds characterization

III.3.2.1 As spun scaffolds

The materials prepared by electrospinning are listed in Table III.1 together with positive and negative voltages applied. Due to the properties (viscosity, surface tension, conductivity) of the solutions the voltages required to obtain a stable Taylor cone were higher to produce fibers containing hydroxyapatite than the voltages used for the pristine polymer fibers (Table III.1).

Table III.1. Preparations conditions and characterization results for the obtained electrospun scaffolds.

	Sample (Core/Shell)			
	PCL/PCL	**PCL-HAn/PCL**	**PCL/PVA**	**PCL-HAn/PVAc**
Applied voltage -/+ (kv)	3.11/10.25	3.54/12.00	2.87/7.21	3.03/8.57
HAn load[a] (wt%)	-	(14.2) (13.8)	-	(11.9) (12.7)
Fiber diameter[b] (nm)	206±62	210±64	264±56	225±47
Porosity (%)	62.0	63.5	65.5	58.6
Pores diameter (nm)	232	210	209	188

[a] From TGA results, theoretical value between brackets.
[b] Obtained by measuring at least 100 fibers in different SEM images.

The HAn load in the fibers was measured by thermogravimetric analysis (TGA, Figure III.2) as the residue after complete polymers elimination at 600 °C (Table III.1). The experimental values of 13.8 and 12.7 wt% for PCL-HAn/PCL and PCL-HAn/PVAC respectively, were close to the theoretical ones (13.2 and 11.9 wt%). The HAn load used was the maximum possible to obtain a stable Taylor cone; higher amount of nanoparticles in the spinning solution increase excessively the viscosity and also hinder good nanoparticles dispersion.

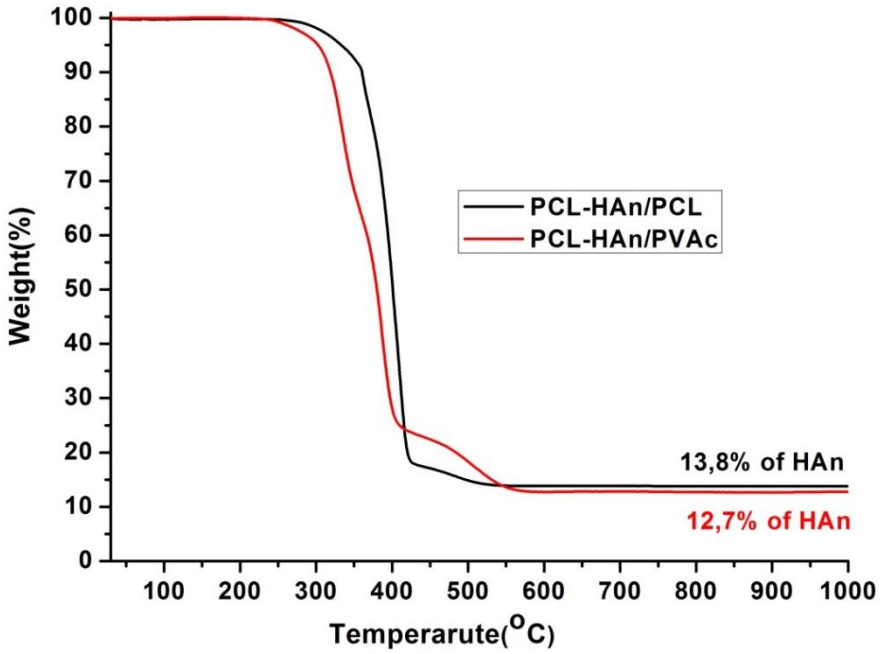

Figure III.2. TGA thermogram of PCL-HAn/PCL and PCL-HAn/PVAc fibers.

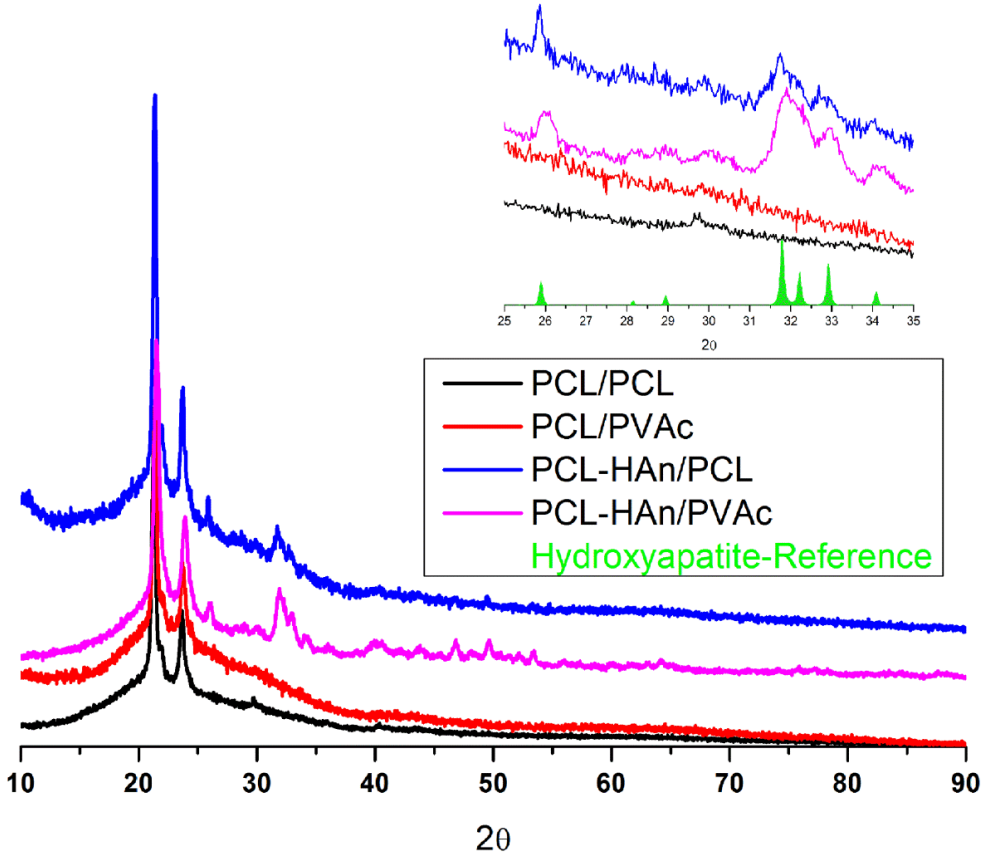

Figure III.3. XRD patterns of PCL/PCL, PCL/PVAc, PCL-HAn/PCL and PCL-HAn/PVAc fibers.

XRD patterns of fibers with HAn are shown in Figure III.3. The XRD diffractgram of PCL-Han/PCL has peaks for both hydroxyapatite and PCL. Both the polymer and ceramic retain their crystalline behavior in the electrospun fibers indicating insignificant change in their crystal structure. This confirms the fact that HAn is finely and uniformly dispersed in the matrix (3). In PCL-HAn/PVAc pattern peaks at 25 and 35° establish the presence of hydroxyapatite incorporated in the scaffold (inset of Figure III.3).

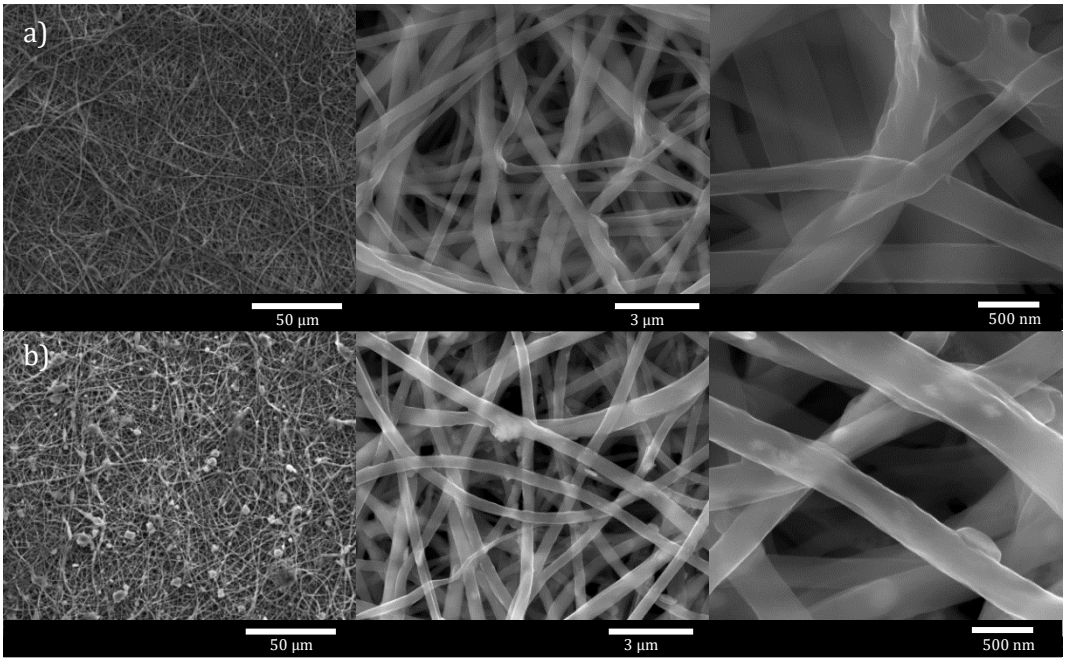

Figure III.4. SEM images of a) PCL/PCL fiber, b) PCL-HAn/PCL fibers.

FE-SEM images of the electrospun scaffolds showed uniform, beadless and nano-scaled fibrous structures randomly oriented for all the prepared materials under the optimum spinning conditions utilized in each case. As an example Figure III.4a) shows SEM micrographs obtained for fibers with PCL in the core and in the shell. Hydroxyapatite nanoparticles are mostly encased inside the fibers, but some agglomerates are observed on the surface (Figure III.4b). The fibers average diameter was measured from SEM images (Table III.1). The presence of hydroxyapatite nanoparticles in the inner solution does not seem to have any effect on the PCL/PCL fiber diameter. It was previously observed for PCL fiber without defects, such as the obtained in this work, that for HA load higher than 5 wt% the average diameter was similar to the pristine fibers (31). This result for

high mass fraction was attributed to the increased viscosity of the dispersion during electrospinning. For the PCL/PVAc material the presence of hydroxyapatite leads to a slightly lower fibers mean diameter, probably due to the higher voltage needed to obtain a stable cone in the case of the hydroxyapatite loaded fibers (32).

The core-shell structure of the PCL/PVAc fibers was investigated by TEM microscopy as shown in Figure III.5a. The PVAc polymer (the transparent part of the outside structure of the fiber) is the shell wrapping uniformly the PCL fiber (the darker part of the inside structure of the fiber) as the core. A TEM micrograph of a PCL/PCL fiber was added in the inset for comparison purpose, as expected core and shell are indistinguishable in this case. The distribution of the HA nanoparticles inside fibers can be observed in Figure III.5b, as mentioned before most of the particles are encapsulated into the polymers.

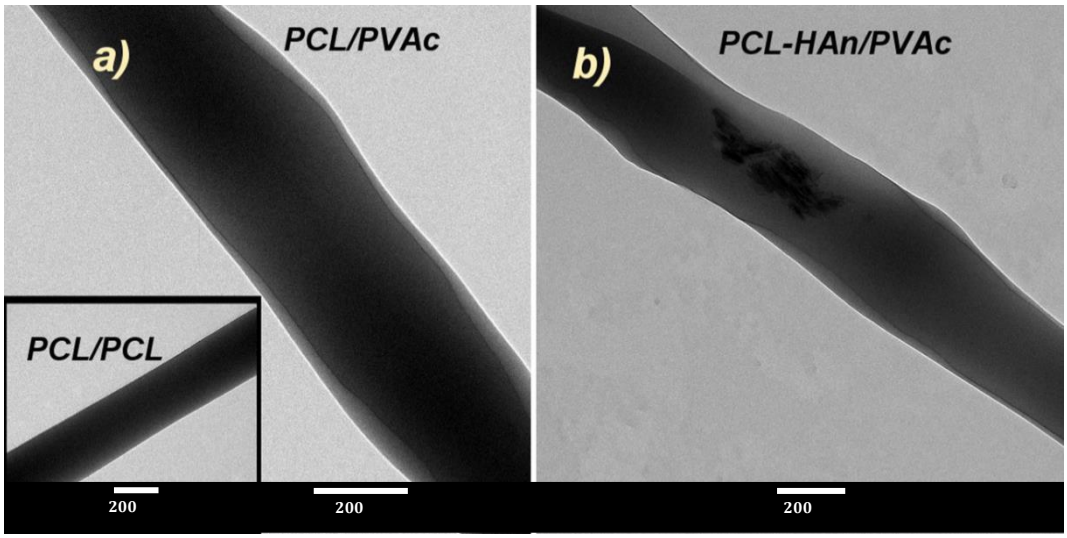

Figure III.5. TEM images of a) PCL/PVAc fiber, inset PCL/PCL fiber, b) PCL-HAn/PVAc fiber.

III.3.2.1 Laser treated scaffolds

After laser irradiation the scaffolds were analyzed by SEM microscopy (Figure III.6). For both materials the laser energy was not sufficient to machine a hole through the electrospun fibers. The images show that the membrane was not significantly affected outside the laser irradiation area. Figure III.6a shows SEM

images of PCL-HAn/PCL ablated scaffolds, the micropores were well obtained with diameters in the range 70–120 µm. It is important to observe the morphology of the remaining fibers since the aim is to improve the porosity without any additional effect (33). Even when some melting and coalescence of the fibers can be observed around the drilled holes, the surface morphology is only slightly changed. For PCL-HAn/PVAC on the other hand, the pores diameter are in the 50–90 µm range and the change in the fibers morphology around the holes is more important. Besides, in this material not all the holes of the rectangular pattern were produced under irradiation. As mentioned in the experimental section different laser were used in order to get the pores in each material.

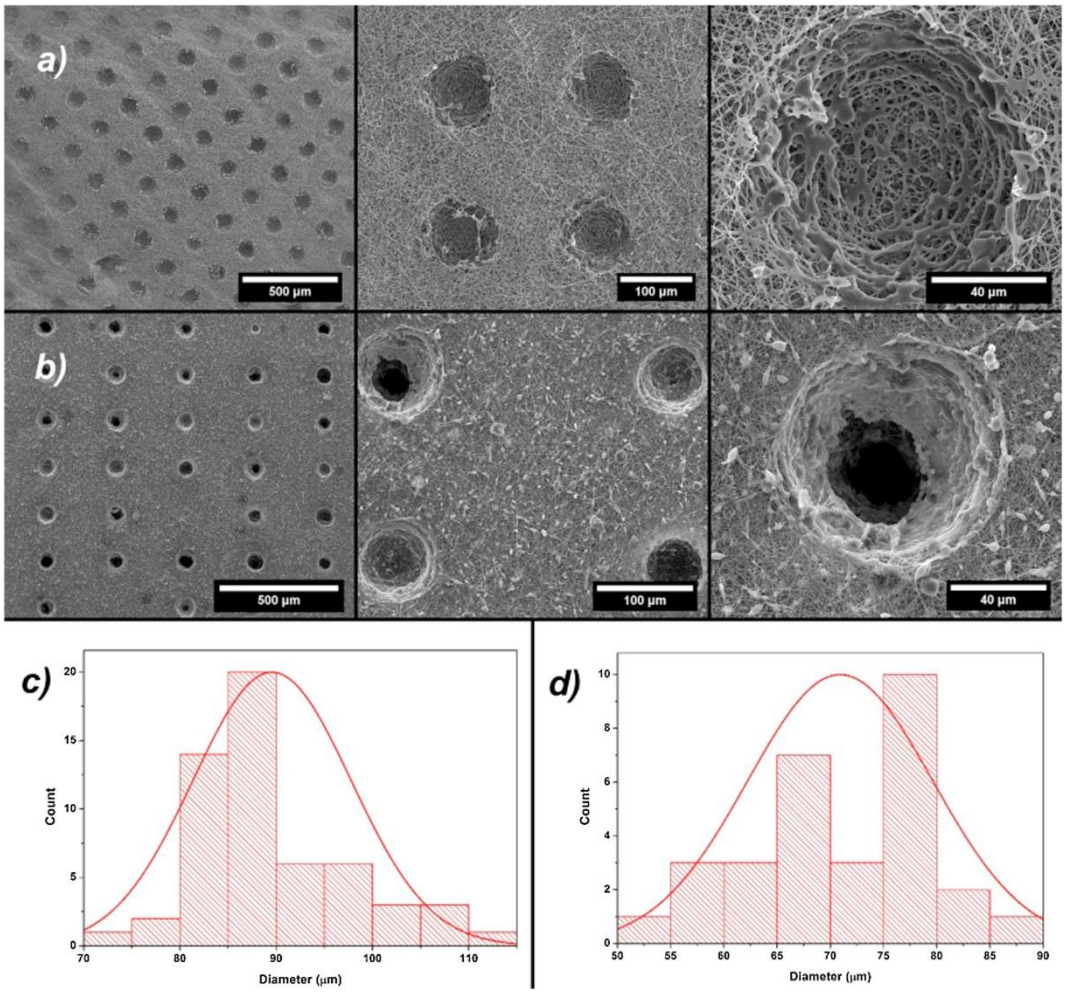

Figure III.6. SEM images and pore size distribution of laser treated a) and c) PCL-HAn/PCL and b) and d) PCL-HAn/PVAc.

III.3.3 *In vitro* bioactivity

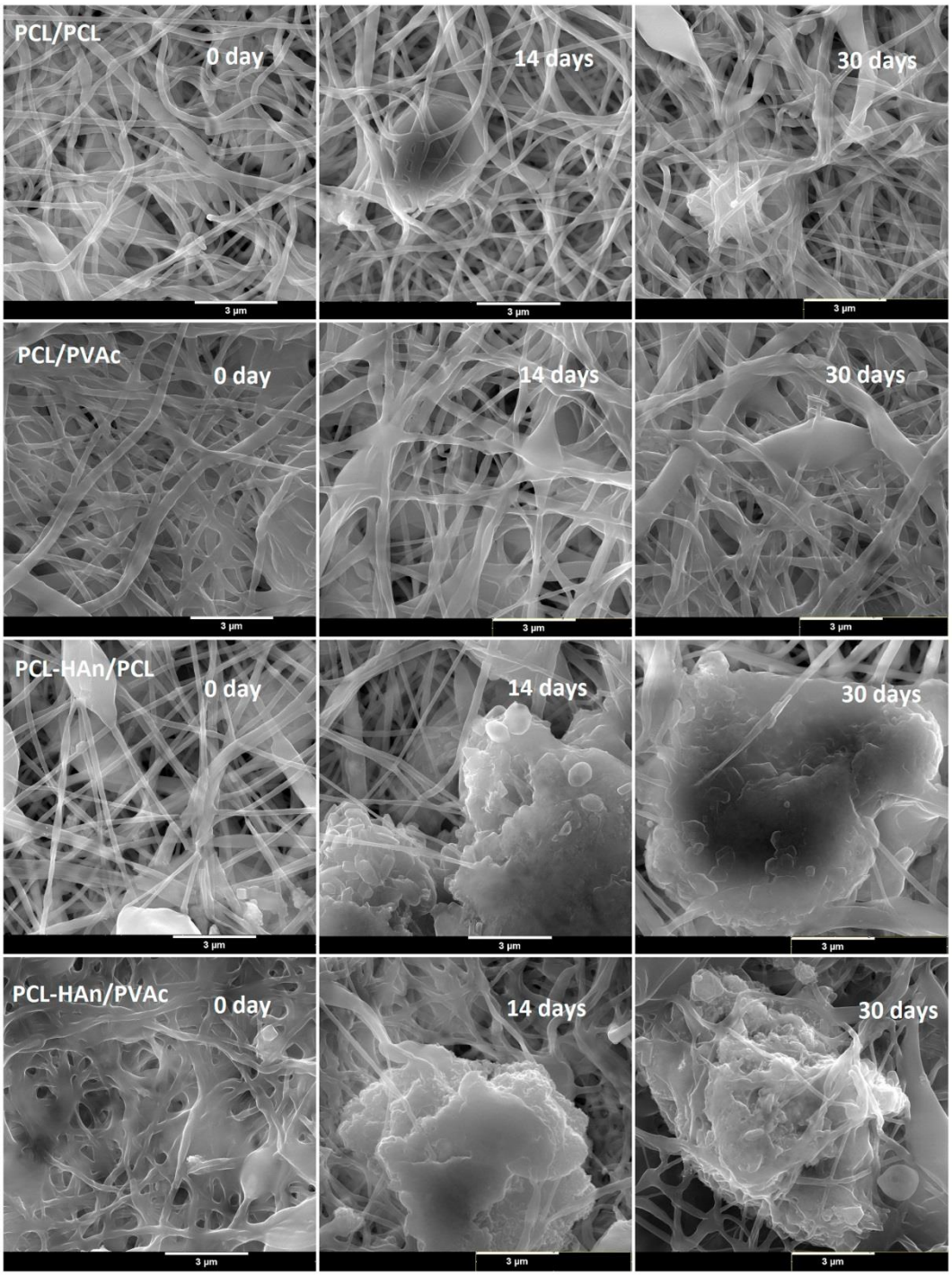

Figure III.7. SEM images of the prepared materials after immersion in SBF solution during different times.

Biomineralization method was used in order to evaluate bone binding ability of the prepared materials. The apatite formation was monitored using the fibers pad before the laser treatment since the most important factor for the bioactivity of materials is the surface nature of fibers (34). Figure III.7 shows SEM images of both kind of fibers unloaded and hydroxyapatite loaded having been soaked in SBF for various times. Hydroxyapatite precipitation can be observed after incubation during 14 and 30 days only in samples containing HAn. The apatite form aggregates that reach size of more than 3 μm. The nanoparticles on the surface of fibers would act as nucleation sites in SBF, thus the presence of HAn is necessary for the apatite formation on the nanofiber surface. Fibers with PVAc shell suffer some structural change due to the poor water resistance of the polymer (35), but they still exhibited a well interconnected pore network structure, which is necessary for mineral deposition and cellular in-growth. Characteristic peaks of calcium, phosphorous and oxygen, the main components of hydroxyapatite in EDX analysis (not shown) confirm the nature of the deposited aggregates. From these analyses Ca/P atomic ratios were 1.6 for PCL-HAn/PCL and 1.7 for PCL-HAn/PVAc.

III.3.4 *In vitro* cell morphology and viability

Human osteoblasts seeded onto the different types of scaffolds fabricated were evaluated regarding their morphology and proliferation until 14 days in order to assess their potential as bone regeneration scaffolds. SEM micrographs (Figure III.8) showed cell adhesion to all the scaffolds and a normal morphology of cells which are homogenously distributed on the surface and with a clear higher cell density after 14 days especially in the scaffolds containing PVAc pointing to a good biocompatibility of the prepared materials.

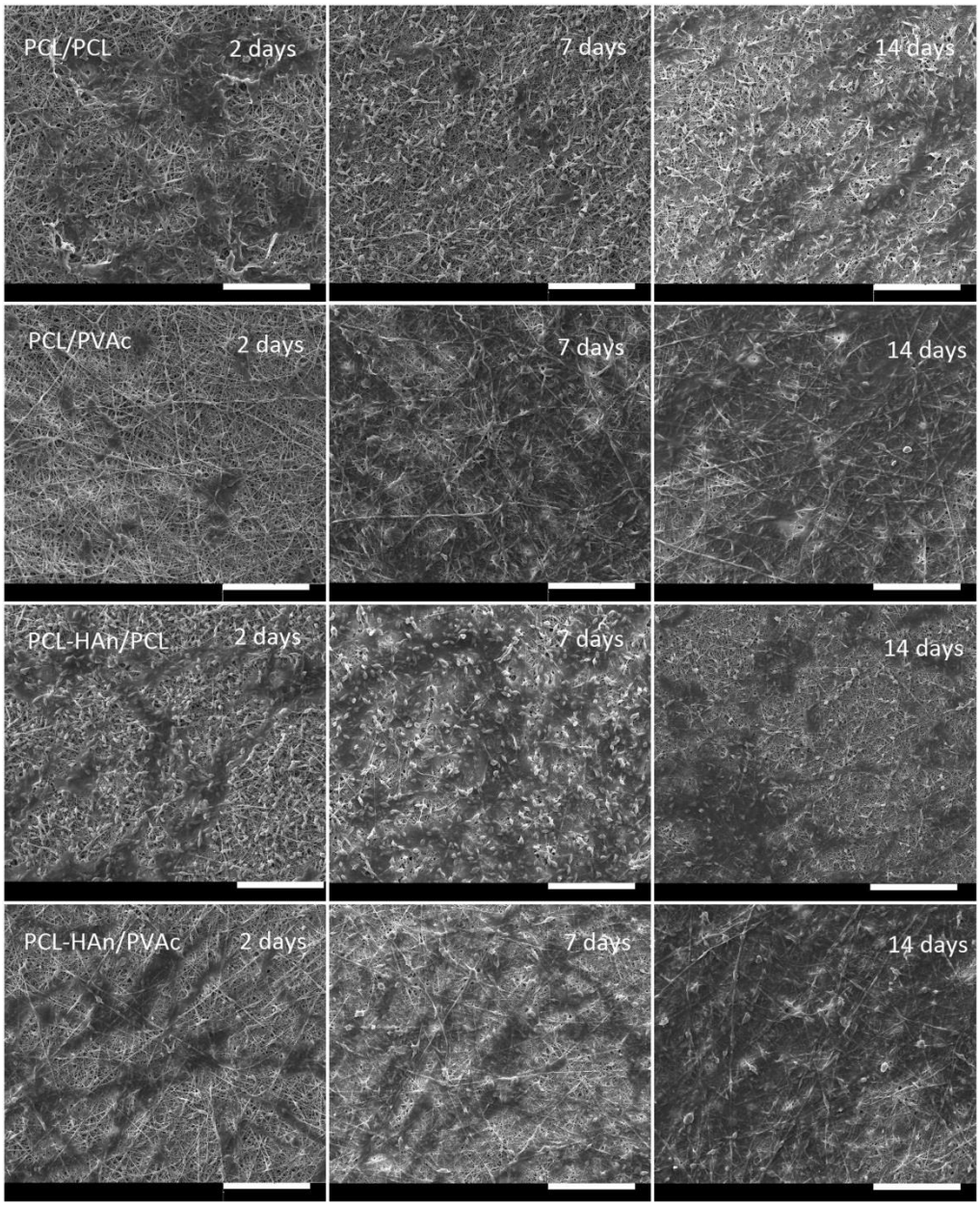

Figure III.8. SEM micrographs showing the morphology and adhesion of human osteoblasts seeded onto the different prepared materials at different time points (2, 7 and 14 days after cell seeding). Scale bars 100 nm.

To further investigate the suitability of these scaffolds for bone tissue engineering, the viability of the osteoblasts seeded was tested after 48 h (Figure III.9), 7 days (Figure III.10) and 14 days (Figures III.11 and III.12). It should be noted that all confocal acquisitions were performed with the same settings. Biocompatibility of our scaffolds is clearly shown exerting high viability, very low mortality, which is even diminished with time, and cell proliferation.

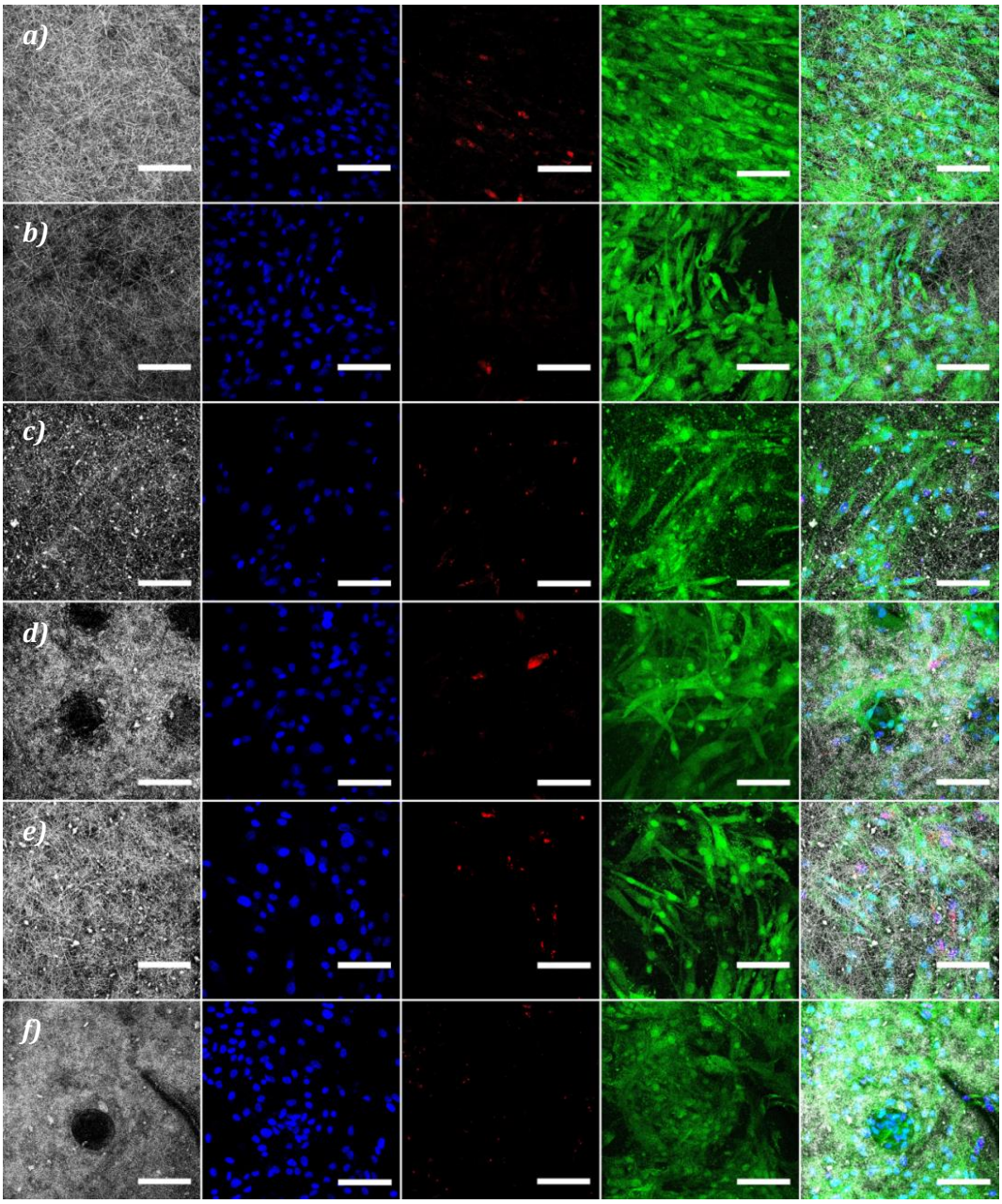

Figure III.9. Osteoblasts adhesion and viability onto the materials studied after 2 days of seeding. Scale bars 100µm.a) PCL/PCL; b) PCL/PVAc; c) PCL-HAnP/PCL; d) PCL-HAnP/PCL (LASER); e) PCL-HAnP/PVAc; f) PCL-HAnP/PVAc (LASER).

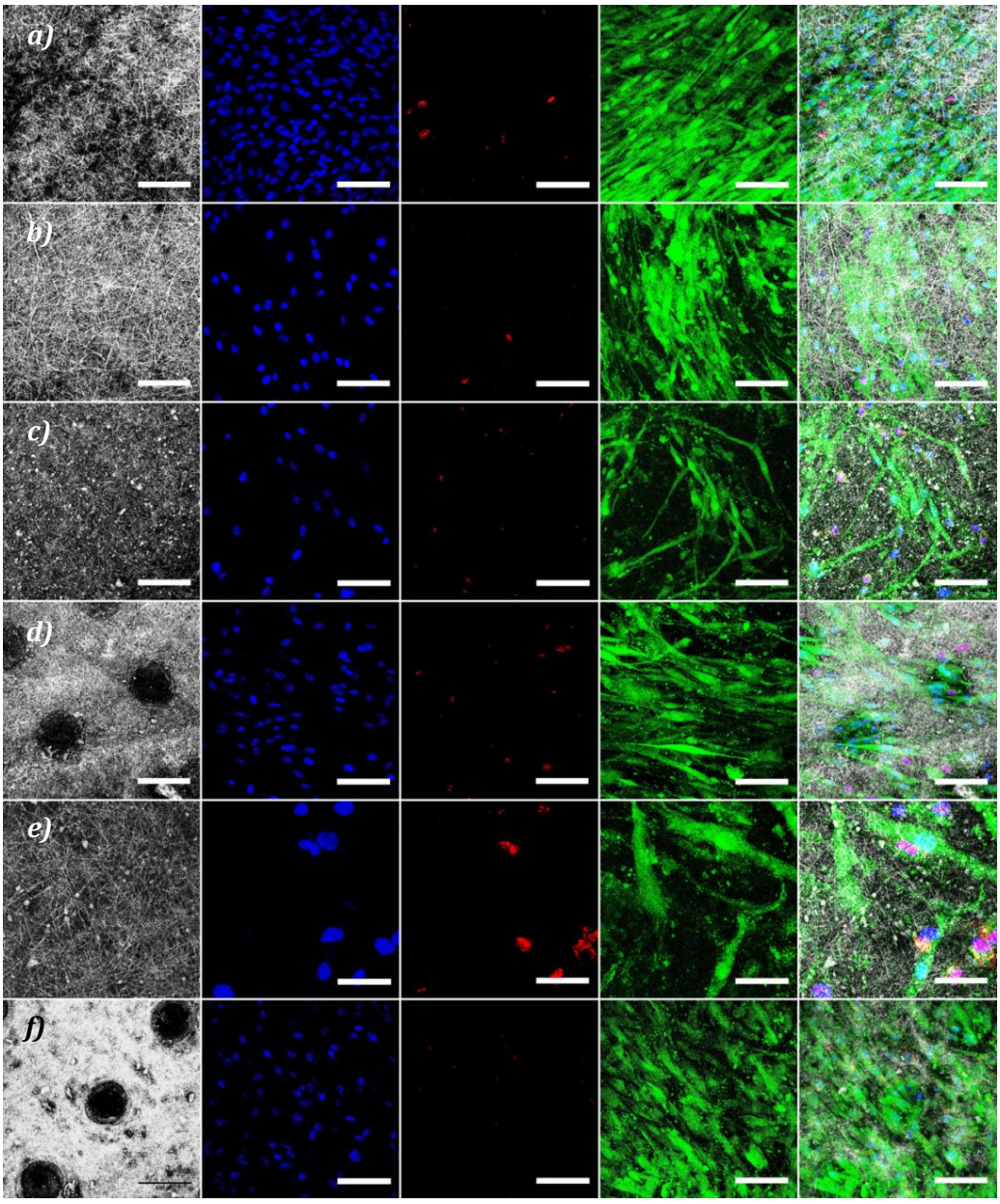

Figure III.10. Osteoblasts adhesion and viability onto the materials studied after 7 days of seeding. Scale bars 100µm .a) PCL/PCL; b) PCL/PVAc; c) PCL-HAnP/PCL; d) PCL-HAnP/PCL (LASER); e) PCL-HAnP/PVAc; f) PCL-HAnP/PVAc (LASER).

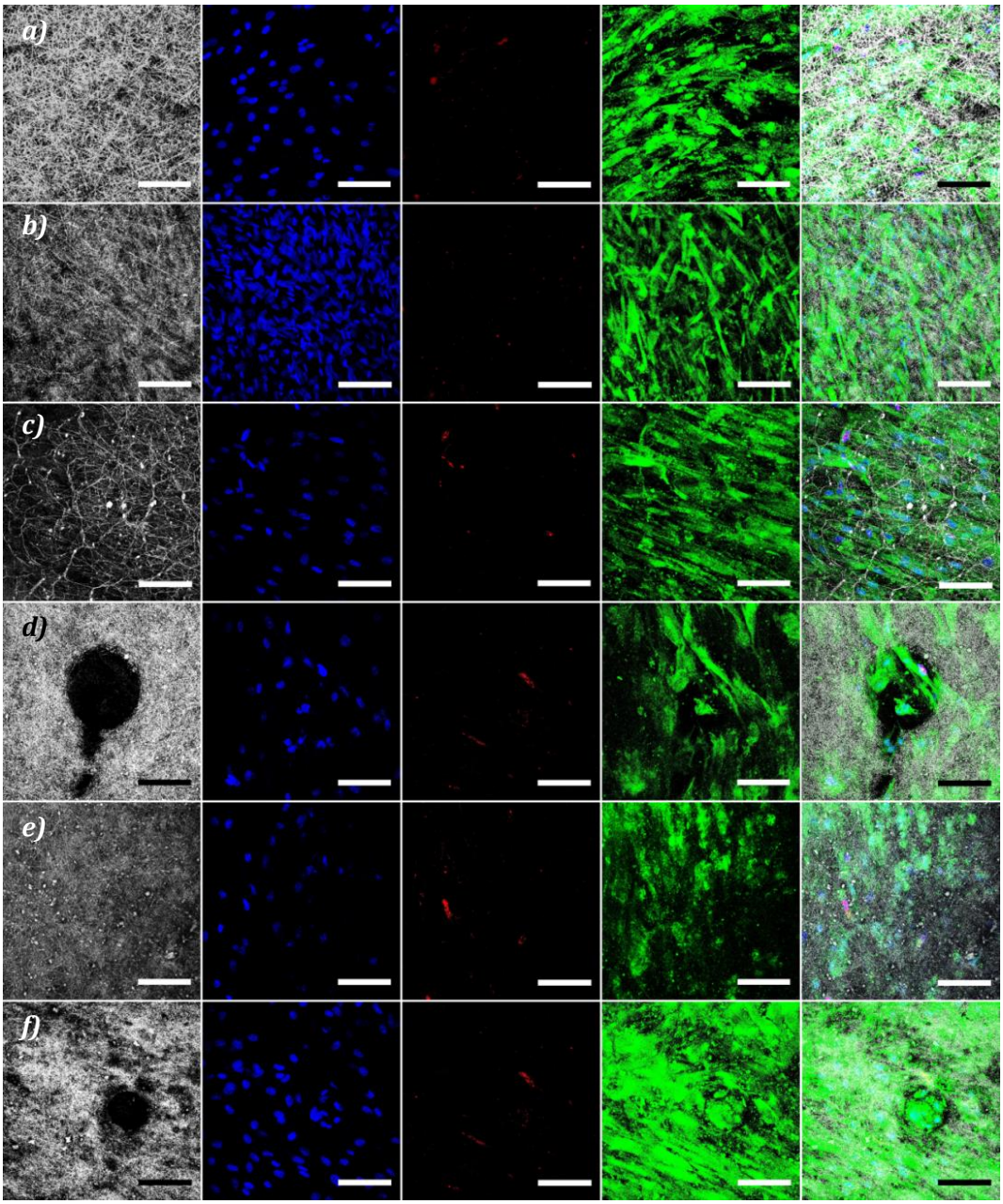

Figure III.11. Osteoblasts adhesion and viability onto the materials studied after 14 days of seeding. Scale bars 100µm.a) PCL/PCL; b) PCL/PVAc; c) PCL-HAnP/PCL; d) PCL-HAnP/PCL (LASER); e) PCL-HAnP/PVAc; f) PCL-HAnP/PVAc (LASER).

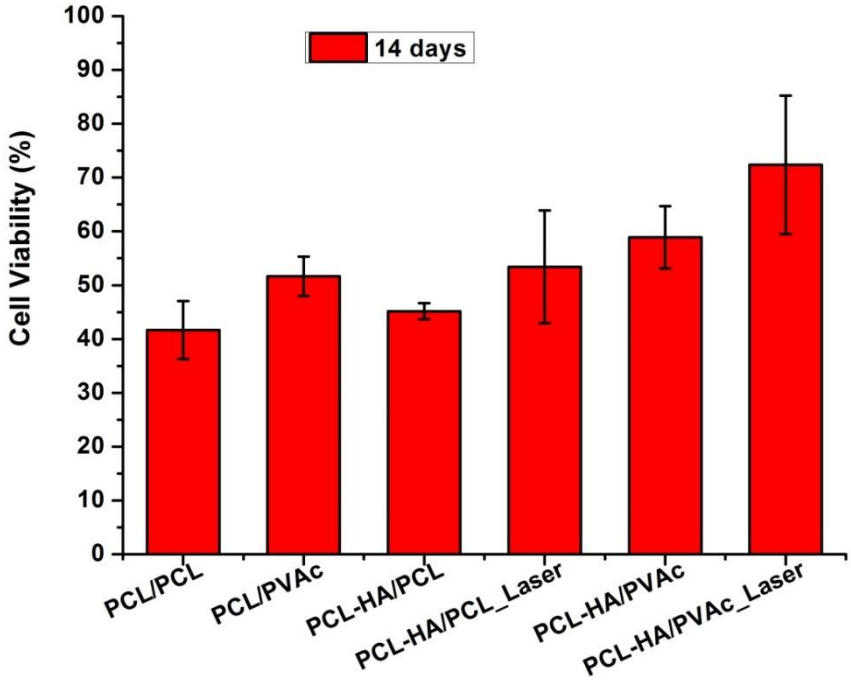

Figure III.12. Cell viability onto the different scaffolds assayed at the end of the experiments (14 days after seeding) calculated by image analysis (Image J software). Five different regions (at least 60 planes per region) of each sample were evaluated.

Furthermore, the laser treatment of the surfaces notably increased the scaffolds biocompatibility observing higher viability and cell density which could be attributed to the modification of the scaffolds surface and porosity (Figure III.13) even in the nanometer scale as has been described for titanium engineered surfaces due to the change in protein adsorption and thus cell adhesion and proliferation (36,37). In all the scaffolds assayed, cell growth was recorded mostly on the seeding surface probably due to the low pore size. In this sense, nano-porosity data of the un-treated scaffolds were very similar in all the different formulations assayed as described in Table III.1, pointing to this factor as the responsible of the homogeneity in the results obtained in the cell viability and proliferation studies.

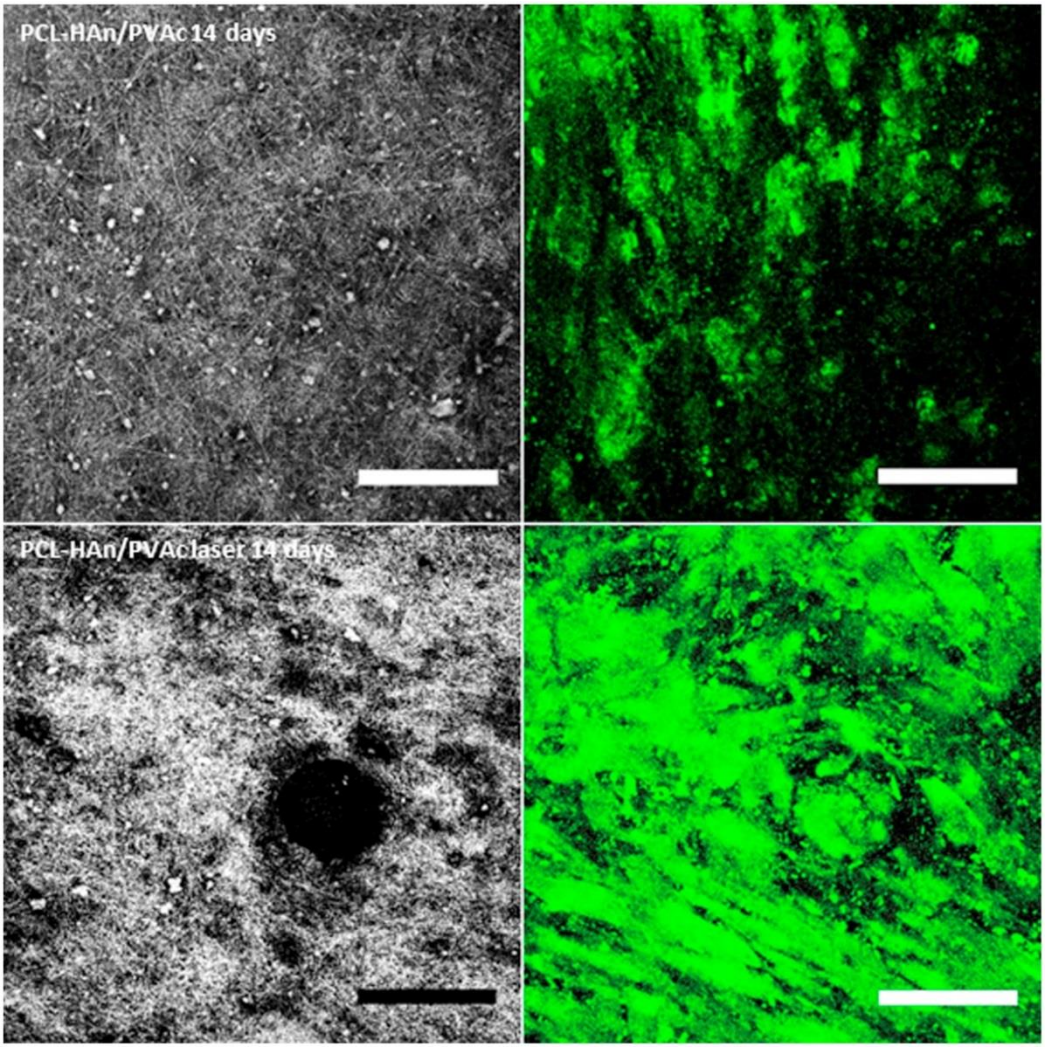

Figure III.13. Confocal microscope images of scaffolds surface (left) and viability (right) of human osteoblasts seeded in PCL-HAn/PVAc scaffolds not treated (above) and treated with laser (below) after 14 days of cell seeding. Scale bars 100 μm.

Previous studies have reported the biocompatibility of PCL electrospun 3D-scaffolds in a human osteoblast *in vitro* model in which the high porosity enabled cells to penetrate into the scaffold (38). The grafting of collagen and chondroitin sulphate on modified surface PCL porous scaffolds synthesized by particulate leaching significantly increased the *in vitro* proliferation of murine chondrocytes four weeks after seeding though porosity was not altered (39) while chemically cross-linked PCL and HAn nanoparticles used to fabricate nanocomposite scaffolds loaded with the growth factor BMP-2 also showed very good cytocompatibility in a rabbit bone marrow stem cells *in vitro* model (40), supporting PCL suitability as biomedical material. In addition, the fabrication of PCL scaffolds treated with a

femtosecond laser to create pores, and therefore to modify the scaffold surface and porosity, has shown enhanced cellular activities compared to those scaffolds with the same pore size and not treated with laser (41), indicating that laser treatment may significantly improve the potential of these types of scaffolds in bone regeneration as our study shows. Though it is controversy regarding the "ideal" size pore for biomedical applications, in osteoregeneration most authors have pointed to 100–400 μm as recommended to facilitate cell adhesion and growth (42). However, smaller pores are able to increase scaffolds surface and lead to higher cell attachment while larger pores facilitate cell migration (41). Our results showed that laser pulse on PCL-HAn/PVAc scaffolds implied the formation of micropores of 50–90 μm while on PCL-HAn/PCL were slightly larger (70–120 μm). These data, together with the apparently higher cell density recorded in PVAc containing scaffolds, suggest that smaller micropore sizes made easier cell adhesion and proliferation.

The incorporation of HAn in the synthesis process of poly(L/DL)-lactide (43) or polylactic acid (PLA) (44) electrospun scaffolds for biomedical applications has been reported in order to improve cell attachment and proliferation. Since this effect is not clear in Figures III.9-III.11, the cell viability 14 days after seeding NHOst on scaffolds with and without HAn was measured by image quantification (Figure III.12). Results show that cell viability on samples with HAn are in the range of the ones without it. Besides, they support our observations pointing to a higher viability of cells seeded on PVAc containing scaffolds, exerting significant differences among PCL-HAn/PVAc group (treated and not treated with laser) vs PCL/PCL and PCL-HAn/PCL groups. Laser treated scaffolds also displayed higher viability percentages than the not treated ones highlighting the laser treatment as an improvement for cell attachment and viability.

To our knowledge, this is the first time that the incorporation of PVAc to PCL electrospun scaffolds and treated with laser to enhance their suitability in biomedical applications has been shown these promising effects regarding human osteoblasts adhesion and proliferation, pointing to its potential application in bone repair approaches.

III.4 Conclusions

Rod shaped hydroxyapatite nanoparticles were successfully synthesized and incorporated into core-shell PCL/PCL and PCL/PVAc electrospun nanofibers. Only HAn loaded fibers presented hydroxyapatite precipitation after been soaked in SBF for 14 and 30 days. The presence HAn particles would be necessary for the apatite formation on the nanofiber surface. Fibers with PVAc shell suffer some structural change but they still exhibited a well interconnected pore network structure. Even when human osteoblasts growth was observed on all seeded surface, the laser treatment of the surfaces notably increased the scaffolds biocompatibility observing higher viability and cell density. This effect was more important on PCL-HAn/PVAc scaffolds with 50–90 μm micropores than on PCL-HAn/PCL (pores of 70–120 μm) suggesting that smaller micropore sizes favor cell adhesion and proliferation.

References

1. Joshi MK, Pant HR, Tiwari AP, Maharjan B, Liao N, Kim HJ, et al. Three-dimensional cellulose sponge: Fabrication, characterization, biomimetic mineralization, and in vitro cell infiltration. Carbohydr Polym. 2016;136:154–62.
2. Pereira IHL, Ayres E, Averous L, Schlatter G, Hebraud A, De Paula ACC, et al. Differentiation of human adipose-derived stem cells seeded on mineralized electrospun co-axial poly(ε-caprolactone) (PCL)/gelatin nanofibers. J Mater Sci Mater Med. 2014;25(4):1137–48.
3. Uma Maheshwari S, Samuel VK, Nagiah N. Fabrication and evaluation of (PVA/HAp/PCL) bilayer composites as potential scaffolds for bone tissue regeneration application. Ceram Int. 2014;40(6):8469–77.
4. Song W, Yu X, Markel DC, Shi T, Ren W. Coaxial PCL/PVA electrospun nanofibers: Osseointegration enhancer and controlled drug release device. Biofabrication. 2013 Sep;5(3):35006.
5. Lee BL-P, Jeon H, Wang A, Yan Z, Yu J, Grigoropoulos C, et al. Femtosecond laser ablation enhances cell infiltration into three-dimensional electrospun scaffolds. Acta Biomater. 2012;8(7):2648–58.
6. Suwantong O, Pankongadisak P, Deachathai S, Supaphol P. Electrospun poly(l-lactic acid) fiber mats containing crude Garcinia mangostana extracts for use as wound dressings. Polym Bull. 2014;71(4):925–49.
7. Kim TG, Chung HJ, Park TG. Macroporous and nanofibrous hyaluronic acid/collagen hybrid scaffold fabricated by concurrent electrospinning and deposition/leaching of salt particles. Acta Biomater. 2008;4(6):1611–9.
8. Kim MS, Kim G. Electrohydrodynamic jet process for pore-structure-controlled 3D fibrous architecture as a tissue regenerative material: Fabrication and cellular activities. Langmuir. 2014;30(28):8551–7.
9. Ortiz R, Moreno-Flores S, Quintana I, Vivanco MM, Sarasua JR, Toca-Herrera JL. Ultra-fast laser microprocessing of medical polymers for cell engineering applications. Mater Sci Eng C. 2014;37(1):241–50.
10. Wu Y, Vorobyev AY, Clark RL, Guo C. Femtosecond laser machining of electrospun membranes. Appl Surf Sci. 2011;257(7):2432–5.
11. Choi HW, Johnson JK, Nam J, Farson DF, Lannutti J. Structuring electrospun polycaprolactone nanofiber tissue scaffolds by femtosecond ablation. J Laser Appl. 2007;19(4):225–31.
12. McCullen SD, Gittard SD, Miller PR, Pourdeyhimi B, Narayan RJ, Loboa EG. Laser ablation imparts controlled micro-scale pores in electrospun scaffolds

for tissue engineering applications. Ann Biomed Eng. 2011;39(12):3021–30.

13. Kim MS, Kim GH. Highly porous electrospun 3D polycaprolactone/β-TCP biocomposites for tissue regeneration. Mater Lett. 2014;120:246–50.

14. Baker SR, Banerjee S, Bonin K, Guthold M. Determining the mechanical properties of electrospun poly-ε-caprolactone (PCL) nanofibers using AFM and a novel fiber anchoring technique. Mater Sci Eng C. 2016 Feb;59:203–12.

15. Chen H, Gigli M, Gualandi C, Truckenmüller R, van Blitterswijk C, Lotti N, et al. Tailoring chemical and physical properties of fibrous scaffolds from block copolyesters containing ether and thio-ether linkages for skeletal differentiation of human mesenchymal stromal cells. Biomaterials. 2016;76:261–72.

16. Dash TK, Konkimalla VB. Poly-ε-caprolactone based formulations for drug delivery and tissue engineering: A review. J Control Release. 2012;158(1):15–33.

17. Ha Y-M, Amna T, Kim M-H, Kim H-C, Hassan MSM, Khil M-S. Novel silicificated PVAc/POSS composite nanofibrous mat via facile electrospinning technique: Potential scaffold for hard tissue engineering. Colloids Surfaces B Biointerfaces. 2013;102:795–802.

18. Sadato A, Taki W, Ikada Y, Nakahara I, Yamashita K, Matsumoto K, et al. Experimental study and clinical use of poly(vinyl acetate) emulsion as liquid embolisation material. Neuroradiology. 1994;36(8):634–41.

19. Abdal-Hay A, Hamdy AS, Khalil KA, Lim JH. A novel simple one-step air jet spinning approach for deposition of poly(vinyl acetate)/hydroxyapatite composite nanofibers on Ti implants. Mater Sci Eng C. 2015;49:681–90.

20. Aragón J, González R, Fuentes G, Palin L, Croce G, Viterbo D. Development and characterization of a novel bioresorbable and bioactive biomaterial based on polyvinyl acetate, calcium carbonate and coralline hydroxyapatite. Mater Res. 2011;14(1):25–30.

21. Jing X, Jin E, Mi H-Y, Li W-J, Peng X-F, Turng L-S. Hierarchically decorated electrospun poly(ε-caprolactone)/nanohydroxyapatite composite nanofibers for bone tissue engineering. J Mater Sci. 2015;50(12):4174–86.

22. Paz A, Guadarrama D, López M, E. González J, Brizuela N, Aragón J. A comparative study of hydroxyapatite nanoparticles synthesized by different routes. Quim Nova. 2012;35(9):1724–7.

23. Mohandes F, Salavati-Niasari M, Fathi M, Fereshteh Z. Hydroxyapatite nanocrystals: Simple preparation, characterization and formation mechanism. Mater Sci Eng C. 2014;45:29–36.

24. Núñez JD, Benito AM, González R, Aragón J, Arenal R, Maser WK. Integration

and bioactivity of hydroxyapatite grown on carbon nanotubes and graphene oxide. Carbon N Y. 2014;79(1):590–604.

25. Nathanael AJ, Seo YH, Oh TH. PVP assisted synthesis of hydroxyapatite nanorods with tunable aspect ratio and bioactivity. J Nanomater. 2015;2015.

26. Taheri MM, Abdul Kadir MR, Shokuhfar T, Hamlekhan A, Assadian M, Shirdar MR, et al. Surfactant-assisted hydrothermal synthesis of Fluoridated Hydroxyapatite nanorods. Ceram Int. 2015;41(8):9867–72.

27. Mary IR, Sonia S, Viji S, Mangalaraj D, Viswanathan C, Ponpandian N. Novel multiform morphologies of hydroxyapatite: Synthesis and growth mechanism. Appl Surf Sci. 2016;361:25–32.

28. An L, Li W, Xu Y, Zeng D, Cheng Y, Wang G. Controlled additive-free hydrothermal synthesis and characterization of uniform hydroxyapatite nanobelts. Ceram Int. 2016;42:3104–12.

29. Dai C-F, Li S-P, Li X-D. Synthesis of nanostructured methotrexate/hydroxyapatite: Morphology control, growth mechanism, and bioassay explore. Colloids Surfaces B Biointerfaces. 2015;136:262–71.

30. Verma G, Barick KC, Manoj N, Sahu AK, Hassan PA. Rod-like micelle templated synthesis of porous hydroxyapatite. Ceram Int. 2013;39(8):8995–9002.

31. Metwally HA, Ardazishvili R V, Severyukhina AN, Zaharevich AM, Skaptsov AA, Venig SB, et al. The Influence of Hydroxyapatite and Calcium Carbonate Microparticles on the Mechanical Properties of Nonwoven Composite Materials Based on Polycaprolactone. Bionanoscience. 2015;5(1):22–30.

32. Cramariuc B, Cramariuc R, Scarlet R, Manea LR, Lupu IG, Cramariuc O. Fiber diameter in electrospinning process. J Electrostat. 2013;71(3):189–98.

33. Rebollar E, Cordero D, Martins A, Chiussi S, Reis RL, Neves NM, et al. Improvement of electrospun polymer fiber meshes pore size by femtosecond laser irradiation. Appl Surf Sci. 2011;257(9):4091–5.

34. Singh RK, Jin G-Z, Mahapatra C, Patel KD, Chrzanowski W, Kim H-W. Mesoporous silica-layered biopolymer hybrid nanofibrous scaffold: A novel nanobiomatrix platform for therapeutics delivery and bone regeneration. ACS Appl Mater Interfaces. 2015;7(15):8088–98.

35. Zhang Y, Gu J, Tan H, Shi J, Di M, Zuo Y, et al. Preparation and characterization of film of poly vinyl acetate ethylene copolymer emulsion. Appl Surf Sci. 2013;276:223–8.

36. Chu S-F, Huang M-T, Ou K-L, Sugiatno E, Cheng H-Y, Huang Y-H, et al. Enhanced biocompatible and hemocompatible nano/micro porous surface as a biological scaffold for functionalizational and biointegrated implants. J

Alloys Compd. 2016;684:726–32.

37. Rosales-Leal JI, Rodríguez-Valverde MA, Mazzaglia G, Ramón-Torregrosa PJ, Díaz-Rodríguez L, García-Martínez O, et al. Effect of roughness, wettability and morphology of engineered titanium surfaces on osteoblast-like cell adhesion. Colloids Surfaces A Physicochem Eng Asp. 2010;365(1–3):222–9.

38. Wang J, Valmikinathan CM, Liu W, Laurencin CT, Yu X. Spiral-structured, nanofibrous, 3D scaffolds for bone tissue engineering. J Biomed Mater Res - Part A. 2010;93(2):753–62.

39. Chang K-Y, Hung L-H, Chu I-M, Ko C-S, Lee Y-D. The application of type II collagen and chondroitin sulfate grafted PCL porous scaffold in cartilage tissue engineering. J Biomed Mater Res - Part A. 2010;92(2):712–23.

40. Liu X, Zhao K, Gong T, Song J, Bao C, Luo E, et al. Delivery of growth factors using a smart porous nanocomposite scaffold to repair a mandibular bone defect. Biomacromolecules. 2014;15(3):1019–30.

41. Kim M, Son J, Lee H, Hwang H, Choi CH, Kim G. Highly porous 3D nanofibrous scaffolds processed with an electrospinning/laser process. Curr Appl Phys. 2014;14(1):1–7.

42. Roosa SMM, Kemppainen JM, Moffitt EN, Krebsbach PH, Hollister SJ. The pore size of polycaprolactone scaffolds has limited influence on bone regeneration in an in vivo model. J Biomed Mater Res - Part A. 2010;92(1):359–68.

43. Rajzer I, Menaszek E, Kwiatkowski R, Chrzanowski W. Bioactive nanocomposite PLDL/nano-hydroxyapatite electrospun membranes for bone tissue engineering. J Mater Sci Mater Med. 2014;25(5):1239–47.

44. Morelli S, Salerno S, Holopainen J, Ritala M, De Bartolo L. Osteogenic and osteoclastogenic differentiation of co-cultured cells in polylactic acid-nanohydroxyapatite fiber scaffolds. J Biotechnol. 2015;204:53–62.

CHAPTER IV

Polymeric electrospun scaffolds for bone morphogenetic protein 2 delivery in bone tissue engineering.

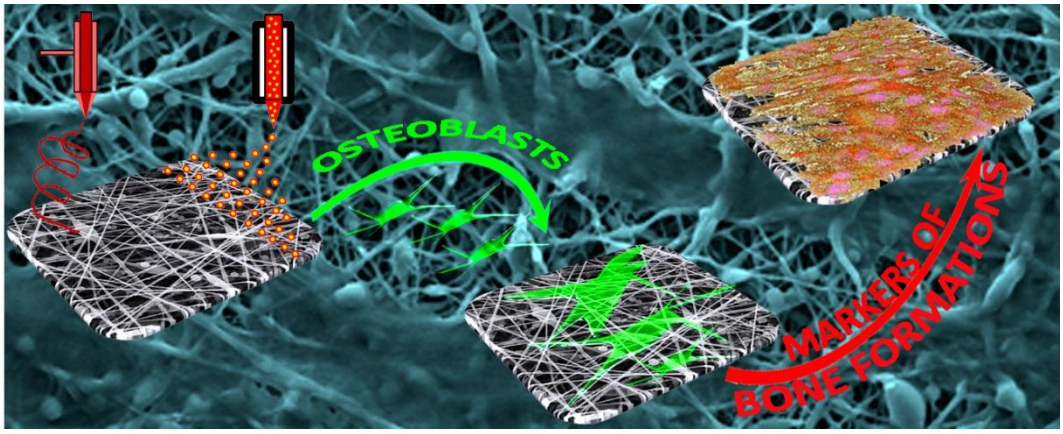

The contents of this chapter have been adapted from the following published work:

Polymeric electrospun scaffolds for bone morphogenetic protein 2 delivery in bone tissue engineering. Javier Aragón, Simona Salerno, Loredana De Bartolo, Silvia Irusta and Gracia Mendoza. Journal of Colloid and Interface Science, 531 (2018) 126–137. DOI:10.1016/j.jcis.2018.07.029.

"The development of novel scaffolds based on biocompatible polymers is of great interest in the field of bone repair for fabrication of biodegradable scaffolds that mimic the extracellular matrix and have osteoconductive and osteoinductive properties for enhanced bone regeneration.

Polycaprolactone (PCL) and polycaprolactone/polyvinyl acetate (PCL/PVAc) core–shell fibers were synthesised and decorated with poly(lactic-co-glycolic acid) [PLGA] particles loaded with bone morphogenetic protein 2 (BMP2) by simultaneous electrospinning and electrospraying. Hydroxyapatite nanorods (HAn) were loaded into the core of fibers. The obtained scaffolds were characterized by scanning and transmission electron microscopy, Fourier-transform infrared spectroscopy, and thermogravimetric analysis. The in vitro potential of these materials for bone regeneration was assessed in biodegradation assays, osteoblast viability assays, and analyses of expression of specific bone markers, such as alkaline phosphatase (ALP), osteocalcin (OCN), and osteopontin (OPN).

PLGA particles were homogeneously distributed in the entire fiber mat. The growth factor load was 1.2–1.7 μg/g of the scaffold whereas the HAn load was in the 8.8–12.6 wt% range. These scaffolds were able to support and enhance cell growth and proliferation facilitating the expression of osteogenic and osteoconductive markers (OCN and OPN). These observations underline the great importance of the presence of BMP2 in scaffolds for bone remodeling as well as the good potential of the newly developed scaffolds for clinical use in tissue engineering."

IV.1 Introduction

The repair of bone defects is still a major challenge in orthopedic and maxillofacial surgery (1). Scaffolds play a crucial role in bone tissue engineering by acting as a template facilitating cell growth and differentiation within bone defects (2). For these purposes, they should mimic the extracellular matrix (ECM); provide mechanical support; be biocompatible, osteoconductive, and osteoinductive; and possess high porosity provided by interconnected pores. Besides, they should be biodegradable to leave room for the new bone to grow. Fibers of mainly submicron sizes produced by electrospinning are a promising material to be used as scaffolds. These fibres resemble the ECM structure and are an excellent framework for cell adhesion, proliferation, and differentiation (3).

Among synthetic polymers, polycaprolactone (PCL) is widely used to obtain electrospun fibers because of its low cost, biocompatibility, and rheological and viscoelastic properties (4). The electrospun scaffolds prepared with this polymer possess flexibility, good mechanical properties, and non-toxicity (3), though its hydrophobicity and low water adsorption may impair its biomedical applications. These limitations may be solved by its association with water-soluble compounds, such as tannins (5), proteins (6), or polysaccharides (7). Furthermore, PCL osteoinduction and osteoconduction may be improved by addition of hydroxyapatite (HA) as we recently reported (4). The addition of HA nanorods (HAn) to PCL/polyvinyl acetate (PVAc) core–shell fibers yields apatite formation on the nanofiber surface while the PVAc shell increases hydrophilicity and cell viability.

Even when HAn is an important osteoconductive biomaterial, incorporation of osteogenic growth factors, such as bone morphogenetic protein 2 (BMP2), is an interesting alternative way to increase the osteogenic activity (8). Bone healing is a complex physiological process that is initiated and controlled by many growth factors such as bone morphogenetic proteins (BMPs). These proteins not only can enhance bone repair but also promote new blood vessel formation (9). BMP2 is a necessary component of the signaling cascade that governs fracture repair because BMP2 is essential for initialization of bone regeneration (10). However, this protein may lose

bioactivity after a short period owing to its short half-life under physiological conditions because of rapid degradation and deactivation by enzymes and other chemical and physical reactions that limit its local delivery (11). To achieve therapeutic efficacy, a carrier is needed to deliver BMP2 locally at a stable concentration to avoid a burst release and uncontrolled ectopic bone formation in soft tissues (12).

Poly(lactic-*co*-glycolic acid) [PLGA] has been extensively used to encapsulate osteogenic growth factors into micro- and nanoparticles for a controlled drug release (13–15). This polyester has interesting characteristics such as solubility in various solvents and approval by the US Food and Drug Administration (FDA). Several techniques have been developed for fabricating polymeric nanoparticles and for encapsulating drugs in a polymeric matrix, including emulsification. Even when this process is simple, it has multiple disadvantages, such as poor encapsulation and loading efficiency rates as well as possible denaturation of the encapsulated drug (16). To overcome these drawbacks, electrospraying or electrohydrodynamic atomization (EHDA) is a promising method for producing micro- and nanoparticles with high encapsulation efficiency of drugs (hydrophilic or hydrophobic molecules). It is a simple and inexpensive approach that enables researchers to preserve bio-functionalities of active ingredients (17). A few examples of BMP2 encapsulation in polymer nanoparticles by electrospraying found in the literature show the sustained release of the protein for 35 days, thus allowing for mesenchymal-stem-cell proliferation and differentiation (18). A stable release of BMP2 from PLGA electrosprayed spheres has been achieved, and new bone formation, accompanied by abundant in-growth of blood vessels, has been attained by *in vivo* implantation of these particles (1).

Objective

The combination of the unique properties of electrospun nanofibers with proven advantages of polymer particles for drug release can result in an innovative drug delivery system (19). This approach allows for a homogeneous distribution of the BMP2-loaded particles along the entire fiber mats, thereby ensuring a continuous release of the growth factor, in contrast to the BMP2 immobilization techniques that involve protein functionalization only on the scaffold surface (20), limiting its efficiency.

For this reason, the objective of this work was to develop a core-shell electrospun scaffold with HAn containing BMP2–loaded PLGA particles to provide the necessary biochemical cues for bone repair and regeneration. The core of PCL would provide the necessary mechanical resistance while the PVAc shell increases hydrophilicity and cell viability. On the other hand HAn particles yield apatite formation on the nanofiber surface. The prepared membranes were intended to have structural, physico-chemical, and biodegradation properties required to address the architectural, biochemical, and functional features of bone tissue.

IV.2 Scaffold fabrication

Different types of fibers (PCL-HAn fibers for the core, and PCL fibers and PVAc fibers for the shell) and PLGA particles loaded with BSA and BMP2, were fabricated to obtain four types of electrospun scaffolds (Table IV.1).

PLGA particles were prepared using an Yflow 2.2.D-500 electrospinner (Electrospinning Machines/R&D Microencapsulation, Spain). BMP2 (10 µg) was dissolved in 100 µL of a BSA aqueous solution (2 %), while PLGA (1.05 g) was dissolved in 10 mL of DMF. Then, the BSA aqueous solution was added to the PLGA solution, and the mixture was incubated with magnetic stirring for 12 h at 4 °C. The addition of a surfactant was not needed to obtain the emulsion (10 mL), which was loaded into a 10 mL plastic syringe and fed through a needle (inner diameter 0.9 mm, outer diameter 1.7 mm) connected to a positive-voltage power supply with voltage 11.65 kV. The tip of the needle was fixed 30 cm above an aluminum foil–covered flat collector. A negative-voltage power supply (-4.5 kV) was connected to the collector. The solution flow rate was 0.5 mL/h. The synthesis of HAn [$Ca_{10}(PO_4)_6(OH)_2$] nanoparticles was conducted as previously described (4). In brief, $CaCO_3$ was dissolved in a 0.3 M H_3PO_4 solution (100 mL), and we maintained a Ca/P ratio of 1.67 and pH 9 by the addition of NH_4OH during precipitation. After incubation in the stock solution for 5 days, the precipitate was washed with deionized water and dried at 110 °C for 2 h.

The aforementioned electrospinner was also used to obtain fibrous scaffolds (Table IV.1): 0.32 g of a HAn powder was dispersed in 5 mL of a DCM–DMF mixture (1:1) with Tween® 80 (0.5 %, v/v) by stirring overnight at room temperature. The dispersion

was then added to 1.27 g of PCL dissolved in 5 mL DCM–DMF (1:1) and stirred overnight at room temperature in order to obtain a solution of PCL and HAn for the fiber core synthesis (Table IV.1). On the other hand, PCL (0.60 g) and PVAc (1.05 g) were dissolved in 10 mL of DCM–DMF (1:1) and 10 mL of DMF, respectively, to prepare a PCL solution or PVAc solution for fabrication of the two types of shells that we developed (Table IV.1). Then, these solutions were stirred overnight at room temperature.

All the solutions were loaded into plastic syringes. A coaxial system was employed to obtain PCL-HAn/PCL or PCL-HAn/PVAc fibers; a PCL-HAn suspension was fed through the inner needle (0.5 mL/h) and PCL or PVAc solutions were fed through the outer needle at a 0.5 mL/h rate (Figure IV.1). All the needles had an inner diameter of 0.9 mm while the outer diameter was 1.7 mm.

Table IV.1. Composition of the scaffolds prepared in this study.

Sample	**Fibers**		**Particles**
	Core	**Shell**	
PCL	PCL-HAn	PCL	
PCL:PLGA-BMP2	PCL-HAn	PCL	PLGA:BSA:BMP2
PVAc	PCL-HAn	PVAc	
PVAc:PLGA-BMP2	PCL-HAn	PVAc	PLGA:BSA:BMP2

To obtain particle-decorated fibers, the coaxial needle (to produce fibers) and the one feeding the solution of PLGA, BSA, and BMP2 (to produce particles) were connected to the positive-voltage power supply (voltage range 9 to 12 kV; Figure IV.1). The tips of coaxial and single needles (inner diameter 0.9 mm, outer diameter 1.7 mm) were fixed 18 and 30 cm above a rotating collection drum (100 rpm), respectively. The collector was connected to the negative-voltage power supply (4 to –5 kV) for 8 h.

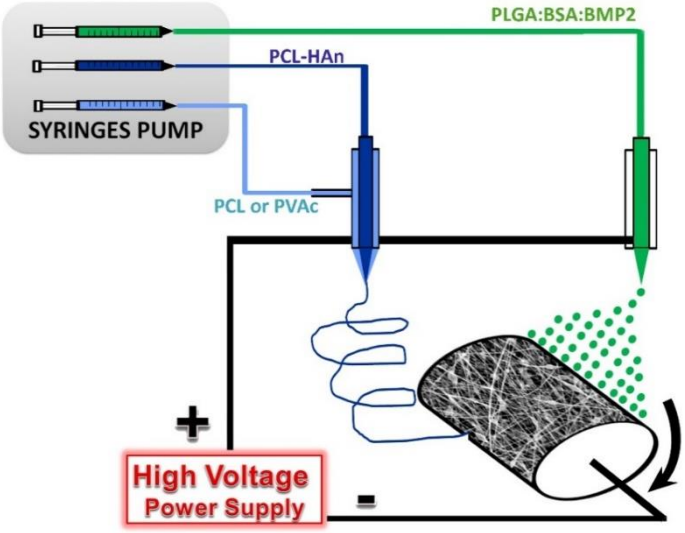

Figure IV.1. Schematic illustration of the coaxial and single electrospinning during the fabrication of PCL-HAn or PCL-HAn/PVAc fibers decorated with PLGA-BMP2 particles.

The characterization techniques and different evaluation methods are described in **Appendix 1**.

IV.3 Results and discussion

IV.3.1 Scaffold characterization

Scaffolds were obtained by electrodynamic techniques, fibers by electrospinning, and particles by electrospraying. In the last two techniques, a polymer solution flowing out of a nozzle is forced into an electric field. Solvents evaporate on the way from the nozzle to the collector and depending on the parameters, such as solution viscosity, density, and conductivity, and polymer molecular weight, fibers or particles are obtained. Several conditions were tested to fabricate PLGA particles with a uniform size distribution: three polymer concentrations (3, 5, and 10 wt%), three flow rates (0.1, 0.5, and 1.0 mL/h), two solvents (DMF and DCM–DMF), and two tip-to-collector distances (15 and 30 cm). The best results were obtained with solutions containing 10 wt% of PLGA in DCM, a flow rate of 0.5 mL/h, and a distance of 30 cm.

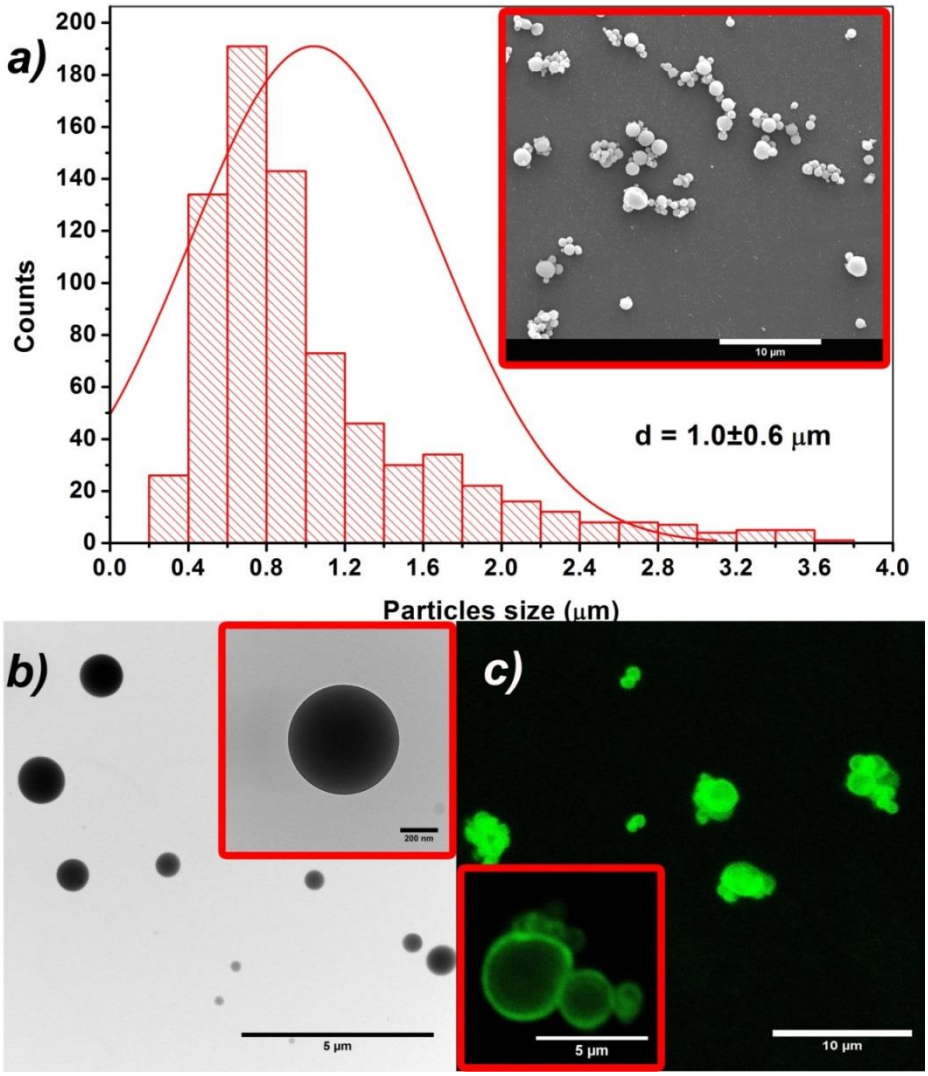

Figure IV.2. SEM (a), TEM (b), and confocal microscopy (c) images of the electrosprayed PLGA particles obtained.

The size distribution and morphology of the electrosprayed PLGA particles were investigated by means of SEM and TEM (Figures IV.2a and IV.2b), and the mean diameter was found to be 1.0 ± 0.6 μm. The histogram clearly showed the presence of a relevant type of particles in the range of 0.4–1.2 μm but also the presence of bigger particles that could be more than 3 μm in diameter. TEM images (Figure IV.2b) confirmed the spherical shape of the particles produced by electrospraying. To estimate the drug distribution inside the synthesized particles, a BSA–fluorescein conjugate (BSA-FITC) was added to the PLGA solution. The obtained particles were examined by confocal laser scanning microscopy (Figure IV.2c), which showed that even when there

was a slightly higher concentration in the shell, the fluorescent compound was almost uniformly distributed inside the microparticles. No significant phase separation of the polymer and/or drug was observed.

HAn was also characterized by means of the SEM and TEM (Figure IV.3). These images confirmed our previous results (4), in which fibrous needle-like particles with a rod-like shape were also seen (length and diameter of approximately 150 and 20 nm, respectively).

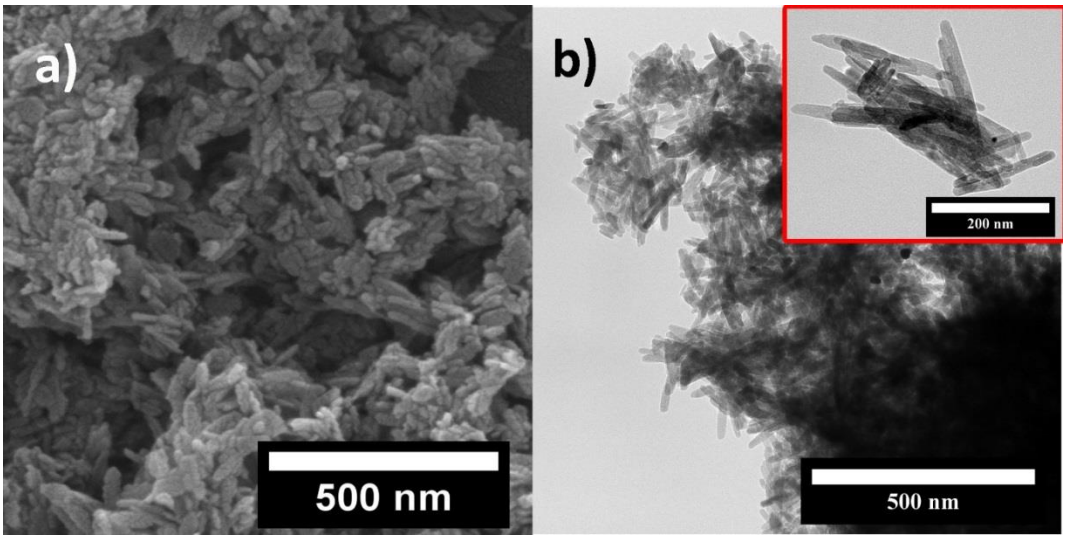

Figure IV.3. SEM (a) and TEM (b) images of synthesized HAn.

Once the particle synthesis was optimized, the simultaneous electrospray-electrospinning process was carried out to generate the final scaffolds of HAn-loaded PCL/PVAc fibers decorated with PLGA particles (Figure IV.4). The optimized electrospray-electrospinning process produced fibers with uniform morphology and a random distribution that led to the creation of a scaffold with porosity of ≈60–64%. Because of the simultaneous synthesis, PLGA particles with a mean diameter of 1.2 ± 0.5 μm were homogeneously distributed in the entire fiber mat. It is noteworthy that the attachment of particles onto fibers did not influence fiber morphology (Figure IV.4). However, some of the particles slightly deviated from the spherical shape (Figures IV.2 and IV.4). The mean diameter of fibers (380 ± 108 nm) forming the scaffolds was in the range of collagen fibers (from 50 to 500 nm), mimicking the nanostructures of the

natural ECM. SEM images clearly revealed the formation of scaffolds with an interconnected network of large pores with size between 0.9 and 2.5 μm for PCL and PVAc scaffolds and smaller pores ranging from 0.2 to 0.6 μm. The mean pore size was 1.14 μm for PVAc and 1.46 μm for PVAc:PLGA-BMP2 owing to the presence of a nanofibrous structure that confers microporosity on the scaffold (Figure IV.4). This structure provides a large surface area-to-volume ratio for cell attachment as well as sufficient porosity for nutrient diffusion. Indeed, the measured hydraulic permeance was 8.00 ± 0.30 and 6.60 ± 0.03 L/h m^2 mbar for PVAc and PCL scaffolds, respectively. An increase in hydraulic permeance by 16% was observed in the PVAc:PLGA-BMP2 scaffolds (9.5 ± 0.4 L/h m^2 mbar) with respect to the non-loaded scaffold.

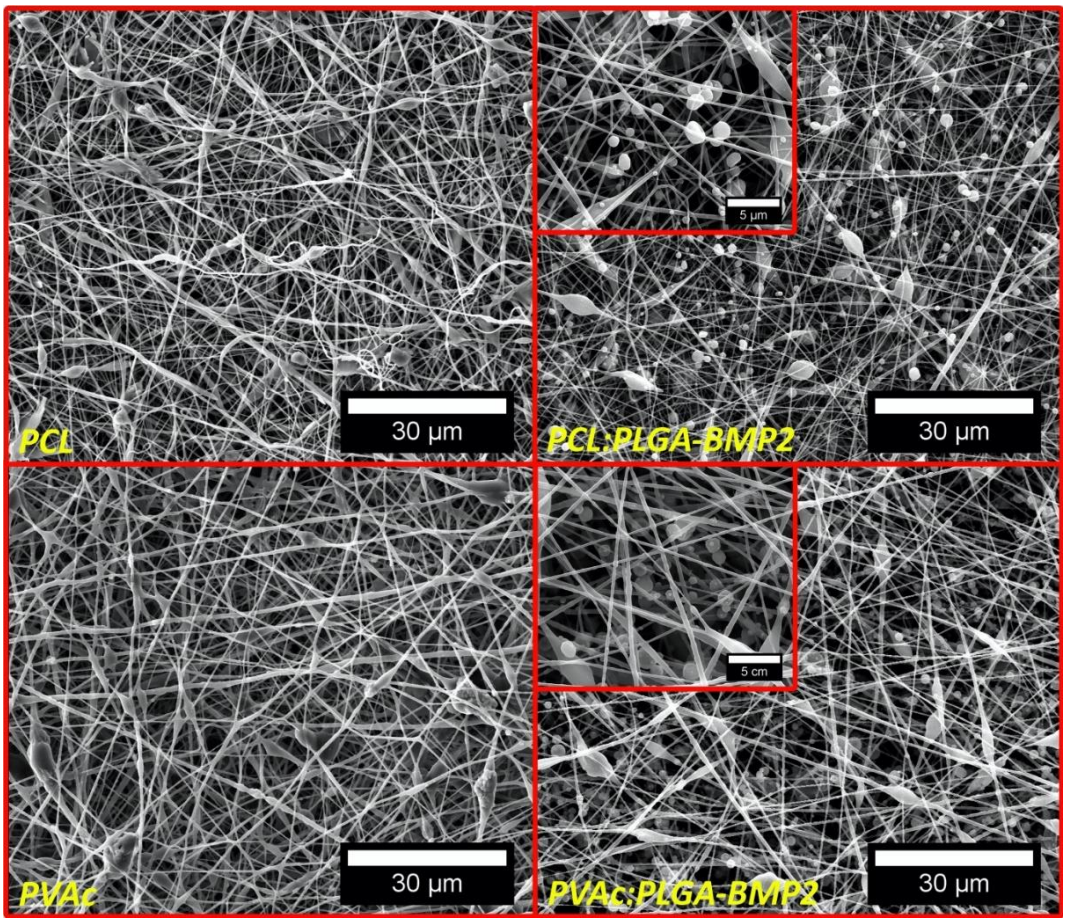

Figure IV.4. SEM images of the synthesised electrospun fibres (left) decorated with BMP2-loaded PLGA electrosprayed particles (right).

TGA analyses (Figure IV.5) confirmed HAn loads of 13.8 and 12.7 wt% for PCL and PVAc fibers, respectively, in agreement with our previous results (4). In PCL:PLGA-BMP2 and PVAc:PLGA-BMP2 scaffolds, owing to the presence of the PLGA polymer, the HAn load was reduced to 12.6 and 8.8 wt%, respectively. However, BMP2 encapsulation efficiency was similar between the two formulations, reaching percentages of 39% ± 5% for PCL:PLGA-BMP2 and 40% ± 11% for PVAc:PLGA-BMP2. A final BMP2 concentration of 39 and 40 μg/ml was achieved in the scaffolds, in line with the clinical required dose (21). These similar efficiency rates led to growth factor loads of 1.2 and 1.7 μg/g in PCL and PVAc composite fibers, respectively.

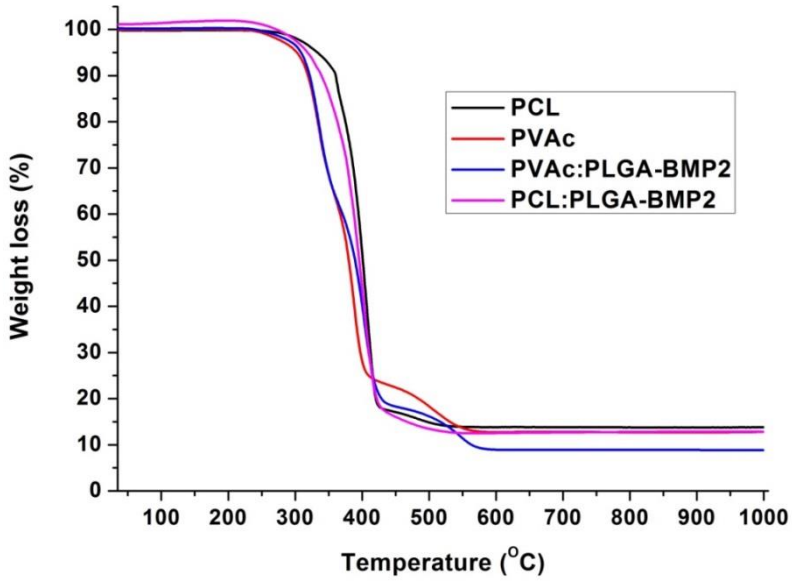

Figure IV.5. TGA thermogram of the four types of scaffolds synthesized: PCL, PVAc,PCL:PLGA-BMP2 and PVAc:PLGA-BMP2.

IV.3.2 *In vitro* protein release

The kinetic profile of the BMP2 release from both kinds of scaffolds was determined in the course of 28 days (Figure IV.6a) and the morphology of PVAc:PLGA-BMP2 scaffolds after the release for 28 days was also studied under the SEM (Figure IV.7).

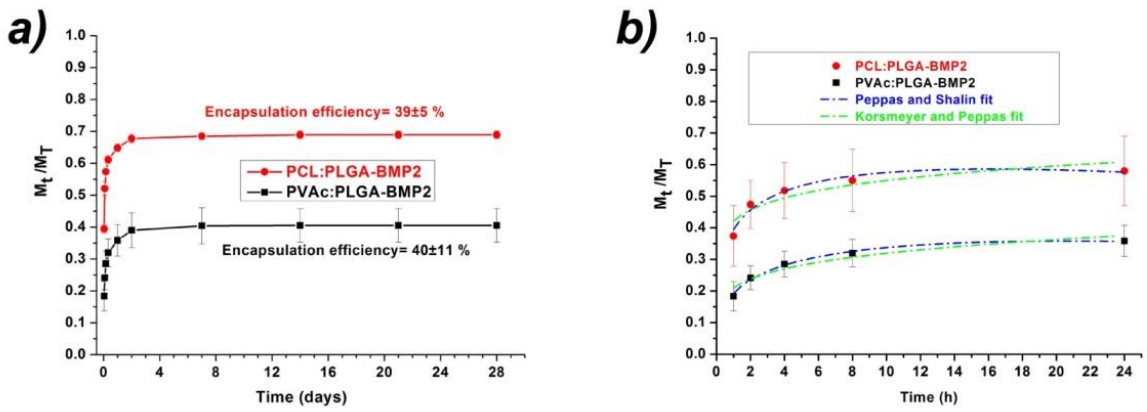

Figure IV.6. BMP2 release kinetic curves obtained for both types of scaffolds (a) and their mathematical adjustment (b).

The pattern of the growth factor release from both scaffolds showed a strong initial burst within the first 8 h, followed by a slow release until the end of the experiment. This behavior should synergistically enhance bone generation because it was suggested that the ideal BMP2 release strategy includes both an initial burst and a subsequent sustained release. The reason is that the former helps to recruit osteoprogenitor cells to the delivery system and the latter promotes osteogenic differentiation (22). The burst release reached ≈ 68 % of the BMP2 load for PCL:PLGA-BMP2 and only 40 % for PVAc:PLGA-BMP2. The difference could be due to the absorption capacity of PVAc (350 % water absorption in 24 h (23)) that may retain the protein released from the PLGA particles during the swelling process. It is important to point out that the hydrophilicity of both membranes is determined by the presence of HA, which turns both scaffolds into highly hydrophilic materials. SEM images of scaffolds (Figure IV.7) after the release (28 days) confirmed this pattern: there were no PLGA particles on the surface of the scaffolds or only a few damaged ones.

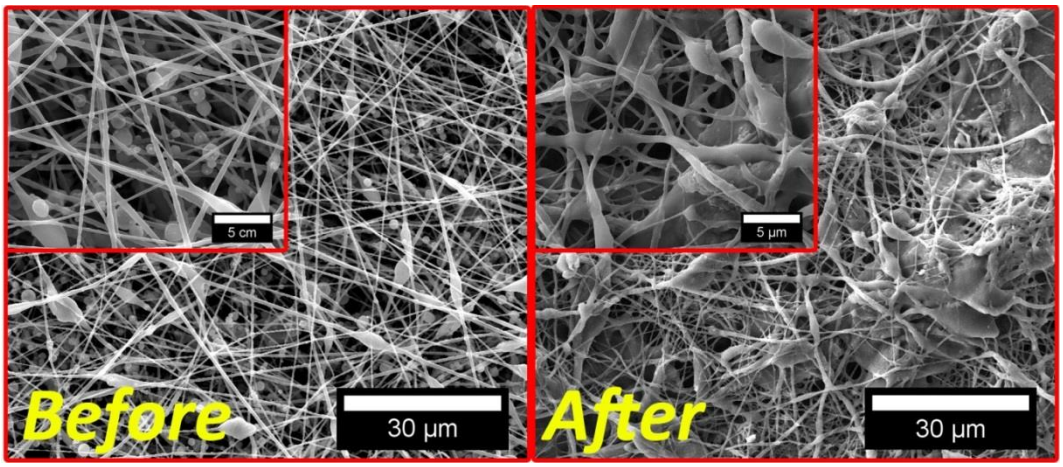

Figure IV.7. SEM images of PVAc:PLGA-BMP2 scaffolds before and after release for 28 days.

The kinetic mathematical models were fitted to the experimental results of the release (Table IV.2, Figure IV.6b). Preliminary calculations (not shown) indicate that the Higuchi model was not satisfactory for fitting to the experimental release data. Given that some of these models should be used only for the first 60% of the release, only the data representing the first 24 h were fitted because it was the release from PCL:PLGA-BMP2 achieved at that time (24). The best fit solution was identified by evaluating coefficient of correlation R^2. The highest values of the coefficient indicated that both samples were better described by the Peppas–Sahlin release kinetic model (Figure IV.6b). In this model, term $k_{1P}t^n$ represents the Fickian diffusional contribution to the release (F), whereas term k_2t^{2n} is the case-II relaxational contribution (R). The negative values obtained for k_2 should be interpreted in terms of a relaxation mechanism being insignificant compared to the diffusion process (25). In accordance with the Peppas–Sahlin equation, the value of exponent n for the Fickian release mechanism from a polymeric system with sphere geometry should be ≈0.43 (26). The lower values found for PCL and PVAc samples may be related to the wide particle size distribution mentioned before (27).

Table IV.2. Release modeling parameters.

Model	Parameter	PCL:PLGA-	PVAc:PLGA-
Korsmeyer-Peppas	k_{1K}	0.42	0.21
	n	0.12	0.18
	R^2	0.77	0.89
Peppas-Sahlin	k_{1P}	0.50	0.23
	k_2	-0.11	-0.04
	n	0.30	0.38
	R^2	0.91	0.98

IV.3.3 *In vitro* enzymatic degradation

An ideal scaffold for bone tissue engineering should be biodegradable and bioresorbable while being able to support the growth of new bone. The degradation behavior of biomaterials in physiological environments plays an important role in the engineering process of a new tissue. The greatest advantage of degradable polymers such as PCL, PVAc, and PLGA is that they are broken down into biologically acceptable molecules that are metabolized and removed from the body via normal metabolic pathways (28). To investigate the effect of enzymes on the degradation behavior of the synthesized scaffolds, they were incubated in phosphate-buffered saline in the presence of lipase or lysozyme for different periods at the same concentrations as those found in human serum. The degradation was followed by gravimetric measurements (Figure IV.8). PVAc and PCL scaffolds manifested similar behavior in the presence of lysozyme, thus reaching degradation of 10 % ± 1 % and 13 % ± 1 %, respectively, after 60 days. This value for PCL-based fibers was higher than the one expected based on the results of Banerjee el at. (29). These authors did not find any significant PCL film degradation in the presence of lysozyme. The greater degradation observed in our PCL scaffolds could be explained by the fibrous structure and high porosity that increase the surface area exposed to the enzyme solution. In the presence of lipase, the degradation profile of all scaffolds was similar to that observed in other studies, showing a significant weight loss with time, which reached values ≈ 90 % after 60 days (29).

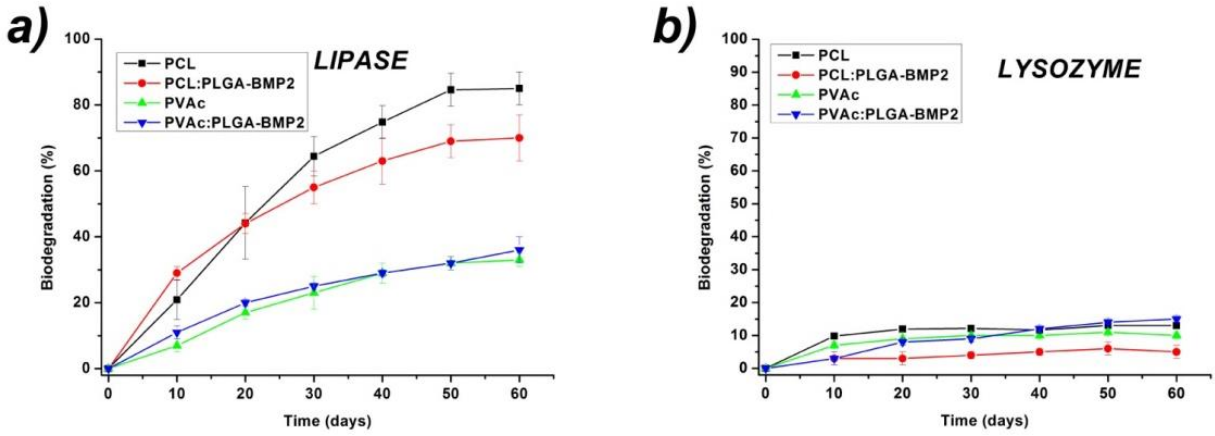

Figure IV.8. Enzymatic degradation of membranes by lipase (a) and lysozyme (b).

Table IV.3. Area ratio in lipase and lysozyme degradation media.

SAMPLE	Area ratio	
	C=O/ PO_4^{-3}	C-O-C/PO_4^{-3}
PCL	2.9	0.7
PCL_LIPASE	0.5	0.2
PCL_LYSOZYME	2.2	0.6
PCL:PLGA-BMP2	2.1	0.6
PCL:PLGA-BMP2_LIPASE	0.2	0.1
PCL:PLGA-BMP2_LYSOZYME	1.9	0.6
PVAC	2.4	1.8
PVAC_LIPASE	1.7	1.7
PVAC_LYSOZYME	2.2	2.0
PVAC:PLGA-BMP2	2.1	1.4
PVAC:PLGA-BMP2_LIPASE	2.3	2.0
PVAC:PLGA-BMP2_LYSOZYME	2.2	1.6

The effects of lipase and lysozyme on the PCL were corroborated by infrared (IR) spectroscopy (Figure IV.9). Bands at 1725 and 1240 cm^{-1}, related to C=O and C-O-C

bonds, respectively, slightly changed after enzymatic degradation. Besides, the ratios between signals assigned to PO_4^{3-} (1040 cm^{-1}), owing to the presence of HAn, and the above-mentioned polymer bands indicate a minor change in sample polymer content after the enzymatic attack (Table IV.3). Even when it is known that PVAc can be degraded by microorganisms, especially filamentous fungi (30,31), to our knowledge, there is no published study about PVAc degradation by lysozyme. The mass decrease observed in the PVAc scaffold may be related only to the PCL degradation.

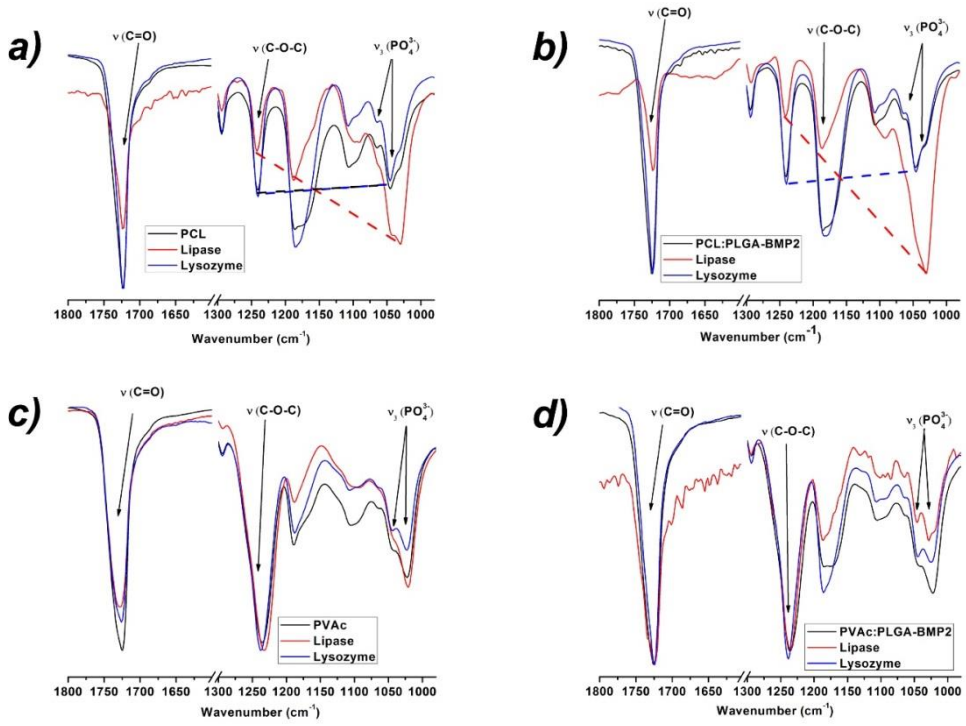

Figure IV.9. FTIR spectra of PCL (a, b) and PVAc (c, d) scaffolds loaded (b, d) and not loaded (a, c) with PLGA-BMP2 particles after enzymatic degradation with lipase and lysozyme.

In the presence of lipase, the fibers with PVAc in the shell showed lower degradation than did the fibers consisting only of PCL (Figure IV.8a). After 40 days, PCL lost almost 75% of the mass, while PVAc scaffolds lost only 29% of their mass, as expected because PCL can be hydrolytically and enzymatically degraded by lipase through hydrolysis of the ester bond (32). On the other hand, each lipase has distinct specificity towards the side chain hydrolysis of PVAc (33). The polymer backbone is not hydrolyzed, and only the side chains containing ester linkages undergo hydrolysis

catalyzed by lipase. The smaller mass loss of PVAc fibers could be due not only to the smaller amount of PCL in the sample (48 and 86 wt% for PVAc and PCL samples, respectively) but also to the reported reduction in the degradation of PCL with the addition of PVAc in PCL–PVAc blends (34). PCL degradation was also confirmed by IR spectroscopy (Figure IV.5a), which revealed relative enhancement of a band at 1040 cm^{-1} associated with HAn, thereby implying a polymer mass decrease.

On the other hand, the addition of PLGA particles to the fibers slightly changed the degradation of PVAc scaffolds in the presence of lysozyme and did not affect the behavior with lipase. PLGA particles synthesized from different polymer formulations may possess different degradation rates because the average molecular weight and lactide:glycolide ratio affect the diffusion rate and permeability of the PLGA polymeric matrix, which consequently affect the degradation rate (35). PLGA (75:25) requires more than 56 days to lose ≈ 8 % of its mass in the presence of lysozyme (36). The polymer used in this work (50:50) is a more degradable formulation because of the preferential degradation of the glycolic acid domain owing to its higher hydrophilicity (37). However, it is frequently used to encapsulate lysozyme, and the release in PBS takes place via diffusion through pre-existing pores and channels in the polymer matrix (38). This fact suggests that the degradation of PLGA 50:50 should be very slow, and therefore the release of the remaining protein (32 % for PCL:PLGA-BMP2 and 60 % for PVAc:PLGA-BMP2) may be sustained long-term while PLGA particle degradation proceeds. This process may enable a BMP2 release in the nanogram range as reported to take place during *in vivo* normal bone regeneration (39) as well as during successful *in vivo* bone repair in an experimental model (40). As a consequence, the prepared scaffold may manifest both required release types (an initial burst followed by a sustained release) to enhance bone regeneration.

It has been extensively studied and proven that biodegradation of HAn is very limited. However, due to the highly osteoconductive nature of HAn, its use in bone graft substitutes is crucial for improving the cellular response and the mineralization process (41).

IV.3.4 Cell viability and morphology

Human osteoblasts seeded onto the different types of the newly developed scaffolds adhered and spread, thus forming (after 2 weeks) a layer that covered the surface as a result of their proliferation (Figures IV.10, IV.11 and IV.12). The nanofibrous structure of scaffolds mimicking the architecture of the ECM favored adhesion and proliferation of osteoblasts as well as the maintenance of their phenotype.

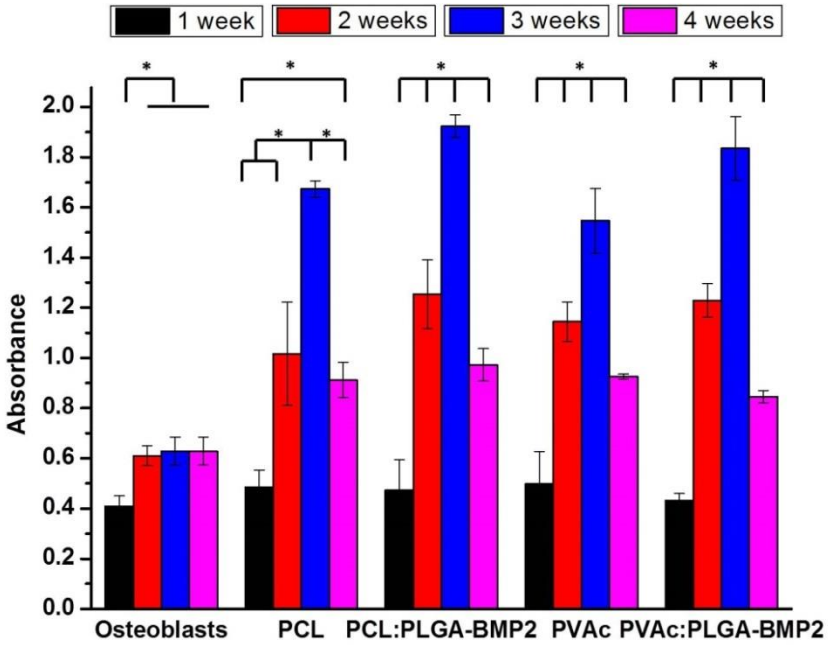

Figure IV.10. Cell viability of osteoblasts seeded in a 2D system and onto PCL and PVAc scaffolds, decorated and not decorated with PLGA-BMP2 particles, at different time points. Mean ± SD (9 samples). Differences between groups were considered significant when $p < 0.05$.

MTT assays (Figure IV.10) showed cell viability and proliferation during the experiments for up to 4 weeks after seeding. Osteoblast seeding in a 2D environment (directly onto a culture plate well) yielded slightly faster growth after 2 and 3 weeks, as compared to the absorbance recorded in the first week, and decreased again after 4 weeks. This decrease is consistent with saturation of the growth surface, preventing cell proliferation and decreasing cell viability. Furthermore, the results obtained clearly show the significant differences in cell viability and proliferation between 2D and 3D

environments because after 2 weeks, viability significantly increased in the 3D scaffolds owing to the larger surface for cell proliferation. On the other hand, the 3D experiments revealed a large increase in viability until 3 weeks in all the investigated scaffolds, followed by a decrease after 4 weeks. This finding may be attributed to the rapid proliferation of cells during this time that led to saturation of the adhesion area as indicated in Figures IV.11 and IV.12. After 4 weeks, a decrease in viability was detected on all the scaffolds tested up to values that are nonetheless significantly higher with respect to those observed after 1 week. These findings point to the scaffold's ability to maintain cell viability for an extended period. Furthermore, absorbance data at the highest cell viability (3 weeks) highlighted significant differences ($p < 0.05$) among the scaffolds including PLGA-BMP2 particles versus non-loaded scaffolds, although no statistically significant differences were observed between PCL:PLGA-BMP2 and PVAc:PLGA-BMP2 scaffolds.

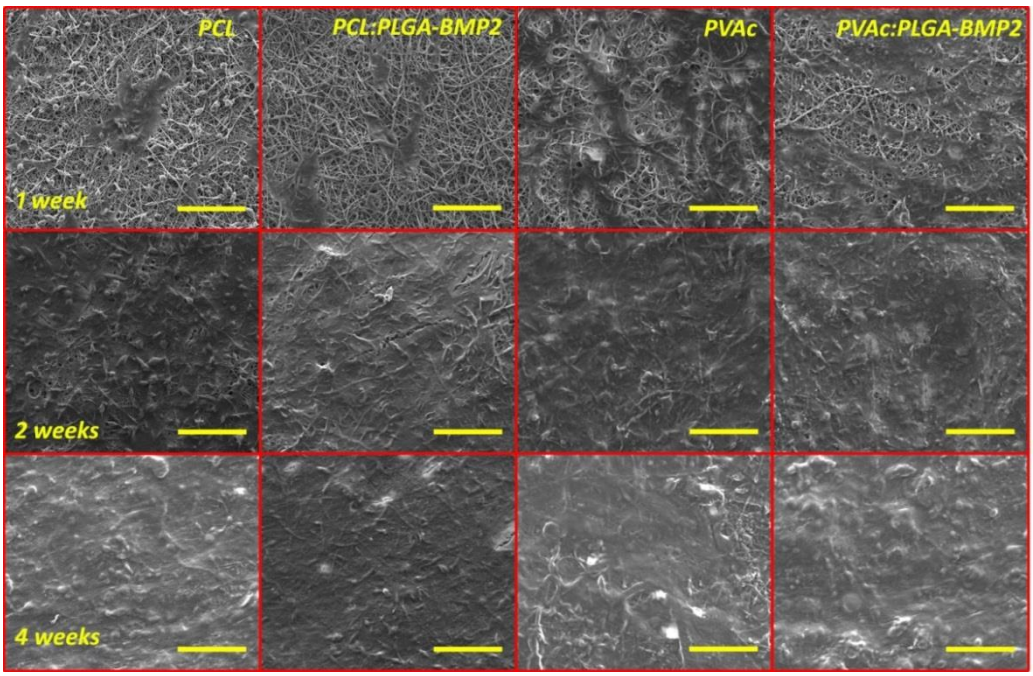

Figure IV.11. Cell proliferation at different time points on PCL and PVAc scaffolds loaded or not loaded with PLGA-BMP2 particles. Scale bar, 50 µm.

The presence of BMP2 in the scaffolds improved the cell response while promoting cell proliferation and viability. These findings are in agreement with other studies that

describe the improvement of cell interactions on composite scaffolds that were modified by surface immobilization of collagen and BMP2 (42) or surface adsorption of BMP2 with erythropoietin (43). By contrast, in our study, BMP2 was encapsulated into PLGA particles and released with time to ensure constant exposure of the cell microenvironment to the growth factor.

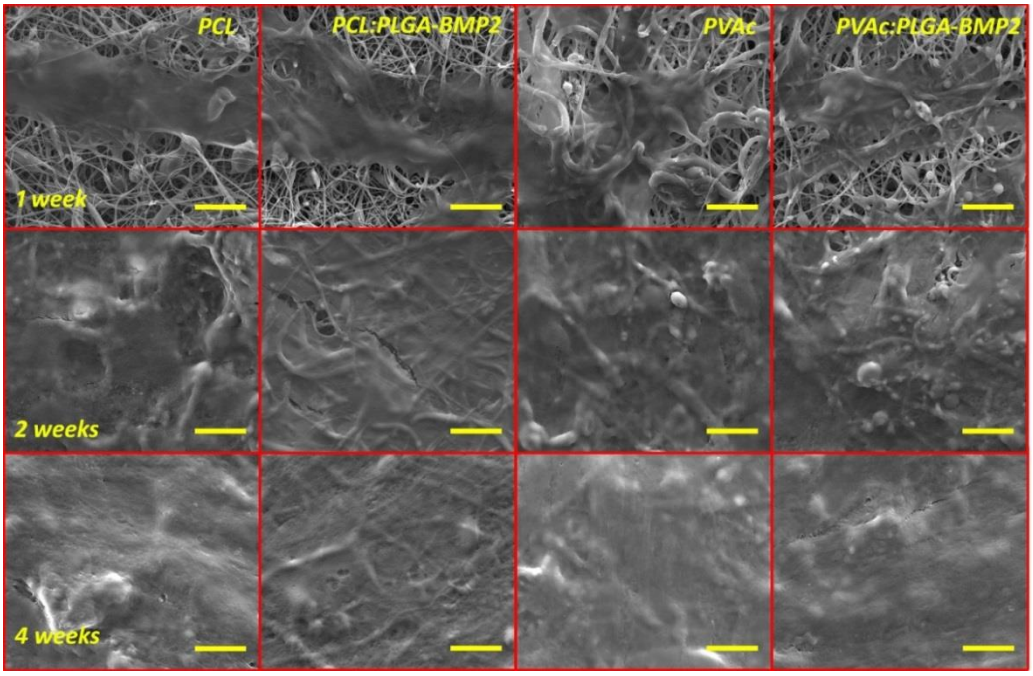

Figure IV.12. SEM images of osteoblasts proliferation onto PCL and PVAc scaffolds loaded or not loaded with PLGA-BMP2 particles at different time points. Scale bar 10 µm.

IV.3.5 Osteogenic, osteoinductive, and osteoconductive activities of scaffolds

The capability of the scaffolds to stimulate bone matrix formation was evaluated by investigating the expression of specific markers such as the secretion of ALP, OCN, and OPN, which perform a crucial function in bone regeneration. Given that the ALP is an early-stage marker of osteogenic differentiation (44,45), we evaluated its secretion by osteoblasts cultured on the different scaffolds. The ALP activity of cells increased with time, reaching a stationary phase after 3 weeks independently from the type of scaffold (Figure IV.13). An improvement of the enzymatic function was observed when the cells were cultured on PCL scaffolds loaded with BMP2 during the first 3 weeks.

These results are in agreement with data from other studies revealing the ALP activity enhancement by cells cultured on PCL scaffolds in a medium containing BMP2 (46). Similarly, Fu et al. (47) have found a significant increase in cellular enzymatic activity after surface immobilization of BMP2 on PLGA-HA microcarriers, for up to 14 days. In our study, the BMP2-loaded particles along the entire fiber mats ensured a continuous release of the growth factor, thus increasing the osteogenic activity, in contrast to the BMP2 immobilized on the surface or dissolved in the culture medium.

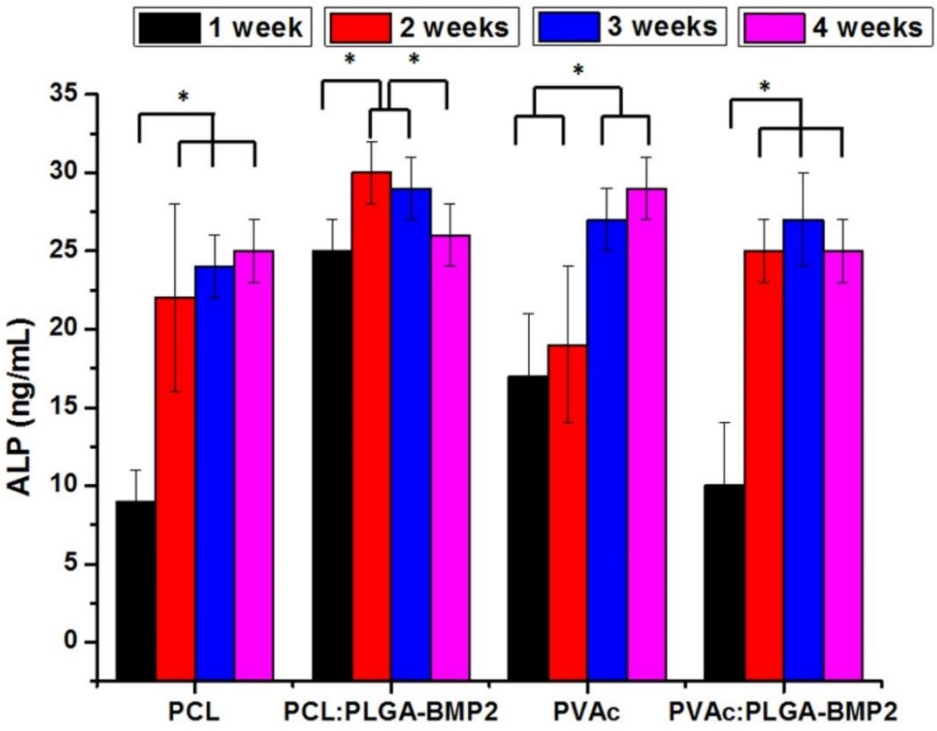

Figure IV.13. ALP concentration in osteoblast cultures seeded onto the investigated scaffolds at different time points. Mean ± SD (9 samples). Differences between groups were considered significant when $p < 0.05$.

The cell behavior indicated that the mineralization process occurred on all scaffolds within 3 weeks and then, as expected, ALP was downregulated.

ALP activity is associated with cell differentiation and precedes the secretion of other proteins such as OCN because ALP helps to prepare the ECM for the deposition before the start of mineralization.

OCN expression corresponds to the onset of mineralization, and this protein plays a pivotal role in bone formation and mineralization but also in metabolic functions of osteoblasts (48). Due to the presence of glutamic acid regions in its chemical structure, OCN has strong affinity for Ca^{2+} and HA, whose equilibrium binding properties are involved in bone turnover and mineralization (49). In contrast to other proteins, OCN is a bone-specific protein that modulates the mineralization process.

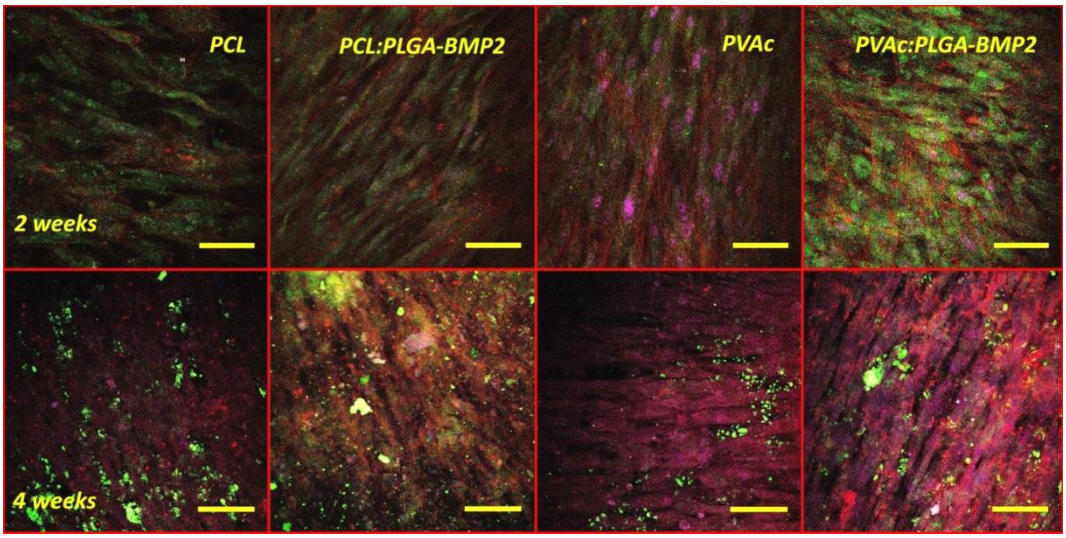

Figure IV.14. Confocal microscopy merged images of osteoblasts seeded onto the scaffolds after 2 weeks (upper images) and 4 weeks (lower images). The cells were stained for actin (red), osteocalcin (OCN; green), and osteopontin (OPN; purple). Scale bar, 100 μm.

OPN also participates in the ECM and bone formation although its function is more prominent in later stages of bone development, showing peaks of expression in remodeling phases because it plays a key part in supporting osteoclastic resorption (50). Figure IV.14 shows a comparison of the expression of actin (red), OCN (green), and OPN (purple) among the four types of electrospun scaffolds investigated at an early stage (2 weeks) and at a later stage (4 weeks) of the study. These confocal images clearly reveal the changes in OCN and OPN expression within this period, with OCN being more prevalent at 2 weeks after seeding, while OPN showed an increase in its expression after 4 weeks. The newly developed scaffolds were able to support the bone-related protein expression in accordance with other studies in the literature that used PCL-HA to

promote the osteoconductivity of MSC-derived osteoblasts (51). Furthermore, their expression was more pronounced in BMP2-loaded scaffolds, especially in PVAc scaffolds (Figures IV.15 and IV.16). The distribution of cells in BMP2-loaded PVAc scaffolds is also shown, suggesting a cell distribution on the seeding surface in accordance with pore size as we previously described (4). BMP2 induced osteogenic activity as demonstrated in other works concerning BMP2 immobilized on PLGA-HA microcarriers that exerted an improved bioactivity of pre-osteoblastic cells (47).

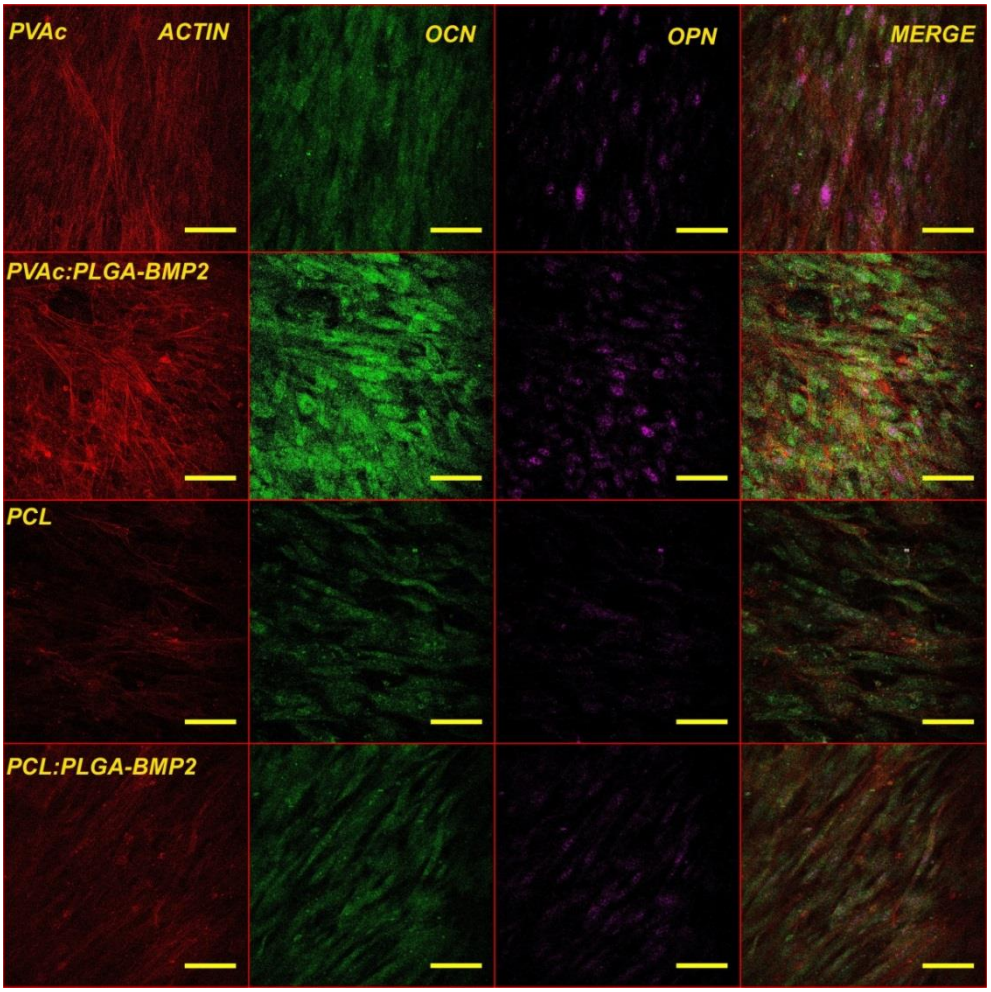

Figure IV.15. Confocal microscopy images of cells seeded onto the scaffolds assayed after 2 weeks. Scale bar 100 μm.

This protein is one of the most important osteogenic cytokines that regulate the transcription of *Runx2* and thus exert a direct effect on osteoblastic differentiation (44,52). Its addition to the scaffold enhanced osteoblastic differentiation, as highlighted by the morphology and the prominent localization and distribution of both proteins, OCN and OPN. These results confirm our previous observations (4) and suggest that these PCL/PVAc-loaded PLGA-BMP2 scaffolds are a potential therapeutic approach for bone tissue engineering.

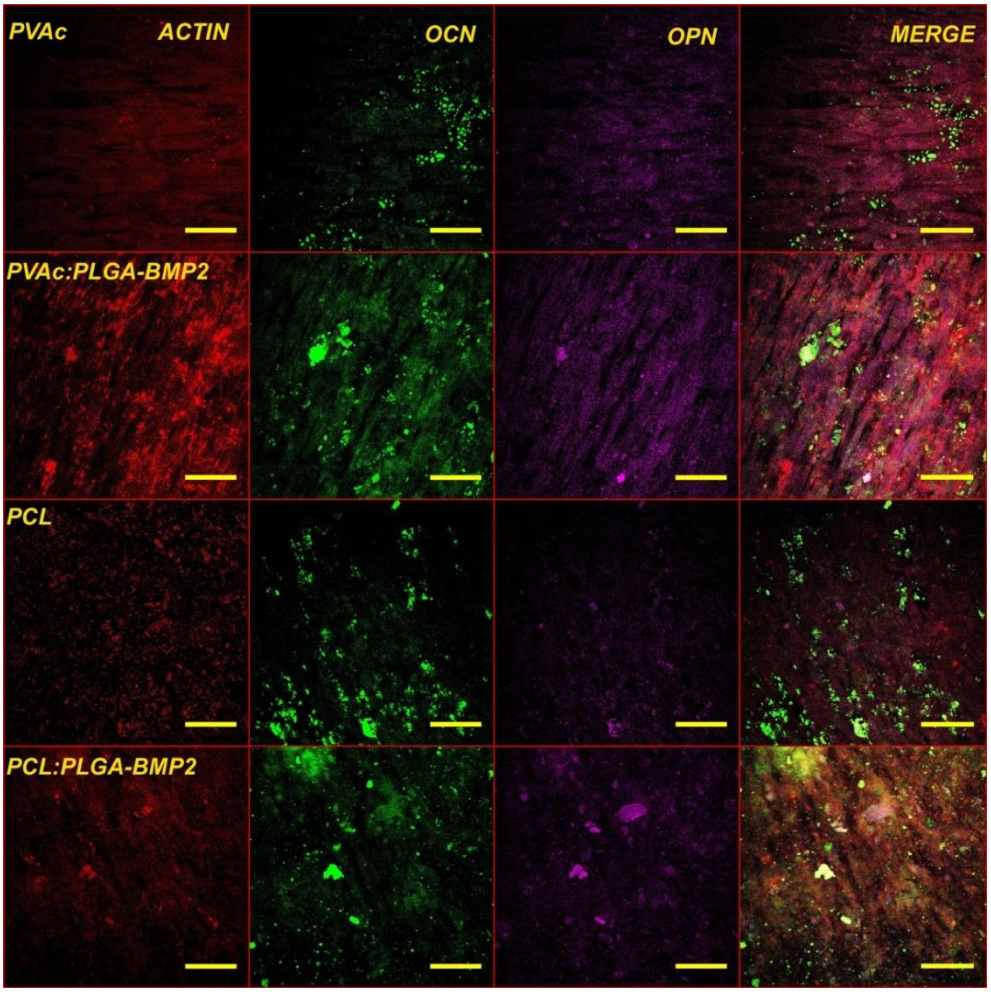

Figure IV.16. Confocal microscopy images of cells seeded onto the scaffolds assayed after 4 weeks. Scale bar 100 μm.

IV.4 Conclusions

It has been previously reported that electrospun PCL nanofibers loaded with HA promote apatite formation, whereas the presence of PVAc in the fiber shell increases hydrophilicity and favors osteoblast adhesion and proliferation (4). Given that BMP2 could be an alternative way to increase osteogenic activity (8), in this work, those fibers were decorated with PLGA-BMP2 particles obtained by electrospraying for osteoinductive and osteoconductive purposes in bone regeneration. Fibers and particles kept their size and structure after the particles were electrosprayed, though HAn loading was slightly lower (≤ 3.9 %) when PLGA was present in the samples. BMP2 was successfully loaded into PLGA particles, and their loading and activity after electrospraying were confirmed, yielding growth factor loads up to 1.7 μg/g in PCL:PLGA-BMP2 and PVAc:PLGA-BMP2 scaffolds with a final BMP2 concentration of 39 and 40 μg/mL, respectively; a mid-range concentration can fuse bone defects without adverse effects (53). The BMP2 release was 40–68 %, being lower for PVAc-containing scaffolds; this phenomenon may be attributed to their absorption capacity. Enzymatic degradation of the scaffolds highlighted their good biodegradation profile, supporting their good potential for bone regeneration. In addition, osteoblast viability and proliferation increased when the FDA-approved growth factor BMP2 was present in the scaffolds; the expression of bone formation and maturation markers was also improved by BMP2. Taken together, these results suggest that BMP2 is a key factor for the potential improvement of PCL/PVAc scaffolds. Besides, the combination of PCL, PVAc, and PLGA-BMP2 is a novel and promising therapeutic approach to bone repair.

References

1. Wang Y, Wei Y, Zhang X, Xu M, Liu F, Ma Q, et al. PLGA/PDLLA core shell submicron spheres sequential release system: Preparation, characterization and promotion of bone regeneration in vitro and in vivo. Chem Eng J. 2015;273:490–501.

2. Goonoo N, Khanbabaee B, Steuber M, Bhaw-Luximon A, Jonas U, Pietsch U, et al. κ-Carrageenan Enhances the Biomineralization and Osteogenic Differentiation of Electrospun Polyhydroxybutyrate and Polyhydroxybutyrate Valerate Fibers. Biomacromolecules. American Chemical Society; 2017 May;18(5):1563–73.

3. Tiwari AP, Joshi MK, Lee J, Maharjan B, Ko SW, Park CH, et al. Heterogeneous electrospun polycaprolactone/polyethylene glycol membranes with improved wettability, biocompatibility, and mineralization. Colloids Surfaces A Physicochem Eng Asp. Elsevier; 2017 May;520:105–13.

4. Aragon J, Navascues N, Mendoza G, Irusta S. Laser-treated electrospun fibers loaded with nano-hydroxyapatite for bone tissue engineering. Int J Pharm. 2017 Jun;525(1):112–22.

5. Martins AF, Facchi SP, da Câmara PCF, Camargo SEA, Camargo CHR, Popat KC, et al. Novel poly(ε-caprolactone)/amino-functionalized tannin electrospun membranes as scaffolds for tissue engineering. J Colloid Interface Sci. 2018 Sep;525:21–30.

6. Ren K, Wang Y, Sun T, Yue W, Zhang H. Electrospun PCL/gelatin composite nanofiber structures for effective guided bone regeneration membranes. Mater Sci Eng C. Elsevier; 2017 Sep;78:324–32.

7. Hong S, Kim G. Fabrication of electrospun polycaprolactone biocomposites reinforced with chitosan for the proliferation of mesenchymal stem cells. Carbohydr Polym. Elsevier; 2011 Jan;83(2):940–6.

8. Cao L, Yu Y, Wang J, Werkmeister JA, McLean KM, Liu C. 2- N , 6- O -sulfated chitosan-assisted BMP-2 immobilization of PCL scaffolds for enhanced osteoinduction. Mater Sci Eng C. 2017 May;74:298–306.

9. Bezemer JM, Radersma R, Grijpma DW, Dijkstra PJ, van Blitterswijk CA, Feijen J. Microspheres for protein delivery prepared from amphiphilic multiblock copolymers. 1. Influence of preparation techniques on particle characteristics and protein delivery. J Control Release. 2000 Jul;67(2–3):233–48.

10. Tsuji K, Bandyopadhyay A, Harfe BD, Cox K, Kakar S, Gerstenfeld L, et al. BMP2

activity, although dispensable for bone formation, is required for the initiation of fracture healing. Nat Genet. 2006 Dec;38(12):1424–9.

11. Li L, Zhou G, Wang Y, Yang G, Ding S, Zhou S. Controlled dual delivery of BMP-2 and dexamethasone by nanoparticle-embedded electrospun nanofibers for the efficient repair of critical-sized rat calvarial defect. Biomaterials. 2015 Jan;37:218–29.

12. Li X, Min S, Zhao X, Lu Z, Jin A. Optimization of entrapping conditions to improve the release of BMP-2 from PELA carriers by response surface methodology. Biomed Mater. 2014 Dec;10(1):15002.

13. Crecente-Campo J, Borrajo E, Vidal A, Garcia-Fuentes M. New scaffolds encapsulating TGF-β3/BMP-7 combinations driving strong chondrogenic differentiation. Eur J Pharm Biopharm. 2017 May;114:69–78.

14. Hassan A, Hosny K, Murshid Z, Alhadlaq A, Yamani A, Naguib G. Depot injectable biodegradable nanoparticles loaded with recombinant human bone morphogenetic protein-2: preparation, characterization, and in vivo evaluation. Drug Des Devel Ther. Dove Press; 2015 Jul;9:3599.

15. Zhang H-X, Zhang X-P, Xiao G-Y, Hou Y, Cheng L, Si M, et al. In vitro and in vivo evaluation of calcium phosphate composite scaffolds containing BMP-VEGF loaded PLGA microspheres for the treatment of avascular necrosis of the femoral head. Mater Sci Eng C. 2016 Mar;60:298–307.

16. Zhang L, Si T, Fischer AJ, Letson A, Yuan S, Roberts CJ, et al. Coaxial Electrospray of Ranibizumab-Loaded Microparticles for Sustained Release of Anti-VEGF Therapies. Jablonski MM, editor. PLoS One. Public Library of Science; 2015 Aug;10(8):e0135608.

17. Karimi Zarchi AA, Abbasi S, Faramarzi MA, Gilani K, Ghazi-Khansari M, Amani A. Development and optimization of N-Acetylcysteine-loaded poly (lactic-co-glycolic acid) nanoparticles by electrospray. Int J Biol Macromol. 2015 Jan;72:764–70.

18. Yoo S-Y, Kim S-K, Heo S-J, Koak J-Y, Lee J-H, Park J-M. Biochemical Responses of Anodized Titanium Implants with a Poly(lactide-co-glycolide)/Bone Morphogenic Protein-2 Submicron Particle Coating. Part 1: An In Vitro Study. Int J Oral Maxillofac Implants. 30(3):512–8.

19. Lavielle N, Hébraud A, Schlatter G, Thöny-Meyer L, Rossi RM, Popa A-M. Simultaneous Electrospinning and Electrospraying: A Straightforward Approach for Fabricating Hierarchically Structured Composite Membranes. ACS Appl Mater Interfaces. American Chemical Society; 2013 Oct;5(20):10090–7.

20. Kim SE, Yun Y-P, Han Y-K, Lee D-W, Ohe J-Y, Lee B-S, et al. Osteogenesis induction of periodontal ligament cells onto bone morphogenic protein-2 immobilized PCL fibers. Carbohydr Polym. 2014 Jan;99:700–9.

21. Zara JN, Siu RK, Zhang X, Shen J, Ngo R, Lee M, et al. High Doses of Bone Morphogenetic Protein 2 Induce Structurally Abnormal Bone and Inflammation *In Vivo*. Tissue Eng Part A. 2011 May;17(9–10):1389–99.

22. Lee HJ, Koh W-G. Hydrogel Micropattern-Incorporated Fibrous Scaffolds Capable of Sequential Growth Factor Delivery for Enhanced Osteogenesis of hMSCs. ACS Appl Mater Interfaces. American Chemical Society; 2014 Jun;6(12):9338–48.

23. Gupta SC, Baheti G., Gupta B. Application of hydrogel system for neutron attenuation. Radiat Phys Chem. Pergamon; 2000 Jul;59(1):103–7.

24. Kannan R, Muthuvijayan V, Prasad E. In vitro study of a glucose attached poly(aryl ether) dendron based gel as a drug carrier for a local anaesthetic. New J Chem. The Royal Society of Chemistry; 2017 Jul;41(15):7453–62.

25. SIMONI RC, LEMES GF, FIALHO S, GONÇALVES OH, GOZZO AM, CHIARADIA V, et al. Effect of drying method on mechanical, thermal and water absorption properties of enzymatically crosslinked gelatin hydrogels. An Acad Bras Cienc. 2017 May;89(1 suppl):745–55.

26. Siepmann J, Peppas NA. Higuchi equation: Derivation, applications, use and misuse. Int J Pharm. 2011 Oct;418(1):6–12.

27. Ritger PL, Peppas NA. A simple equation for description of solute release I. Fickian and non-fickian release from non-swellable devices in the form of slabs, spheres, cylinders or discs. J Control Release. Elsevier; 1987 Jun;5(1):23–36.

28. Chaerunisaa M, Chaerunisaa AY. Polymer combination for parenteral drug delivery. Int J Pharm Sci Res. 2017;8(5):1993–2002.

29. Banerjee A, Chatterjee K, Madras G. Enzymatic degradation of polycaprolactone–gelatin blend. Mater Res Express. IOP Publishing; 2015;2(4):45303.

30. Cappitelli F, Sorlini C. Microorganisms attack synthetic polymers in items representing our cultural heritage. Appl Environ Microbiol. American Society for Microbiology (ASM); 2008 Feb;74(3):564–9.

31. Takasu A, Baba M, Hirabayashi T. Preparation and Biodegradation of Sugar-Containing Poly(vinyl acetate) Emulsions. Macromol Biosci. 2008 Feb;8(2):193–8.

32. Gámiz-González MA, Vidaurre A, Gómez Ribelles JL. Biodegradable chitosan-poly(Ɛ-caprolactone) dialdehyde copolymer networks for soft tissue engineering.

Polym Degrad Stab. 2017 Apr;138(138):47–54.

33. Chattopadhyay S, Sivalingam G, Madras G. Lipase specificity for the hydrolysis of poly (vinyl acetate). Polym Degrad Stab. Elsevier; 2003 Jan;80(3):477–83.

34. Sivalingam G, Chattopadhyay S, Madras G. Enzymatic degradation of poly (ε-caprolactone), poly (vinyl acetate) and their blends by lipases. Chem Eng Sci. Pergamon; 2003 Jul;58(13):2911–9.

35. Qodratnama R, Serino LP, Cox HC, Qutachi O, White LJ. Formulations for modulation of protein release from large-size PLGA microparticles for tissue engineering. Mater Sci Eng C. 2015 Feb;47:230–6.

36. Zhou X, Cai Q, Yan N, Deng X, Yang X. In vitro hydrolytic and enzymatic degradation of nestlike-patterned electrospun poly(D,L-lactide-co-glycolide) scaffolds. J Biomed Mater Res Part A. 2010 Dec;95A(3):755–65.

37. Makadia HK, Siegel SJ. Poly Lactic-co-Glycolic Acid (PLGA) as Biodegradable Controlled Drug Delivery Carrier. Polymers (Basel). NIH Public Access; 2011 Sep;3(3):1377–97.

38. Jiang G, Woo BH, Kang F, Singh J, DeLuca PP. Assessment of protein release kinetics, stability and protein polymer interaction of lysozyme encapsulated poly(D,L-lactide-co-glycolide) microspheres. J Control Release. 2002 Feb;79(1–3):137–45.

39. Gamradt SC, Lieberman JR. Genetic modification of stem cells to enhance bone repair. Ann Biomed Eng. 2004 Jan;32(1):136–47.

40. Huber E, Pobloth A-M, Bormann N, Kolarczik N, Schmidt-Bleek K, Schell H, et al. * Demineralized Bone Matrix as a Carrier for Bone Morphogenetic Protein-2: Burst Release Combined with Long-Term Binding and Osteoinductive Activity Evaluated In Vitro and In Vivo. Tissue Eng Part A. 2017 Dec;23(23–24):1321–30.

41. Venkatesan J, Pallela R, Bhatnagar I, Kim S-K. Chitosan–amylopectin/hydroxyapatite and chitosan–chondroitin sulphate/hydroxyapatite composite scaffolds for bone tissue engineering. Int J Biol Macromol. 2012 Dec;51(5):1033–42.

42. Song M-J, Amirian J, Linh NTB, Lee B-T. Bone morphogenetic protein-2 immobilization on porous PCL-BCP-Col composite scaffolds for bone tissue engineering. J Appl Polym Sci. 2017 Sep;134(33):45186.

43. Patel JJ, Modes JE, Flanagan CL, Krebsbach PH, Edwards SP, Hollister SJ. Dual Delivery of EPO and BMP2 from a Novel Modular Poly-ε-Caprolactone Construct to Increase the Bone Formation in Prefabricated Bone Flaps. Tissue Eng Part C

Methods. 2015 Sep;21(9):889–97.

44. Rutkovskiy A, Stensløkken K-O, Vaage IJ. Osteoblast Differentiation at a Glance. Med Sci Monit Basic Res. International Scientific Literature, Inc.; 2016 Sep;22:95–106.

45. Jensen ED, Gopalakrishnan R, Westendorf JJ. Regulation of gene expression in osteoblasts. Biofactors. NIH Public Access; 2010;36(1):25–32.

46. Yilgor P, Sousa RA, Reis RL, Hasirci N, Hasirci V. Effect of scaffold architecture and BMP-2/BMP-7 delivery on in vitro bone regeneration. J Mater Sci Mater Med. 2010 Nov;21(11):2999–3008.

47. Fu C, Yang X, Tan S, Song L. Enhancing Cell Proliferation and Osteogenic Differentiation of MC3T3-E1 Pre-osteoblasts by BMP-2 Delivery in Graphene Oxide-Incorporated PLGA/HA Biodegradable Microcarriers. Sci Rep. 2017 Dec;7(1):12549.

48. Wei J, Karsenty G. An overview of the metabolic functions of osteocalcin. Rev Endocr Metab Disord. NIH Public Access; 2015 Jun;16(2):93–8.

49. Hauschka P V., Wians FH. Osteocalcin-hydroxyapatite interaction in the extracellular organic matrix of bone. Anat Rec. 1989 Jun;224(2):180–8.

50. Chen J, Singh K, Mukherjee BB, Sodek J. Developmental expression of osteopontin (OPN) mRNA in rat tissues: evidence for a role for OPN in bone formation and resorption. Matrix. 1993 Mar;13(2):113–23.

51. Morelli S, Facciolo D, Messina A, Piscioneri A, Salerno S, Drioli E, et al. Polycaprolactone-Hydroxyapatite Composite Membrane Scaffolds for Bone Tissue Engineering. MRS Proc. Cambridge University Press; 2013 Jan;1502:mrsf12-1502-t01-09.

52. Chen D, Harris MA, Rossini G, Dunstan CR, Dallas SL, Feng JQ, et al. Bone morphogenetic protein 2 (BMP-2) enhances BMP-3, BMP-4, and bone cell differentiation marker gene expression during the induction of mineralized bone matrix formation in cultures of fetal rat calvarial osteoblasts. Calcif Tissue Int. 1997 Mar;60(3):283–90.

53. Halling Linder C, Ek-Rylander B, Krumpel M, Norgård M, Narisawa S, Millán JL, et al. Bone Alkaline Phosphatase and Tartrate-Resistant Acid Phosphatase: Potential Co-regulators of Bone Mineralization. Calcif Tissue Int. Springer US; 2017 Jul;101(1):92–101.

CHAPTER V

Electrospun asymmetric membranes for wound dressing applications

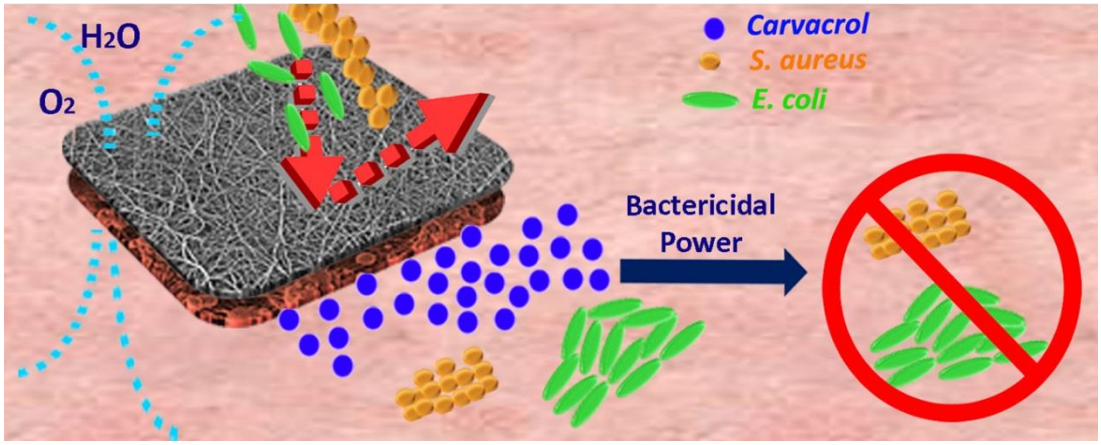

The contents of this chapter have been adapted from the following submitted work (under review):

Electrospun asymmetric membranes for wound dressing applications. Javier Aragón, Clarinda Costa, Isabel Coelhoso, Gracia Mendoza, Ana Aguiar-Ricardo and Silvia Irusta. **Materials Science and Engineering C (MSEC_2018_3013)**

"To accomplish a rapid wound healing it is necessary to develop an asymmetric membrane with interconnected pores consisting of a top layer that prevents rapid dehydration of the wound and bacteria penetration and a sub-layer with high absorption capacity and bactericidal properties. Polycaprolactone (PCL)/polyvinyl acetate (PVAc) asymmetric membranes loaded with the bactericidal monoterpene carvacrol (CRV) were synthesized and characterized by scanning electron microscopy and Fourier transform infrared spectroscopy. Mechanical properties in dry and wet conditions and fluid handling behavior were also assessed. In addition, biological studies regarding their bactericidal effects, cytocompatibility and wound closure properties were also developed. Loading efficiencies of 40-50 % were achieved in the prepared samples and 85-100 % of the loaded CRV was released in simulated wound pH evolution medium. The significant inhibition of Gram negative (Escherichia coli S17) and Gram positive (Staphylococcus aureus ATCC 25923) bacteria growth clearly showed the suitability of the fabricated membranes for wound healing applications. Furthermore, cytocompatibility of the loaded membranes was demonstrated both in 2D and 3D human dermal fibroblast cultures, as well as cell migration was not impaired by released carvacrol from the membranes. These results highlight the potential of these polymeric electrospun membranes for wound healing."

GENERAL CONCLUSIONS

The materials prepared in this work have demonstrated the potential of electrodynamic technique to obtain biomaterials for two different applications, bone scaffolds and wound dressing membranes. The most relevant conclusions of each prepared material are summarized in this chapter.

Three polymeric multifunctional scaffolds were developed using electrospinning and electrospray for bone repair and the prevention or treatment of bone infection.

- PCL and PCL/PVAc core/shell fibers obtained by electrospinning can be decorated with RFP or BMP2 loaded PLGA microparticles using the electrospraying technique.

- The incorporation of HAn particles in the polymer fibers favors the apatite formation on nanofiber surface.

- The combination of PCL, PVAc, and PLGA-BMP2 is a novel and promising therapeutic approach for bone repair. Given that BMP2 could be an alternative way to increase osteogenic activity and the PVAc fiber shell increases hydrophilicity and favors osteoblast adhesion and proliferation.

- Enzymatic degradation of the scaffolds highlighted their potential for bone regeneration.

- Laser treatment of the surfaces notably increases the scaffolds cytocompatibility resulting in higher viability and cell density.

- The synthesized scaffold shows a porous network providing a large surface area-to-volume ratio for cell attachment as well as sufficient porosity for nutrient diffusion.

- The obtained scaffold presents a homogeneous distribution of RFP-PLGA microparticles along the entire scaffolds thereby ensuring a continuous release of the RFP.

- RFP release was initially pronounced to be followed by a sustained stage until the end of the experiments. The release profile obtained from the scaffold loaded with RFP is suitable for the clinical application, as bone infection is initially controlled to keep later the prophylaxis in order to avoid bone reinfection.

- The microbiological studies support the potential of the fabricated scaffolds loaded with RFP for bone infection treatment. The scaffolds loaded with RFP-PLGA microparticles are able to eliminate *E. coli* and *S. aureus*, and RFP levels are in the range of the serum therapeutic dosages clinically recommended.

- Human osteoblasts seeded on these scaffolds decorated with RFP-PLGA microparticles displayed cell proliferation and completely colonizing their surface. Scaffolds decorated with RFP-PLGA microparticles act as potential candidates for bone repair when infection may impair the regeneration of the tissue.

- Results suggest that BMP2 is a key factor for the potential improvement of PCL/PVAc scaffolds. Osteoblast viability and proliferation increased when the growth factor (BMP2) was present in the PCL/PVAc scaffolds; the expression of bone formation and maturation markers was also improved by BMP2.

Asymmetric membranes loaded with carvacrol were obtained by electrospinning and electrospraying intended for wound dressing applications. The mechanical properties, fluid handling capacity, antimicrobial properties and non-cytotoxicity to human dermal fibroblasts (HDFs) point to the potential of these asymmetric membranes for wound dressing applications.

- Strain to failure values obtained was in the range of that observed in human skin, highlighting the potential of the fabricated membranes as dressings to be placed over a wound surface.

- WVTR values are in the required range to keep good moisture balance with water loss from the wound at the optimal rate.

- Carvacrol release produces inhibitory effects against *S. aureus* and *E. coli* growth and does not induce cytotoxicity to human dermal fibroblasts nor impair cell migration, pointing to their suitability for the clinical application.

CONCLUSIONES GENERALES

En este trabajo se ha demostrado que la técnica electrodinámica presenta un gran potencial para obtener materiales que pueden ser utilizados como biomateriales en dos aplicaciones diferentes: *scaffolds* para tratamientos óseos y apósito para heridas en forma de membranas. En este capítulo se resumen las conclusiones más relevantes de material preparado.

Mediante la técnica de electrohilado y electropulverización se desarrollaron tres *scaffolds* poliméricos multifuncionales que pueden ser utilizados en la regeneración y prevención o tratamiento de la infección ósea.

- Mediante la técnica de electropulverización se adicionaron micropartículas de PLGA cargadas con RFP o BMP2 a fibras de PCL y PCL/PVAc con estructura núcleo/cubierta obtenidas por electrohilado.

- La partículas de HAn incorporadas en las fibras poliméricas favorece la formación de apatita biologica en la superficie de la nanofibra.

- La combinación de PCL, PVAc y PLGA-BMP2 proporciona un enfoque terapéutico novedoso y prometedor en la reparación ósea. Debido a que la BMP2 podría ser una forma alternativa de aumentar la actividad osteogénica y el PVAc que recubre las fibras aumenta la hidrofilicidad del *scaffold* y favorece la adhesión y proliferación de osteoblastos.

- Los *scaffolds* presentan una degradación enzimática para ser utilizados en la regeneración ósea.

- El tratamiento láser en la superficie de los *scaffolds* aumenta notablemente su citocompatibilidad, provocando en una mayor viabilidad y densidad celular.

- Los *scaffolds* sintetizados presenta un enrejado poroso con una alta relación área de superficie/volumen que facilita la adhesión celular así como la difusión de nutrientes a través de él.

• Las micropartículas de RFP-PLGA se distribuyen homogéneamente a lo largo de todo el *scaffold* obtenido, garantizando de esta forma una liberación continua de RFP.

• En el proceso de liberación se libera una gran cantidad de RFP en la etapa inicial, seguida de una liberación sostenida hasta el final del estudio. El perfil de liberación de RFP obtenido en este caso es adecuado para la aplicación clínica, ya que se puede controlar inicialmente la infección ósea y mantener la profilaxis evitando la reinfección ósea.

• El uso de los *scaffolds* fabricados cargados con RFP en el tratamiento de la infección ósea fue respaldado por los estudios microbiológicos obtenidos. Los *scaffolds* cargados con micropartículas de RFP-PLGA son capaces de eliminar tanto la *E. coli* como el *S. aureus* y mantener unos niveles de RFP liberada en el rango clínicamente recomendado en suero de las dosis terapéuticas.

• Los osteoblastos humanos sembrados sobre los *scaffolds* decorados con micropartículas de RFP-PLGA fueron capaces de proliferar y colonizar completamente su superficie. Actuando como posibles candidatos para la reparación ósea cuando una posible infección puede perjudicar la regeneración del tejido.

• Los resultados sugieren que la BMP2 es un factor clave para mejora los *scaffolds* de PCL/PVAc. La presencia del factor de crecimiento (BMP2) en los *scaffolds* de PCL/PVAc aumenta la viabilidad y proliferación de osteoblastos; así como también la expresión de marcadores específicos de formación ósea.

Se obtuvieron membranas asimétricas cargadas con carvacrol mediante electrohilado y electrospulverización para aplicaciones como apósitos para heridas. El potencial que presentan estas membranas para ser utilizada como apósitos para heridas quedo demostrado con sus propiedades mecánicas, su capacidad para manejar los fluidos, sus propiedades antimicrobianas y la falta de citotoxicidad en fibroblastos dérmicos humanos (HDF).

• Los valores obtenidos de deformación antes de la rotura, están en el rango de los valores reportados en la piel humana, destacando la utilidad de estas membranas como apósitos que pueden ser colocados sobre la superficie de una herida.

• Los valores de WVTR están en el rango requerido para mantener un adecuado balance entre la humedad y la pérdida de agua de la herida.

• El carvacrol liberado no induce citotoxicidad a los fibroblastos dérmicos humanos ni altera la migración celular y produce efectos inhibitorios en el crecimiento de *S. aureus* y *E. coli*, lo que indica su idoneidad en la aplicación clínica.

CONCLUSIONI GENERALI

I materiali preparati in questo lavoro hanno dimostrato il potenziale della tecnica elettrodinamica per ottenere biomateriali per due diverse applicazioni, scaffold ossei e membrane per medicazione delle ferite. Le conclusioni più rilevanti di ogni materiale preparato sono riassunte in questo capitolo.

Tre scaffold polimerici multifunzionali sono stati sviluppati utilizzando elettrofilatura ed elettrospray per la riparazione ossea e la prevenzione o il trattamento dell'infezione ossea.

- Le fibre core/shell PCL e PCL/PVAc ottenute per elettrofilatura possono essere decorate con microparticelle PLGA caricate con RFP o BMP2 utilizzando la tecnica dell'elettrospray.

- L'incorporazione di particelle di HAn nelle fibre polimeriche favorisce la formazione di apatite sulla superficie di nanofibre.

- La combinazione di PCL, PVAc e PLGA-BMP2 è un approccio terapeutico innovativo e promettente per la riparazione ossea. Dato che BMP2 potrebbe essere un modo alternativo per aumentare l'attività osteogenica e il guscio di fibra PVAc aumenta l'idrofilia e favorisce l'adesione e la proliferazione degli osteoblasti.

- Il degrado enzimatico degli scaffold ha evidenziato il loro potenziale di rigenerazione ossea.

- Il trattamento laser delle superfici aumenta notevolmente la citocompatibilità degli scaffold, con conseguente maggiore vitalità e densità cellulare.
- Lo scaffold sintetizzato mostra una rete porosa che fornisce un ampio rapporto superficie-volume per l'attacco cellulare e una porosità sufficiente per la diffusione dei nutrienti.

- Lo scaffold ottenuto presenta una distribuzione omogenea di microparticelle RFP-PLGA lungo l'intero scaffold, garantendo in tal modo un rilascio continuo della RFP.

- Il rilascio della RFP è stato inizialmente pronunciato per essere seguito da uno stadio prolungato fino alla fine degli esperimenti. Il profilo di rilascio ottenuto dallo scaffold caricato con RFP è adatto per l'applicazione clinica, poiché l'infezione ossea è inizialmente controllata per mantenere in seguito la profilassi al fine di evitare la reinfezione ossea.

- Gli studi microbiologici supportano il potenziale degli scaffold fabbricati caricati con RFP per il trattamento delle infezioni ossee. Gli scaffold caricati con microparticelle RFP-PLGA sono in grado di eliminare E. coli e S. aureus e i livelli di RFP sono nell'intervallo dei dosaggi terapeutici sierici raccomandati clinicamente.

- Gli osteoblasti umani seminati su questi scaffold decorati con microparticelle RFP-PLGA hanno mostrato la proliferazione cellulare e colonizzano completamente la loro superficie. Le impalcature decorate con microparticelle RFP-PLGA fungono da potenziali candidati per la riparazione ossea quando l'infezione può compromettere la rigenerazione del tessuto.

- I risultati suggeriscono che BMP2 è un fattore chiave per il potenziale miglioramento degli scaffold PCL/PVAc. La vitalità e la proliferazione dell'osteoblasto sono aumentate quando il fattore di crescita (BMP2) era presente negli scaffold PCL/PVAc; l'espressione della formazione dell'osso e dei marker di maturazione è stata migliorata anche dalla BMP2.

Le membrane asimmetriche caricate con carvacrolo sono state ottenute elettrofilando e elettrofilando per applicazioni di medicazione. Le proprietà meccaniche, la capacità di gestione dei fluidi, le proprietà antimicrobiche e la non citotossicità dei fibroblasti dermici umani (HDF) indicano il potenziale di queste membrane asimmetriche per le applicazioni di medicazione delle ferite.

- I valori di deformazione fino a rottura ottenuti erano nella gamma di quella osservata nella pelle umana, evidenziando il potenziale delle membrane fabbricate come condimenti da posizionare su una superficie della ferita.

- I valori WVTR rientrano nell'intervallo richiesto per mantenere un buon equilibrio idrico con la perdita d'acqua dalla ferita alla frequenza ottimale.

- Il rilascio di Carvacrol produce effetti inibitori contro la crescita di S. aureus ed E. coli e non induce citotossicità nei fibroblasti dermici umani né compromette la migrazione cellulare, indicando la loro idoneità per l'applicazione clinica.

CONCLUSÕES GERAIS

Os materiais preparados neste trabalho demonstraram o potencial da técnica eletrodinâmica para obtenção de biomateriais para duas diferentes aplicações, arcabouços ósseos e membranas de curativos. As conclusões mais relevantes de cada material preparado estão resumidas neste capítulo.

Três scaffolds multifuncionais poliméricos foram desenvolvidos utilizando eletrofiação e eletropulverização para reparo ósseo e prevenção ou tratamento de infecção óssea.

- Fibras núcleo/casca PCL e PCL/PVAc obtidas por eletrofiação podem ser decoradas com micropartículas de PLGA carregadas com RFP ou BMP2 usando a técnica de eletropulverização.

- A incorporação de partículas de HAn nas fibras de polímero favorece a formação de apatita na superfície da nanofibra.

- A combinação de PCL, PVAc e PLGA-BMP2 é uma abordagem terapêutica inovadora e promissora para o reparo ósseo. Dado que a BMP2 poderia ser uma maneira alternativa de aumentar a atividade osteogênica e a casca de fibra PVAc aumenta a hidrofilicidade e favorece a adesão e proliferação de osteoblastos.

- A degradação enzimática dos scaffolds destacou seu potencial para regeneração óssea.

- O tratamento a laser das superfícies aumenta notavelmente a citocompatibilidade dos scaffolds, resultando em maior viabilidade e densidade celular.

- O andaime sintetizado mostra uma rede porosa que fornece uma grande proporção entre área e volume para a conexão das células, bem como porosidade suficiente para difusão de nutrientes.

• O andaime obtido apresenta uma distribuição homogênea de micropartículas de RFP-PLGA ao longo de todos os andaimes, garantindo assim uma liberação contínua do RFP.

• Liberação de RFP foi inicialmente pronunciada para ser seguida por um estágio sustentado até o final dos experimentos. O perfil de liberação obtido a partir do andaime carregado com RFP é adequado para a aplicação clínica, pois a infecção óssea é inicialmente controlada para manter a profilaxia tardia, a fim de evitar a reinfecção óssea.

• Os estudos microbiológicos suportam o potencial dos andaimes fabricados carregados com RFP para tratamento de infecção óssea. Os suportes carregados com micropartículas de RFP-PLGA são capazes de eliminar E. coli e S. aureus, e os níveis de RFP estão na faixa das dosagens terapêuticas séricas clinicamente recomendadas.

• Os osteoblastos humanos semeados nesses arcabouços decorados com micropartículas de RFP-PLGA apresentaram proliferação celular e colonizaram completamente sua superfície. Andaimes decorados com micropartículas de RFP-PLGA agem como candidatos potenciais para reparo ósseo quando a infecção pode prejudicar a regeneração do tecido.

• Os resultados sugerem que o BMP2 é um fator chave para a melhoria potencial dos arcabouços PCL/PVAc. A viabilidade e proliferação de osteoblastos aumentaram quando o fator de crescimento (BMP2) estava presente nos arcabouços PCL/PVAc; a expressão da formação óssea e marcadores de maturação também foi melhorada pela BMP2.

As membranas assimétricas carregadas com carvacrol foram obtidas por electrospinning e electrospraying destinadas a aplicações de curativos. As propriedades mecânicas, capacidade de manipulação de fluidos, propriedades antimicrobianas e não-citotoxicidade para fibroblastos dérmicos humanos (HDFs) apontam para o potencial destas membranas assimétricas para aplicações de curativos.

• Os valores da tensão até a falha obtidos estavam na faixa do observado na pele humana, destacando o potencial das membranas fabricadas como curativos para serem colocados sobre uma superfície da ferida.

• Os valores de WVTR estão dentro do intervalo necessário para manter um bom equilíbrio de umidade com a perda de água da ferida na taxa ideal.

• A liberação de carvacrol produz efeitos inibitórios contra o crescimento de S. aureus e E. coli e não induz citotoxicidade aos fibroblastos dérmicos humanos, nem prejudica a migração celular, indicando sua adequação para a aplicação clínica.

APPENDIX 1

Materials and methods

A.1.1 Materials

Polycaprolactone (PCL) with an average molecular weight of 80,000 Da, polyvinyl acetate (PVAc) with an average molecular weight of 140,000 Da RFP (≥97%), N,N-dimethylformamide (DMF; ≥99.8%), dichloromethane (DCM; ≥99.8%), acetic acid (≥99%), dimethyl sulfoxide (DMSO; ≥99.8%), ethanol absolute (ETOH; ≥ 99.5 %), calcium carbonate ($CaCO_3$; ≥95%), phosphoric acid (H_3PO_4; ≥85%), ammonium hydroxide solution (NH_4OH; 28–30%), sodium chloride(NaCl; ≥99%), calcium chloride dihydrate ($CaCl_2.2H_2O$; ≥99%), phosphate-buffered saline (PBS), tris(hydroxymethyl)aminomethane (Tris; ≥99.8%), ammonium sulfate ($(NH_4)_2SO_4$; ≥99%), sodium nitrate ($NaNO_2$; ≥97%), sodium hydroxide (NaOH; ≥98%), potassium acetate (CH_3COOK; (≥99%)), carvacrol (CRV; ≥99%), naproxen sodium (≥98-102%), TWEEN® 80, bovine serum albumin (BSA; ≥98%), albumin–fluorescein isothiocyanate conjugate (BSA-FITC), 3-(3,4-dimethylthiazol-2-yl)-2,5-diphenyltetrazoliumbromide (MTT; ≥98%), human lysozyme (≥100,000 U/mg protein, lyophilised powder; ≥90%), lipase from *Aspergillus oryzae* (50 U/mg), and CellCrown™ inserts (24 well plate inserts) were purchased from Sigma-Aldrich (Spain).

Poly(D,L-lactide-co-glycolide)lactide:glycolide 50:50 (PLGA) ester terminated at molecular weight 38,000–54,000 Da was purchased from Evonik Industries (Spain), and bone morphogenetic protein 2 (BMP2; ≥95%) is from R&D Systems (US). Sodium dodecyl sulfate (SDS) and Triton X-100 were obtained from Bio-Rad (USA). Trypticasein soy broth (TSB) and trypticasein soy agar (TSA) were acquired from Conda-Pronadisa (Spain). Trypsin-EDTA, Dulbecco's phosphate-buffered saline (DPBS) high-glucose DMEM (DMEM w/stable glutamine) and antibiotic-antimycotic (60 µg/mL penicillin, 100 µg/mL streptomycin and 0.25 µg/mL amphotericin B) were obtained from Biowest (France).

Escherichia coli S17 was kindly gifted by Professor J. A. Aínsa Claver from Department of Microbiology, Preventive Medicine, and Public Health, University of Zaragoza, while *Staphylococcus aureus* (ATCC®25923) was purchased from Ielab (Spain). Human dermal fibroblasts (HDFs) were obtained from Lonza (US) and fetal bovine serum (FBS) was purchased from Gibco (UK). Osteoblast cells were

provided by two companies; human osteoblasts (HOBs) and osteoblast growth medium (OGM) were obtained from PromoCell (Germany), and Clonetics™ normal human osteoblasts (NHOst) and Clonetics™ OGM™ osteoblast growth medium (OGM) were purchased from Lonza (Belgium).

A.1.2 Physical-chemical characterization

The morphology of HAn and PLGA particles and electrospun scaffolds or asymmetric membranes was analyzed using a Transmission Electron Microscope (TEM) operated at 300 kV (Tecnai F30, FEI, USA) and two Scanning Electron *Microscope* (SEM; Field Emission Scanning Electron Microscope CSEM-FEG INSPECT 50, FEI, USA and Field Emission SEM, by Nova 200 NanoLab Dual Beam-SEM/FIB, FEI, equipped with a cryogenic module, Quorum Technologies PP200T). Particles and fibers diameter was measured by Image J software (Version 1.48f, NIH, US). The size distribution statistics was obtained by measuring at least 100 fibers or particles in different images.

Fourier transform infrared (FTIR) spectrum and XRPD were used to evaluate the molecular structure and to identify the crystallographic phases in the case of the HAn. Fourier-transform infrared (FTIR) spectra were recorded on a Vertex-70 FTIR spectrophotometer (Bruker, US) and a Spectrum 1000, Perkin Elmer to evaluate the molecular structure. The powder diffraction pattern was measured in a diffractometer (Rigaku RINT 2000) with a monochromatic Cu Kα radiation. Thermal analyses of membranes were conducted with a thermogravimetric analyzer (TGA) from METTLER TOLEDO (TGA/SDTA 851e; US).

The mean pore size and pore size distribution were determined by means of a Capillary Flow Porometer CFP 1500 AEXL (Porous Materials Inc. PMI, Ithaca, New York, US). Porosity of membranes was also measured by mercury intrusion using a mercury porosimeter (Poremaster, Quantachrome and Micromeritics' AutoPore IV 9500 Series). At least five samples were tested for each type of membrane.

Contact angle of each face of the prepared membranes was evaluated with water droplets (6 µL) using a Dataphysics OCA-Series equipment (Dataphysics instruments GmbH, Germany) at room temperature.

A.1.3 *In vitro* studies in simulated body fluid (SBF) on "Laser-treated electrospun fibers loaded with nano-hydroxyapatite" (Chapter III)

In vitro studies in simulated body fluid (SBF) were carried out using the SBF composition and the standard procedures described by Kokubo and Takadama (1). Electrospun scaffolds membranes were immersed in 10 mL of SBF for 30 days at 37 °C and, every 72 h in the first 15 days and every week in the last 15 days, the liquid phase was replaced with 10 mL of fresh SBF. After immersion in SBF the samples were characterized by SEM to verify whether HAn was formed on the surfaces of the scaffolds.

A.1.4 Mechanical properties

A.1.4.1 Mechanical properties of "Composite scaffold loaded with RFP" (Chapter II)

Mechanical properties of the RFP loaded scaffolds were determined at room temperature through a Uniaxial Instron test machine (Instron, US) with video extensometer 5548 (1 KN load cell, 1 mm/min). Five samples per membrane were cut into 50 mm x 5 mm strips and subjected to a tensile test. A full-scale load of 20 N and maximum extension of 100 mm were used.

A.1.4.2 Mechanical properties on "Electrospun asymmetric membranes" (Chapter V)

In order to mimic a real wound environment, asymmetric membranes were soaked in 3 different pH solutions and tested during 3 weeks at 37 ºC: 1st week in 0.1M TRIS solution at pH 8; 2nd week in 0.1M PBS solution at pH 7.4; 3rd week in artificial exudates solutions (AES) at pH 5 (142 mmol of Na^{+} and 2.5 mmol of Ca^{+2}). In this case mechanical properties were evaluated at room temperature with a tensile testing machine (MINIMAT firm-ware v.3.1). Five samples per membrane in dried and wet conditions (soaked during 3 weeks) were cut into 30 mm x 10 mm

strips and subjected to a tensile test. A full-scale load of 20 N and maximum extension of 50 mm were used.

A.1.5 Membranes permeability in "Polymeric electrospun scaffolds for bone morphogenetic protein" (Chapter IV)

To test membranes permeability, pure water was used to determine flux values at different levels of trans-membrane pressure (ΔP^{TM}, mbar). Hydraulic permeance Lp, expressed in units of flux per pressure, L/m^2 h mbar, was estimated by applying the following equation [Eq. A.1] in which a linear dependence between water flux (J, L/m^2h) and the convective driving force is expressed:

$$L_p = \left(\frac{J_{Solvent}}{\Delta P^{TM}}\right)_{\Delta C=0} \qquad \text{[Eq. A.1]}$$

A.1.6 Encapsulation efficiency

Encapsulation efficiency (EE) of RFP, CRV and BMP2 was analyzed by different technique.

EE was calculated with the following equation [Eq. A.2]:

$$EE = \frac{Experimental\ amount}{Theoretical\ amount} \times 100 \qquad \text{[Eq. A.2]}$$

The theoretical amount was calculated based on the amount of drug added to the solution.

A.1.6.1 Encapsulation efficiency in "Composite scaffold loaded with RFP" (Chapter II)

In samples containing rifampicin (RFP) the EE was evaluated by absorbance measurement at 334 nm in a microplate reader (Multimode Synergy HT Microplate Reader; Biotek, US). Approximately 10-20 mg of PCL-PLGA-RFP scaffold was put in contact with 1 mL of DMF with constant agitation during 3 h at 4 ºC to extract the loaded RFP. RFP calibration curves in DMF was prepared in the range of 0-50 ppm and measured in triplicate.

A.1.6.2 Encapsulation efficiency in "Polymeric electrospun scaffolds for bone morphogenetic protein" (Chapter IV)

A solvent extraction technique was used to measure the EE of BMP2. Approximately 15 mg of each scaffold were dissolved in 1 mL of DCM at 37 °C. After 6 h, BMP2 was extracted by adding 5 mL of DPBS (pH 7.4) and keeping the mixture for 24 h at 37 °C. The resultant emulsion was centrifuged at 150 × g for 10 min. The water phase was carefully collected and kept at -20 °C. The protein amount in collected solutions was measured with the BMP2 Quantikine ELISA Kit (R&D Systems, US). Absorbance of samples was measured at 450 nm on a microplate reader (Multimode Synergy HT Microplate Reader; BioTek, US), and the concentration was determined by interpolation of the absorbance data obtained from the samples on a standard calibration curve (0-2,000 pg/mL) provided by the manufacturer.

A.1.6.3 Encapsulation efficiency in "Electrospun asymmetric membranes" (Chapter V)

In case of CRV gas chromatography mass spectrometry (GC-MS), GCMS-QP2010 SE (Shimadzu, Japan) equipped with an AOC 20i auto-injector was used to determine EE of CRV. Approximately 15-20 mg of each asymmetric membrane was dissolved in DCM/Acetonitrile (1:1) to extract the loaded CRV.

A.1.7 *In vitro* release study and kinetic modeling

A.1.7.1 *In vitro* release study and kinetic modeling of "Composite scaffold loaded with RFP" (Chapter II)

An *in vitro* release from RFP loaded electrospun scaffolds (15-20 mg) was performed at 37 ºC (Heater Memmert, Germany) in DPBS (1.5 mL; n = 5). According to scheduled time intervals (from 1 h to 28 days), DPBS was harvested and added again the same volume of fresh DPBS. The collected samples (five replicas per time) were kept at -20 ºC until analysis. To determine RFP concentration, three aliquots (150 µL) per sample were taken and added to a 96-well plate to measure the absorbance. RFP calibration curves in DPBS was prepared in the range of 0-50 ppm and measured in triplicate.

A.1.7.2 *In vitro* release study and kinetic modeling of "Polymeric electrospun scaffolds for bone morphogenetic protein" (Chapter IV)

An *in vitro* release of BMP2 from loaded scaffolds was carried out at 37 °C in a heater (Memmert, Germany) in DPBS (1.5 mL; n = 5). According to scheduled time intervals (from 30 min to 28 days), all DPBS was collected and replaced with an equal volume of fresh DPBS. The collected samples were stored at -20 °C until analysis and measured BMP2 Quantikine ELISA Kit as described above in section A.1.6.2.

A.1.7.3 *In vitro* release study and kinetic modeling of "Electrospun asymmetric membranes" (Chapter V)

In vitro CRV release from asymmetric membranes was carried out during 7 days in TRIS and AES solutions. On the other hand, in order to mimic real wound healing process, the release was also measured during 3 weeks: 1st week in 0.1 M TRIS solution at pH 8; 2nd week in 0.1 M PBS solution at pH 7.4; 3rd week in AES at pH 5 (142 mmol of Na^{+} and 2.5 mmol of Ca^{+2}). According to scheduled time intervals (from 1, 2, 4, 8, 24, 72 and 168 hours), 1 mL of each solution was collected and replaced with equal volume of fresh solutions. The collected samples were stored at -20 ºC until analysis by high-performance liquid chromatography (HPLC) using a Agilent 1100 series chromatography system coupled with a UV-vis multiwavelength detector. The monitoring wavelength was 275 nm. The column used was a Phenomenex Kinetex 2.6 um XB-C18 100A 100x4.6 mm. The mobile phase was an isocratic combination of acetonitrile (ACN):H2O (50:50) with a flow rate of 0.4 ml/min. Injection volume for all samples and standard solutions was 25µl. The carvacrol calibration curve (0-50 ppm) was made with naproxen sodium as internal standard.

A.1.8 Drug release kinetics

To fit the obtained results, release kinetics from scaffolds or asymmetric membrane was evaluated using the Higuchi (2), Korsmeyer-Peppas (3), Peppas-Sahlin (4)and Lindner-Lippold's (5) models. Experimental data were analyzed by a linear and a non-linear least-squares regression. The Higuchi, Korsmeyer-Peppas

and Peppas-Sahlin models are valid only for the first 60% of the drug release, while the Lindner-Lippold's model is valid for the first 80% (4,5). The equations [Eq. A.3-A.6] for these kinetic models were as follows:

Higuchi model: $\frac{M_t}{M_T} = k\, t^{1/2}$ [Eq. A.3]

Korsmeyer-Peppas model: $\frac{M_t}{M_T} = k_{1K}\, t^n$ [Eq. A.4]

Peppas-Sahlin model: $\frac{M_t}{M_T} = k_{1P}\, t^n + k_2\, t^{2n}$ [Eq. A.5]

Lindner-Lippold's model: $\frac{M_t}{M_T} = k_{1L}\, t^n + b$ [Eq. A.6]

Where M_t/M_T is the drug release fraction at time t, k is the Higuchi rate constant, k_{1K}, k_{1L} are kinetic constants incorporating structural and geometric features of the system and the term b describes the burst effect (fast release from surface). In the Peppas and Sahlin model, k_{1P} and k_2 are constants, and the first term on the right hand side represents the Fickian diffusional contribution (F), whereas the second term represents the case-II relaxation contribution (R). The ratio of both contributions can be calculated as follows: $R/F = (k_2/k_1)\, t^n$ (4). In all of them, n is the diffusional exponent that can be related to the drug transport mechanism. For a spherical sample, when n = 0.43, the drug release mechanism follows a Fickian diffusion and when n = 0.85, the case II transport occurs, leading to zero-order release (polymer chains swelling or relaxing). When n value is between 0.43 and 0.85, an anomalous transport is observed (6).

Correlation coefficient (R^2) values obtained were calculated and compared. Besides the coefficient of determination (R^2), the smaller value of sum of the squared residuals (SSR) and the Akaike Information Criterion (AIC) [Eq. A.7] were applied to discriminate the model that best described the drug release mechanism (7).

$AIC = N\,(\ln SSR) + 2p$ [Eq. A.7]

Where N is the number of experimental data points and p is the number of parameters. When comparing several models, the one associated with the smallest

value of *AIC* is given the best fit for the given data set. Additionally, the fit of the predicted curve to the experimental data was also evaluated.

A.1.9 Swelling studies of "Electrospun asymmetric membranes" (Chapter V)

The swelling was measured via gravimetric method by immersing dry membranes with initial weight W_d in a TRIS solution, after 24 h the medium was changed for AES. Membranes were removed from solutions at a prescribed time interval and weighed after wiping the excess water from the surface to get its final weight, W_t. Membranes swelling was calculated using the following equation:

$$Swelling = \frac{W_t - W_d}{W_d} \times 100\% \qquad \text{[Eq. A.8]}$$

Water retention of membranes was calculated as follows:

$$Water\ retention = \frac{W_t - W_d}{W_s - W_d} \times 100\% \qquad \text{[Eq. A.9]}$$

Where W_s is the weight of the membrane removed from TRIS solution, when the swelling equilibrium is reached.

A.1.10 Water vapor transmission of "Electrospun asymmetric membranes" (Chapter V)

The water vapor transmission rate (WVTR) was measured according to ASTM Standard E96/E96M-10 (8). Three different driving forces were imposed to determine the water vapor permeability of the asymmetric membranes. Square pieces of the membrane (2x2 cm) were conditioned at room temperature and relative humidity of 81% overnight. Then they were mounted on a glass dish with a diameter of 5 cm and placed on a top of a cup with 15 mL of a solution with a specific relative humidity. The device was introduced in a desiccator containing a saturated salt solution (CH_3COOK solution with RH = 28%) and equipped with a fan to promote air circulation, in order to minimize the mass transfer resistance in the air boundary layer above the membrane. Room temperature and relative humidity (RH) inside the desiccator were monitored using a thermohygrometer HM40 (Vaisala, Finland). The WVTR was determined by measuring the rate of

change of mass in regular time intervals for 24 h at three different driving forces of RH: 100 %, 81 % ($(NH_4)_2SO_4$ solution) and 65 % ($NaNO_2$ solution) to 28 % (CH_3COOK solution), following this equation:

$$WVTR\ (^{g}/_{m^2\ h}) = \frac{mass}{t \times area} \qquad \text{[Eq. A.10]}$$

Three independent runs were performed.

A.1.11 Biodegradation studies

The biodegradation percentage was calculated by the following equation [Eq. A.11]:

$$Biodegradation\ (\%) = \frac{M_t - M_i}{M_i} \times 100 \qquad \text{[Eq. A.11]}$$

Where M_i is the initial mass and M_t *is* the dry mass at time t after incubation.

A.1.11.1 Enzymatic degradation in "Polymeric electrospun scaffolds for bone morphogenetic protein" (Chapter IV)

Enzymatic degradation experiments were carried out at 37 °C in DPBS to mimic biodegradation conditions. Square samples (2.5 × 2.5 × 0.2 mm) of the fabricated scaffolds were cut out and placed in 6-well culture plates containing 1 mL of DPBS with 0.12 U/mL lipase from *Aspergillus oryzae* or 1 mL of DPBS containing 1300 U/mL human lysozyme, to emulate the enzymatic activities of human serum (9). Every 10 days until 60 days, three scaffolds per sample and enzyme were withdrawn from the degradation medium. Then, they were dried at 37 °C for 4 h to be weighed. After weighing, the enzymatic solution (1 mL) was refreshed, and the scaffolds were immersed again until the next weight measurement (every 10 days up to 60 days).

A.1.11.2 Biodegradability in a mimic real wound environment of "Electrospun asymmetric membranes" (Chapter V)

The biodegradability of asymmetric membranes was studied *in vitro* over 3 weeks at 32 ºC. Five samples per membrane were soaked in the 3 different pH solutions (one per week) with the same order described before for the samples in

wet conditions. Samples were taken out from the solutions every week, washed with distilled water, freeze-dried and placed in the solution at different pH. The weight was measured before and after lyophilization.

A.1.12 Bactericidal tests

A.1.12.1 Bactericidal tests in "Composite scaffold loaded with RFP" (Chapter II)

To evaluate the antimicrobial efficiency of the fabricated materials, the minimum inhibitory concentration (MIC) and the minimum bactericidal concentration (MBC) were determined against *E. coli S17* as Gram negative model, and *S. aureus* as Gram positive infective model.

Antibacterial activities of the RFP loaded in PCL-PLGA-RFP electrospun scaffolds against *E. coli* and *S. aureus* were studied using the ASTM E-2180 (10). Briefly, an overnight stationary growth phase of bacteria in TSB was diluted in sterile TSA solution at 40 ºC to obtain a starting bacteria concentration of 10^5 colony forming units per milliliter (CFU/mL). Samples were placed in a 12-well plate and the electrospun scaffolds were weighed to obtain RFP concentrations ranging from 0.5 to 90 ppm, considering the total amount of RFP loaded in the scaffolds, and then placed on the bacteria inoculated TSA and incubated at 37 ºC during 24 h. After incubation, the samples were collected in 10 mL of sterile TSB to be sonicated in an ultrasonic bath (50 kHz) for 1 min, and then stirred with vortex for 1 min. Subsequently, the samples were diluted in PBS and spot-plated on TSA plates (four replicas per sample). Viable bacterial colonies were counted after overnight incubation at 37 ºC. Each experiment was performed in triplicate and the results are reported as mean ± S.D. PCL-PLGA electrospun scaffolds without RFP were used as control sample.

A.1.12.2 Bactericidal tests in "Asymmetric membranes loaded with CRV" (Chapter V)

Asymmetric membranes antibacterial activity loaded with CRV against *E. coli* and *S. aureus* was studied using the Antimicrobial Disk Susceptibility Tests of the US Clinical and Laboratory Standards Institute (CLSI) (11). Briefly, TSA plates were

inoculated with 0.2 mL of a bacterial suspension containing 10^7 CFU/mL. Membrane discs (14 mm diameter) were placed on the top of the agar plate (with the PVAc-CRV layer in contact with the agar) and incubated at 37 °C for 24 h. After incubation, agar discs (10 mm in diameter) were obtained from the inhibition zone, cut and aseptically placed in a tube with TSB These tubes were sonicated 1 min and stirred 1 min to assure the bacteria release. Then, bacterial suspensions were diluted in PBS, plated on TSA and viable colonies counted after incubation (37 ºC, 24 h). Control samples (untreated bacteria) were also run. Each experiment was done in triplicate and the results are reported as mean ± S.D.

A.1.13 Cell attachment, morphology, viability, and immunohistochemistry

A.1.13.1 Cell culture on "Composite scaffold loaded with RFP" (Chapter II)

Electrospun scaffolds (15 mm of diameter, surface area 1.54 cm^2) were sterilized on both sides by UV-irradiation for 1 h and successively soaked with OGM culture medium for 1 h to avoid floating. HOBs were grown in OGM culture medium in a 5 % CO_2 atmosphere at 37 ºC. Then, the culture medium was removed and 10 µL of cell suspension (3.2 x 10^6 cells/mL) were seeded on the top region of the scaffolds. To promote cell adhesion to the scaffold, the samples were incubated for 1 h (5% CO_2, 37 ºC) and then 500 µL of OGM were added to each sample. The seeded scaffolds were cultured up to 3, 7, 14 and 28 days, renewing the culture medium every 2-3 days. In addition, 2D cultures (HOBs seeded on 24-well plates) were also run as cell growth and proliferation control sample.

A.1.13.2 Cell morphology on "Composite scaffold loaded with RFP" (Chapter II)

SEM microscopy was performed to observe the morphology of the attached cells to the electrospun scaffolds. At the time points indicated above, the seeded scaffolds were washed with DPBS and fixed in a 4% paraformaldehyde solution (Affymetrix, US) for 30 min at room temperature. After fixation, the samples were washed with DPBS and distilled water, air-dried and sputter-coated with a thin

platinum layer prior to visualization by SEM (Field Emission Scanning Electron Microscope CSEM-FEG INSPECT 50, FEI, US).

A.1.13.3 Confocal analysis on "Composite scaffold loaded with RFP" (Chapter II)

Confocal analysis was developed to observe the cytoskeleton protein distribution, actin (Alexa Fluor™ 546 Phalloidin; Molecular Probes, US), after 3, 7, 14 and 28 days of cell culture. Seeded scaffolds were rinsed with DPBS and fixed with 4% paraformaldehyde solution for 15 min. Then, samples were permeabilized on ice-cold acetone (-20 ºC, 5 min), air-dried and rinsed with DPBS. Triton X-100 (0.5 %) was then added to the samples for blocking (30 min) with 5% normal donkey serum (NDS; Jackson ImmunoResearch Europe Ltd, UK). After blocking, actin staining (1:200; Alexa Fluor™ 546 Phalloidin; Molecular Probes, US) was developed for 30 min at room temperature. The scaffolds were then washed with DPBS and incubated with 8 µM anthraquinone dye (DRAQ5; eBiocence, US) for 30 min at room temperature to stain the cellular nuclei. Finally, samples were washed, mounted and visualized under a confocal laser scanning microscope (Leica TCS SP2, Leica, Germany).

A.1.13.4 *In vitro* cytotoxicity studies of "Composite scaffold loaded with RFP" (Chapter II)

Cytotoxicity of seeded electrospun scaffolds, with and without RFP, was determined by the 3-(3,4-dimethylthiazol-2-yl)-2,5-diphenyltetrazoliumbromide (MTT) test at the time points described above (3-28 days) (12). In brief, an MTT solution (5 mg/mL in DPBS) was diluted in OGM (final concentration 0.5 mg/mL), added to the seeded scaffolds at the time points described above, and incubated for 4 h at 37 ºC and 5 % CO_2. Then, the cell medium was discarded and the insoluble formazan crystals obtained were dissolved by the addition of an SDS (Sodium Dodecyl Sulfate; Bio-Rad, US) solution (100 mg/mL in DMSO and 0.6% of acetic acid). Finally, aliquots (100 µL) were transferred to a 96-well plate and the absorbance was read at 570 nm in a Synergy HT microplate reader (Biotek, US). Results were expressed as mean ± S.D of the total absorbance of the samples analyzed in triplicate.

A.1.13.5 Cell culture on "Laser-treated electrospun fibers loaded with nano-hydroxyapatite" (Chapter III)

Electrospun scaffolds membranes were fixed in CellCrown™, sterilized by UV-irradiation for 30 min on both sides and rinsed overnight with OGM. Normal human osteoblasts (NHOst, Lonza, Belgium) were grown in OGM culture medium, supplemented with 10% FBS, ascorbic acid and 5% solution of gentamicin and amphotericin-B (OGM BulletKit, Lonza, USA) as the manufacturer indicates in an atmosphere containing 5 % CO_2 at 37 °C. Electrospun scaffolds membranes fixed in CellCrown™ were incubated for 12-18 h in OGM. Then, culture medium was removed and NHOst at passages between 5 and 6 were seeded on the scaffolds at a density of 3.2×10^6 cells/mL suspended in 10 µL of medium on the scaffolds center. Samples were incubated for 1 h and then more OGM was added to each well. Next, the cells were cultured up to 2, 7 and 14 days, renewing the culture medium every 2 days.

A.1.13.6 Cell viability of "Laser-treated electrospun fibers loaded with nano-hydroxyapatite" (Chapter III)

A Live/Dead® Viability/Cytotoxicity Kit *for mammalian cells* (Molecular Probes, UK) was used to determine cell viability after 48 h, 7 and 14 days of cultivation, according to the manufacturer's protocol. Calcein-AM was used as a marker of esterase activity in living cells, EthD-1 penetrates into dead cells through their damaged membrane and produces red fluorescence and cellular nuclei were stained with an anthraquinone dye (DRAQ5TM). The scaffolds were washed with DPBS five times for five minutes every time and incubated in 0.5 mL of Live/Dead® working solution and 8 µM of DRAQ5. Staining was performed under dark conditions for 30 min at room temperature. Imaging the sample surfaces and cellular morphology were obtained on a confocal laser scanning microscope (Leica TCS SP2).

A.1.13.7 Image processing for cell viability quantification on "Laser-treated electrospun fibers loaded with nano-hydroxyapatite" (Chapter III)

Image J software (Version 1.48f, NIH, US) was used to quantify the viability of NHOst seeded onto the different scaffolds described above. Confocal images were analyzed through a step-by-step procedure on the green channel as it recorded the live cells, setting up the scale and the threshold in this channel. Cell viability was determined by the ratio of green pixel area to the total area of pixels. Five different regions of each sample were evaluated and the maximum projection of at least 60 planes per region was quantified (total area analyzed per region ≈ 0.14 cm^2). Semiautomatic measurement was developed to calculate the percentage of the covered area by live cells stained with calcein.

A.1.13.8 Cell morphology on "Laser-treated electrospun fibers loaded with nano-hydroxyapatite" (Chapter III)

SEM was performed to observe cell morphology and attachment on electrospun scaffolds membranes. After 48 h, 7 and 14 days of cultivation samples were washed with DPBS, fixed in a 4% paraformaldehyde solution at room temperature for 30 min. The samples were sputter-coated with platinum and characterized by SEM microscopy (Field Emission Scanning Electron Microscope CSEM-FEG INSPECT 50, FEI, USA).

A.1.13.9 Cell culture on "Polymeric electrospun scaffolds for bone morphogenetic protein" (Chapter IV)

Human osteoblasts were grown in the OGM culture medium in a 5 % CO_2 atmosphere at 37 °C. Electrospun scaffolds of 15 mm diameter were placed in CellCrown™ inserts and sterilised on both sides by ultraviolet (UV) irradiation for 60 min. After that, the scaffolds were placed into 24-well plates to be successively conditioned with the OGM culture medium for 1 h to soak them and avoid floating. Next, the culture medium was removed, and cells at passage 6 (3.2×10^6 cells/mL) were resuspended in 10 µL of the medium and were seeded onto the middle top region of the scaffolds (surface area 1.54 cm^2). Samples were incubated for 1 h (5

% CO_2, 37 °C) to facilitate cell adhesion to the scaffold and then, 500 µL of OGM were added into each well for subsequent growth and proliferation. The seeded scaffolds were cultured for 1, 2, 3, or 4 weeks, and the culture medium was refreshed every 2-3 days.

A.1.13.10 Cell viability of "Polymeric electrospun scaffolds for bone morphogenetic protein" (Chapter IV)

Cell viability was determined by examination of the cultured scaffolds in a 3-(3,4-dimethylthiazol-2-yl)-2,5-diphenyltetrazolium bromide (MTT) assay (12). Briefly, an MTT solution (5 mg/mL in DPBS) was diluted in OGM to a final concentration of 0.5 mg/mL and added to the seeded scaffolds at the time points described above. After incubation for 4 h (37 °C, 5% CO_2), the cell medium was discarded and an SDS (Sodium Dodecyl Sulfate; Bio-Rad, US) solution (100 mg/mL in 0.6 % acetic acid in DMSO) was added to the samples to dissolve the insoluble formazan obtained. Aliquots (100 µL) of each sample were transferred to 96-well plates in triplicate, and absorbance was recorded at 570 nm on a Synergy HT microplate reader (BioTek, US). The results were expressed as total absorbance of the samples.

A.1.13.11 Cell morphology on "Polymeric electrospun scaffolds for bone morphogenetic protein" (Chapter IV)

The morphology of the cells attached to the scaffolds at the time points indicated above was visualized under an SEM (Field Emission Scanning Electron Microscope CSEM-FEG INSPECT 50, FEI, US). HOBs that were seeded onto the scaffolds, as described in the previous section, and were incubated for 1, 2, 3, or 4 weeks, were washed with DPBS and fixed in a 4% paraformaldehyde solution (Affymetrix, US) for 15 min. Then, the fixed samples were washed with DPBS, dried, and sputter-coated with a thin platinum layer prior to visualization under the SEM.

A.1.13.12 Alkaline phosphatase assay in "Polymeric electrospun scaffolds for bone morphogenetic protein" (Chapter IV)

ALP concentration was determined to elucidate the potential of the seeded cells for bone turnover and mineralization, as previously described (13), by means of the SensoLyte® pNPP Alkaline Phosphatase Assay Kit (Anaspec, US). At different time points (1–4 weeks), scaffolds with and without (control samples) seeded cells were washed with assay buffer, rinsed with a Triton X-100 solution and scraped to release the enzyme through cell membrane leakage. Finally, the scaffolds were discarded, and the samples were collected to be next stirred (250 rpm, 10 min, 4 °C) and centrifuged (10,000 × *g*, 10 min, 4 °C). Then, the supernatants were collected, and aliquots (100 µL) were transferred to 96-well plates in triplicate. The absorbance of the samples was measured at 570 nm on the Synergy HT microplate reader (Biotek, US). The results were expressed as total absorbance of the samples.

A.1.13.13 Immunohistochemistry in "Polymeric electrospun scaffolds for bone morphogenetic protein" (Chapter IV)

The expression of specific osteogenic markers, such as OCN (anti-osteocalcin antibody [G-5] conjugated with Alexa Fluor® 488, Santa Cruz Biotechnology, US) and OPN (anti-OPN antibody [AKm2A1] conjugated with Alexa Fluor® 647, Santa Cruz Biotechnology, US), together with the evaluation of the cytoskeleton protein distribution and actin (Alexa Fluor™ 546–conjugated phalloidin, Molecular Probes, US) in HOBs seeded onto the different types of scaffolds, was analyzed by immunohistochemistry.

Seeded scaffolds at an early (2 weeks) and at a later (4 weeks) time point were rinsed with DPBS and fixed with a 4 % paraformaldehyde solution (Affymetrix, US) for 15 min. After that, paraformaldehyde was discarded, and the samples were permeabilized by incubation in ice-cold acetone (-20 °C, 5 min). Then, acetone was discarded and the scaffolds were air-dried and rinsed with DPBS. Triton X-100 (0.5 %) was then added to the samples for blocking (30 min) with 5 % normal donkey serum (Jackson ImmunoResearch Europe Ltd., UK). After incubation, anti-OCN (G-5) Alexa Fluor® 488 (1:100) and anti-OPN (AKm2A1)

Alexa Fluor® 647 (1:200) mouse monoclonal conjugated antibodies (Santa Cruz Biotechnology, US) diluted in 2.5 % normal donkey serum in DPBS were added to the scaffolds and incubated overnight at 4 °C. Subsequent actin staining (1:200; Alexa Fluor™ 546-conjugated phalloidin) was developed for 30 min at room temperature. Finally, the samples were washed, mounted, and observed by confocal laser scanning microscopy (Leica TCS SP2, Leica, Germany).

A.1.13.14 *In vitro* cytotoxicity studies of "Electrospun asymmetric membranes" (Chapter V)

HDFs were used for the cell viability experiments as cell line model for wound healing. Both 2D and 3D experiments were developed to address cytocompatibility of the target cells for the clinical application.

2D cell viability studies were developed by seeding cells in 24-well plates at a density of 6×10^4 cells/mL and asymmetric membranes previously sterilized with UV were then added to the cell cultures for 1, 2, 3 and 7 days at 37 ºC in a 5 % CO_2 atmosphere in high glucose DMEM supplemented with 10 % v/v FBS and 1% antibiotic-antimycotic. Cytotoxicity of CRV released from asymmetric membranes loaded with and without (control sample) CRV was determined by the 3-(3,4-dimethylthiazol-2-yl)-2,5-diphenyltetrazoliumbromide (MTT) test, as previously described (12). In brief, MTT solution in supplemented medium (0.5 mg/mL) was added to the cells at the time points previously specified. Cells were further incubated (4 h; 37 ºC, 5 % CO_2) and then, the cell medium was discarded to add SDS solution (100 mg/mL in a 0.6 % acetic acid in DMSO) to solubilize the insoluble formazan yielded. Finally, absorbance was recorded in triplicate at 570 nm in a Synergy HT microplate reader (Biotek, US). Results were expressed as viability percentage of the samples related to the control sample (PCL/PVAc not loaded with CRV; 100 % viability).

A.1.13.15 Cell morphology and confocal analysis on "Electrospun asymmetric membranes" (Chapter V)

3D cell morphology and cytocompatibility assays were developed by seeding HDFs onto the asymmetric membrane in contact with the PVAc-CRV layer. First, sterilized membranes were conditioned with DMEM for 1 h to soak them and avoid

floating. Then, the culture medium was removed and cells were seeded onto the middle region of the PVAc-CRV layer of the membranes at a density of 6x 10^4 cells/mL in a volume of 20 µL of supplemented culture medium. Samples were incubated for 1 h (5 % CO_2, 37 ºC) to promote cell adhesion to the membrane and then 500 µL of supplemented DMEM were added to each well to enable cell proliferation. Culture medium was renewed every 2 days in all samples. After 3 days, membranes were washed with DPBS, fixed in a 4 % paraformaldehyde solution in PBS (Affymetrix, US) at room temperature for 30 min. The samples were sputter-coated with platinum and characterized by SEM. Confocal analysis of 3D cell cultures was also achieved to observe the expression of cytoskeleton protein F-actin (Alexa Fluor™ 546 Phalloidin; Molecular Probes, US) after 3 days of cell culture onto the membranes in order to further evaluate cell proliferation and cytocompatibility of the membranes. Cells were fixed with 4% paraformaldehyde solution (Affymetrix, US) for 15 min and permeabilized with 0.5 % Triton X-100 for 30 min, to be then blocked (30 min) with 5 % normal donkey serum (NDS; Jackson ImmunoResearch Europe Ltd, UK). After blocking, the membranes were incubated with Alexa Fluor™ 546 Phalloidin (1:200; Molecular Probes, US) for 30 min at room temperature and then washed three times in DPBS and incubated with 8 µM anthraquinone dye (DRAQ5; eBioscience, US) for 30 min at room temperature for nuclei staining. Finally, stained membranes were washed three times in DPBS and milli-Q water to be then mounted on glass slides and examined under confocal microscopy (Leica TCS SP2, Germany).

A.1.14 Cell scratch model on "Electrospun asymmetric membranes" (Chapter V)

HDFs were seeded in 24-well plates at 1.2 × 10^5 cells/mL and grown until a confluence. Then, cells were washed with DPBS and a manual scratch of 1 mm wide straight-line was made with a 1000 µL sterile pipette tip to emulate a wound. Cells were washed again with DPBS in order to remove cell debris and added fresh DMEM. Scaffolds were then added to the cultures to evaluate the effect of released CRV from Sample I and Sample II on cell migration. Control samples (not treated) were also run to compare cell migration. Scratch closure was qualitative analyzed under an Olympus motorized inverted research microscope model IX81, Japan, by

acquiring images at time 0 (immediately after scratching) and after 1, 2 and 3 days in culture.

A.1.15 Statistical analysis

All the data are reported as mean ± standard deviation (SD). For fiber and particle diameter at least n = 100 were studied. Measurements of porosity, mechanical properties and swelling study were made by quintuplicate (n = 5). Water vapor transmission rate, biodegradations studies, permeability, antibacterial activity, encapsulation efficiency and *in vitro* release of RFP, BMP2, and CRV were measured in triplicate and quintuplicate according to the specific case. For confocal analysis, more than 50 planes per region and at least three regions per sample were evaluated. MTT and ALP were assayed thrice, and three measurements were performed per experiment (9 data points). The statistical analysis of data was performed by the Student-Newman-Keuls t-test and ANOVA or U-Mann-Whitney analysis (Statgraphics® Centurion XV statistical software, StatPoint Technologies, Inc., US). Statistically significant differences were considered when $p \leq 0.05$.

References

1. Kokubo T, Takadama H. How useful is SBF in predicting in vivo bone bioactivity? Biomaterials. 2006;27(15):2907–15.

2. Higuchi T. Mechanism of sustained-action medication. Theoretical analysis of rate of release of solid drugs dispersed in solid matrices. J Pharm Sci. Wiley-Blackwell; 1963 Dec;52(12):1145–9.

3. Korsmeyer RW, Gurny R, Doelker E, Buri P, Peppas NA. Mechanisms of solute release from porous hydrophilic polymers. Int J Pharm. Elsevier; 1983 May;15(1):25–35.

4. Peppas NA, Sahlin JJ. A simple equation for the description of solute release. III. Coupling of diffusion and relaxation. Int J Pharm. Elsevier; 1989 Dec;57(2):169–72.

5. Lindner WD, Lippold BC. Drug release from hydrocolloid embeddings with high or low susceptibility to hydrodynamic stress. Pharm Res. 1995 Nov;12(11):1781–5.

6. Ritger PL, Peppas NA. A simple equation for description of solute release II. Fickian and anomalous release from swellable devices. J Control Release. Elsevier; 1987 Jun;5(1):37–42.

7. Yamaoka K, Nakagawa T, Uno T. Application of Akaike's information criterion (AIC) in the evaluation of linear pharmacokinetic equations. J Pharmacokinet Biopharm. Kluwer Academic Publishers-Plenum Publishers; 1978 Apr;6(2):165–75.

8. ASTM E96 / E96M-16, Standard Test Methods for Water Vapor Transmission of Materials. ASTM International. West Conshohocken, PA; 2016.

9. Azevedo H, Reis RL. Understanding the Enzymatic Degradation of Biodegradable Polymers and Strategies to Control Their Degradation Rate. In: Biodegradable Systems in Tissue Engineering and Regenerative Medicine. 2005.

10. ASTM E2180-18, Standard Test Method for Determining the Activity of Incorporated Antimicrobial Agent(s) In Polymeric or Hydrophobic Materials. ASTM International. 2018.

11. Bauer AW, Kirby WMM, Sherris JC, Turck M. ANTIBIOTIC SUSCEPTIBILITY TESTING BY A STANDARDIZED SINGLE DISK METHOD. Am J Clin Pathol.

1966;45(4):493–6.

12. Morelli S, Piscioneri A, Salerno S, Al-Fageeh MB, Drioli E, De Bartolo L. Neuroprotective effect of didymin on hydrogen peroxide-induced injury in the neuronal membrane system. Cells Tissues Organs. 2014;199:184–200.

13. Halling Linder C, Ek-Rylander B, Krumpel M, Norgård M, Narisawa S, Millán JL, et al. Bone Alkaline Phosphatase and Tartrate-Resistant Acid Phosphatase: Potential Co-regulators of Bone Mineralization. Calcif Tissue Int. Springer US; 2017 Jul;101(1):92–101.

APPENDIX 2

Articles published and participation in scientific forums

Publications

- Composite scaffold obtained by electro-hydrodynamic technique for infection prevention and treatment in bone repair. Javier Aragón, Sergio Feoli, Silvia Irusta, Gracia Mendoza. International Journal of Pharmaceutics. **Submitted work (under review)** (Ms. Ref. No.: IJP-D-18-01794).
- Electrospun asymmetric membranes for wound dressing applications. Javier Aragón, Clarinda Costa, Isabel Coelhoso, Gracia Mendoza, Ana Aguiar-Ricardo and Silvia Irusta. Applied Surface Science. **Submitted work (under review)**.
- Polymeric electrospun scaffolds for bone morphogenetic protein 2 delivery in bone tissue engineering. Javier Aragón; Simona Salerno, Loredana De Bartolo, Silvia Irusta and Gracia Mendoza. Journal of Colloid and Interface Science, 531 (2018) 126–137. DOI:10.1016/j.jcis.2018.07.029.
- Synthesis of a Novel Electrospun Polycaprolactone Scaffold Functionalized with Ibuprofen for Periodontal Regeneration: An In Vitro and In Vivo Study. Fareeha Batool, David-Nicolas Morand, Lionel Thomas, Isaac Maximiliano Bugueno, Javier Aragon, Silvia Irusta, Laetitia Keller, Nadia Benkirane-Jessel, Henri Tenenbaum and Olivier Huck. Materials 11, 580, 2018. DOI:10.3390/ma11040580.
- Production, characterization and testing of antibacterial PVA membranes loaded with HA-Ag3PO4 nanoparticles, produced by SC-CO2 phase inversion. Lucia Baldino, Javier Aragon, Gracia Mendoza, Silvia Irusta, Stefano Cardea, Ernesto Reverchon1. Journal of Chemical Technology & Biotechnology. 2018. DOI:10.1002/jctb.5749.
- Laser-treated electrospun fibers loaded with nano-hydroxyapatite for bone tissue engineering. Javier Aragon, Nuria Navascues, Gracia Mendoza, Silvia Irusta. International Journal of Pharmaceutics 525,112–122, 2017. DOI:10.1016/j.ijpharm.2017.04.022.

- Integration and bioactivity of hydroxyapatite grown on carbon nanotubes and graphene oxide. J. David Núñez, Ana M. Benito, Ramón González, Javier Aragón, Raul Arenal, Wolfgang K. Maser. CARBON, Vol. 79: 590-604, 2014. DOI: 10.1016/j.carbon.2014.08.020.

Presentations at scientific meetings

- 2017. 2nd International Caparica Christmas Congress on Translational Chemistry. Multilayer membrane obtained by electrospinning technique for wound dressing applications.
- 2017. 4th Congress University Nova de Lisboa-University of Yamaguchi-Univesity of Zaragoza: "Engineering at the service of our society: From nanotechnology to megastructures". Polymeric electrospun membrane for tissue engineering applications.
- 2017. 28th European Conference on Biomaterials, Athens, Greece, 4th – 8th September 2017. POLYMERIC NANOFIBROUS MEMBRANES OBTAINED BY ELECTROSPINNING FOR BIOMEDICAL APPLICATIONS
- 2014. XXXII Annual Congress of the Spanish Society of Biomedical Engineering (CASEIB 2014). Core-shell fibers of biocompatible polymers loaded with Hydroxyapatite and Ibuprofen.
- 2014. 6 th Journey of young researchers of Aragon. Development of fibers with biomedical applications by electrospinning technology.

Postgraduate courses

- 2015. International training school on advanced characterization techniques for electrospun nanofibers: hands -on experience. Ankara, Turkey.